APPLICATION OF SEISMIC REFRACTION AND ELECTRIC RESISTIVITY METHODS IN PLACER EXPLORATION

OPEN FILE 84-11

FINAL REPORT

(July 1, 1983 - June 30, 1984)

By

Scott L. Huang

Report On

Contract No. 1134102
U.S. Bureau of Mines
Department of Interior

July, 1984

ABSTRACT

In spite of the success of geophysical methods in subsurface exploration, the applications to gold prospecting in Alaska are limited owing to several reasons. Presence of permafrost and the complicated interpretation procedures of geophysical methods are the two major factors.

This study evaluated the performance of seismic refraction and electric resistivity methods on frozen ground and permafrost free areas in the Fairbanks mining district. Two computer programs, SEISMIC and RESISTIVITY, were developed to assist the field data interpretation.

The seismic refraction proves itself a good technique for determining the depth of a possible deposit in permafrost free area. A survey conducted in frozen ground was unable to accurately detect the gravel-bedrock contact.

The Schlumberger and Wenner arrays produced very consistent results. The resistivity profiling successfully detected a known gold-bearing quartz vein. Profiling data also identified a similar vein pattern which was previously detected by VLF method. The vertical electrical sounding method produced results with less accuracy. It was probably caused by the limitation of the interpretation procedures and the theory used.

ACKNOWLEDGEMENTS

This study was supported by the U.S. Bureau of Mines, Department of the Interior, under Contract No. 1134102 through the Mineral Industry Research Laboratory of the University of Alaska, Fairbanks. The research reported herein was performed by Scott L. Huang. Field surveys were conducted by graduate students, Michael D. Balen, Ming-chee Wu, Frank Wuttig and Stephanie Kutterer.

TABLE OF CONTENTS

	Page
ABSTRACT	i
ACKNOWLEDGEMENTS	ii
TABLE OF CONTENTS	iii
LIST OF FIGURES	v
LIST OF TABLES	vii
I. INTRODUCTION	1
II. REGIONAL GEOLOGY AND STRUCTURE	5
REGIONAL GEOLOGY	5
Yukon-Tanana Metamorphic Complex	5
Mesozoic Rocks	8
Tertiary Rocks	8
Quaternary and Surficial Deposits	8
REGIONAL STRUCTURE	9
III. SEISMIC REFRACTION	12
THEORY	12
Time-Distance Relationship	12
Dipping Beds	15
Refraction Across a Subsurface Structure	19
ROUTINE FIELD PROCEDURES	21
MICROCOMPUTER ANALYSIS	23
CASE STUDIES	33
Willow Creek Survey	34
Local Geology	34
Survey Procedures	34
Results	

TABLE OF CONTENTS (cont'd)

	Page
USA CRREL Tunnel Survey	44
Local Geology	44
Survey Procedures	47
Results	47
IV. ELECTRICAL RESISTIVITY	50
THEORY	50
Schlumberger Configuration	53
Wenner Configuration	53
Vertical Electrical Sounding (VES)	56
ROUTINE FIELD PROCEDURES	57
MICROCOMPUTER ANALYSIS	58
CASE STUDIES	63
Chatham Creek Survey	63
Local Geology	63
Survey Procedures	65
Results	66
USA CRREL Tunnel Survey	66
Survey Procedures	66
Results	71
V. DISCUSSION AND CONCLUSIONS	84
VI. REFERENCES	88
VII. APPENDICES	89
APPENDIX A	89
APPENDIX B	105

LIST OF FIGURES

FIGURE		Page
1.	Significant gold deposits in Alaska (Eakin and Others, 1983)	2
2.	Map showing location of the Fairbanks mining district (Forbes, 1982)	6
3.	Regional geologic map of the Yukon-Tanana Upland (Forbes, 1982)	7
4.	Geological structure map of the Yukon-Tanana Upland (Forbes, 1982)	10
5.	Seismic wave paths of the least time and time-distance curve for a two layer structure	13
6.	Seismic refraction along a dipping bed. Respective shots are at updip and downdip ends of survey line	16
7.	Refraction along the nth dipping layer (after Mota, 1954)	18
8.	Refraction across a subsurface structure	20
9.	Correction of refraction times for elevation	22
10.	Flow chart of the SEISMIC microcomputer program	25
11.	Computer output of the time - distance plot	29
12.	Map showing the site of seismic refraction survey along Willow Creek	35
13.	Time - distance diagram of the track 1 at the Willow Creek site	40
14.	Time - distance diagram of the track 2 at the Willow Creek site	41
15.	Time - distance diagram of the track 3 at the Willow Creek site	42
16.	Map showing the seismic survey sites at USA CRREL permafrost tunnel, Fox, Alaska	45
17.	Geology of the USA CRREL permafrost tunnel	46
18.	Subsurface layering structure at Site I, USA CRREL permafrost tunnel	48

LIST OF FIGURES (cont'd)

FIGURE		Page
19.	Vertical cross-section of the earth showing the electric current lines (solid lines) and the equipotential lines (dashed lines)	51
20.	The Schlumberger electrode configuration	54
21.	The Wenner electrode configuration	55
22.	Flow chart of the RESISTIVITY microcomputer program	59
23.	Map showing the location of resistivity profiling survey along Chatham Creek	64
24.	Profiling measurements and VLF data of the Chatham Creek site	68
25.	Map showing the resistivity survey sites at USA CRREL permafrost tunnel, Fox, Alaska	70
26.	Diagram of theoretical Schlumberger curves and field Wenner and Schlumberger sounding measurements at station A on site I. USA CRREL permafrost tunnel	74
27.	Diagram of theoretical and field Schlumberger VES curves at station B on site I. USA CRREL permafrost tunnel	75
28.	Diagram of theoretical and field Schlumberger VES curves at station C on site I, USA CRREL permafrost tunnel	76
29.	Diagram of theoretical and field Schlumberger VES curves at station A on site II, USA CRREL permafrost tunnel	79
30.	Diagram of theoretical and field Schlumberger VES curves at station B on site II, USA CRREL permafrost tunnel	80
31.	Diagram of theoretical and field Schlumberger VES curves at station C on site II. USA CRREL permafrost tunnel	81
32.	Diagram of theoretical and field Schlumberger VES curves at station D on site II, USA CRREL permafrost tunnel	82

LIST OF TABLES

TABLE		Page
I.	Summary of the time-distance measurements along track 1 at the Willow Creek site	37
II.	Summary of the time-distance measurements along track 2 at the Willow Creek site	38
III.	Summary of the time-distance measurements along track 3 at the Willow Creek site	39
IV.	Results of Seismic survey at the Willow Creek site	43
V.	Apparent resistivity data of profiling survey at the Chatham Creek site	67
VI.	Field Schlumberger VES measurements of stations A, B, and C at site I, USA CRREL permafrost tunnel	72
VII.	Field Wenner VES mesurements of station A at site I, USA CRREL permafrost tunnel	73
VIII.	Results of electric resistivity surveys at site I, USA CRREL permafrost tunnel	77
IX.	Results of electric resistivity surveys at site II, USA CRREL permafrost tunnel	78

INTRODUCTION

Gold mining (Figure 1), the foundation of Alaska's heritage and economy, has played a major role in the exploration and development of the state. Since the discovery made in 1902, the Fairbanks district has been more active than any other mining districts. Statewide operation after World War II declined due to rising operating costs, and during the 1960's nearly all dredging was discontinued. Deregulation of federal restrictions on prices and ownership and the increase in world market price in the 1970's stimulated a revival of gold mining activity in the state. Gold production was up 30 percent in volume from 1981. Exploration expenditures increased steadily from $4.6 million in 1979 to $35.3 million in 1981 and declined to $10.9 million a year later (Eakins and others, 1982). The rapid drop in exploration was due to the worldwide recession and high prospecting cost, and it also reflected decisions made by major companies to proceed toward production of the deposits.

Regardless of the temporary reduction of exploration activities, it will be more and more important to find new reserves as the production increases. It is unfortunate that as the need for gold increases, the chance for finding a new profitable deposit becomes smaller and the prospecting technique for such a site becomes sophisticated.

Geophysical methods have been the basic tools in subsurface investigation for many years. Geophysical prospecting involves systematic measurements of physical properties of a potential deposit and the surrounding materials. These measurements are made in search for the anomalies of the properties. Seismic refraction and electric resistivity methods are widely used in

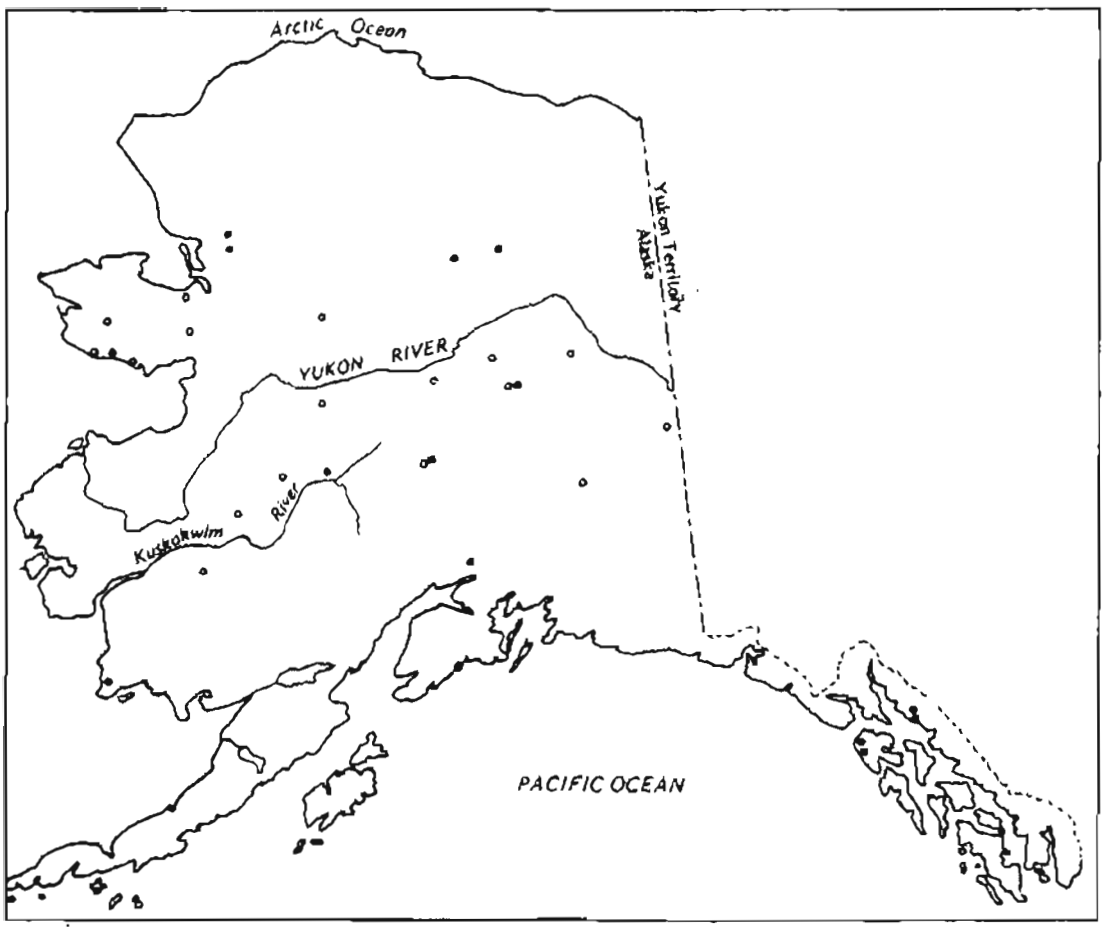

Figure 1. Significant gold deposits in Alaska (Eakin and Others, 1983).

geologic studies, petroleum exploration and mineral prospecting. Depth to the bedrock, type of deposit and other material properties can be investigated and determined quickly without needs for drilling except where occasional field checks are desired. In spite of the unique advantages of these two techniques, the applications to placer and lode gold prospecting have been limited, owing to the following reasons:

- the complex nature of frozen deposits:
- the lack of complete information on velocity and electrical properties of gold deposits and the overburden materials; and
- the complicated interpretation procedures which require considerable background knowledge of the technique.

Wescott (1982) evaluated the performance of three geophysical methods for exploration of auriferous gravels in the Fairbanks mining district. He concluded that the seismic method can determine accurately the depth to unweathered bedrock, even in deep permafrost areas and the resistivity is useful in finding water-bearing gravel and bedrock in non-permafrost areas. Anderson and Johnson (1970) conducted resistivity surveys on the north flank of Cleary Summit about 16 air miles north-northeast of Fairbanks. They indicated that the field data were useful for selecting locations for further detailed study. In areas free of permafrost, depths to bedrocks estimated from the resistivity data were compared favorably with drill-hole data. However, resistivity soundings made over frozen gravel were useful only for determining the depth to the permafrost table.

One of the major objectives of this study was to develop the field operating guidelines which will provide the prospector with step-by-step

introductory procedures of seismic and resistivity surveys. Due to the highly technical nature of these methods, this report also provides two computer programs which were primarily designed for interpretation of the survey data. Prospectors can use these packages to their benefit. The detailed documentation and discussion of these two softwares are listed in chapters III and IV and Appendices A and B.

REGIONAL GEOLOGY AND STRUCTURE

REGIONAL GEOLOGY

The lode and placer deposits of the Fairbanks mining district extend from Ester Dome to Fairbanks Creek and Coffee Dome (Figure 2). It defines a northeast-trending belt which is bounded on the northwest by the valley of the Chatanika River. The southeast boundary is approximately parallel to the Chena River and its northern tributary.

The district is located in the northeastern part of the Yukon-Tanana Upland, which is underlain by a sequence of rocks ranging from the Precambrian formation to recent surficial deposits. Every geologic system except the Jurassic is represented by sedimentary, metamorphic, or volcanic rock units.

Yukon-Tanana Metamorphic Complex

The oldest rock in the district is the Birch Creek schist of the Yukon-Tanana metamorphic complex. This metamorphic complex comprises about 75 percent of the Yukon-Tanana regions (Figure 3). The basement complex is composed of at least two sequences of metamorphic rocks that include parent rocks of late Paleozoic (Ordovician) and Precambrian age. The metamorphic rocks range in grade from greenschist to garnet-amphibolite and eclogite facies. Although micaceous quartzites and peletic schists are the most dominant rocks, the metamorphic complex also contain large gneiss terranes.

The Yukon-Tanana metamorphic complex has been extensively intruded by Mesozoic granitic rocks ranging in composition from quartz diorite to granite. Some of these intrusives are of batholithic sizes. The schists have also been invaded by mafic and ultramafic intrusives, including diorite, gabbro, hornblendite, and peridotite.

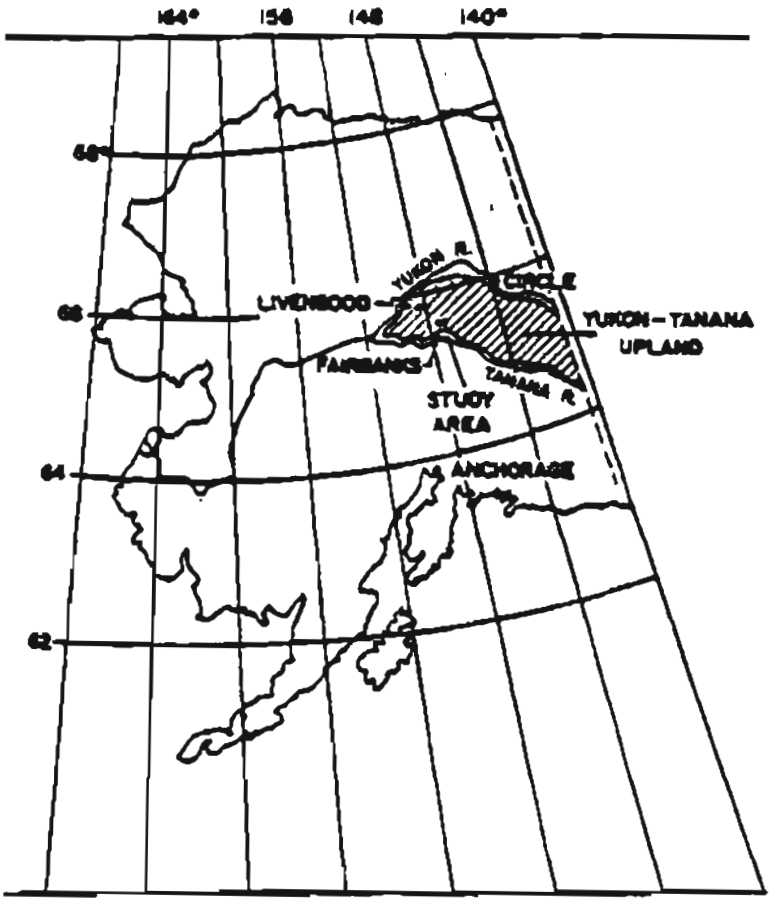

Figure 2. Map showing location of the Fairbanks mining district (Forbes, 1982).

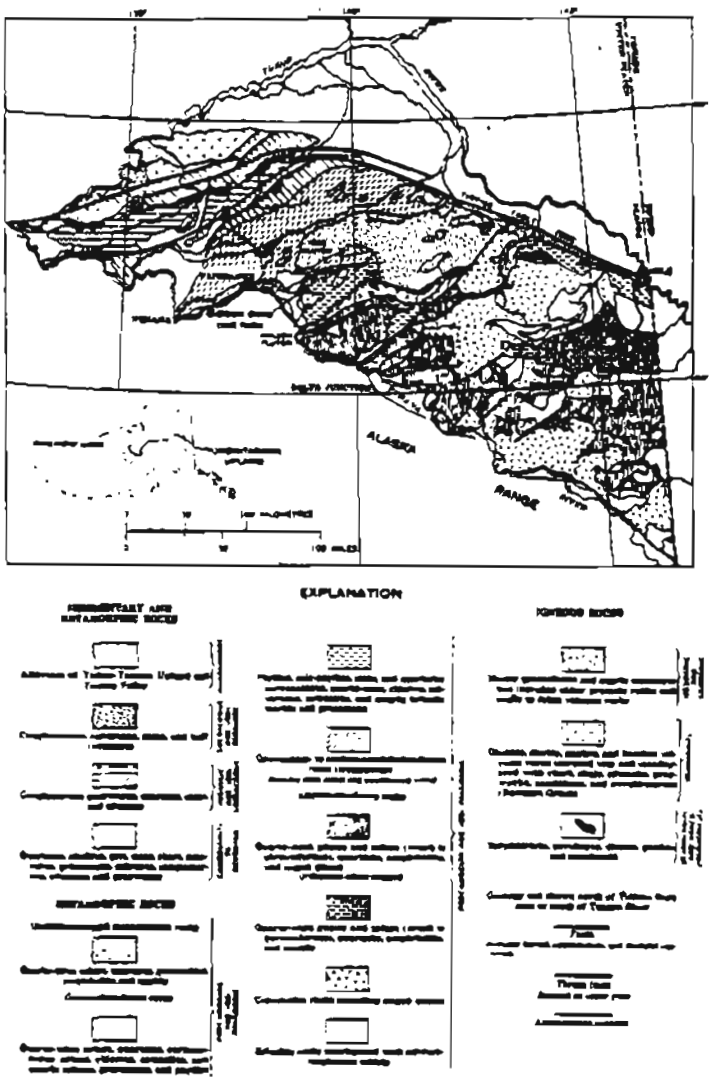

Figure 3. Regional geologic map of the Yukon-Tanana Upland (Forbes, 1982).

Mesozoic Rocks

Although Cretaceous argillaceous sediments, graywackes and conglomerates have been mapped northwest of Fairbanks, the Mesozoic sedimentary rocks have not been found in the southeastern part of the Yukon-Tanana Upland.

Small areas of basaltic rocks occur in the Fairbanks district. These late cretaceous volcanic rocks are preserved in downthrown fault blocks. Basalt also occurs as cross-cutting dikes throughout the Upland.

Tertiary Rocks

Tertiary sediments, including siltstones, sandstones, and conglomerates, occur as small, isolated outcrops in the Yukon-Tanana Upland. All occurrences are of nonmarine origin, and some section are similar to the coal-bearing Tertiary rocks on the north flank of the Alaska Range.

The Tertiary volcanic rocks occur as erosional remnants at higher elevations in the Upland. It has been found in the southeastern part of the area. The volcanic rocks are similar to that of the Tertiary volcanic fields of the Circum-Pacific island arcs. Granitic intrusives are found in the northwestern part of the Upland.

Quaternary and Surficial Deposits

Outcrops of quarternary basalts are present in several localities in the Tanacross Quadrangles. Those occurrences are adjacent to the northeast-trending faults.

Glaciation in the interior Alaska may have been initiated in the late Miocene or Pliocene time. Both Illinoian and Wisconsin glaciations have deposited glaciofluvial sediments on the flood plains of the Tanana, Delta, and Tok River. As a result of the glacial deposits and the southerly winds,

large quantities of silts from the flood plains were deposited as loess on the north sides of the rivers.

During Holocene time, tributary streams in the Upland started a new erosion cycle. The glacial deposits are being reworked by the main streams and colluvial deposits are developing in the area. During Wisconsinan time, the 32°F isotherm may have reached a depth of 1200 ft. in the Yukon-Tanana Upland. During the last 2000 to 3000 years, a warming weather has initiated a long term thawing cycle. Currently, south-facing slopes are generally free of permafrost and the permafrost exists on north-facing slopes and valley floor covered by vegetation.

REGIONAL STRUCTURE

The regional geological structure is dominated by two arcuate lineaments (Figure 4). These are the Denali fault in the Alaska Range and the Tintina fault on the north. The Denali fault is continuous with the Shakwak lineament in Canada. The Tintina fault has been extended into eastern Interior Alaska from Canada. Both of these lineaments are strike-slip faults with large right-lateral displacement. There may have been 40 miles of offset along the Tintina fault in Paleozoic time, with an additional 220 miles of offset during the Mesozoic era. A right lateral offset of 250 miles along the Denali fault since late Cretaceous time has been documented. Lode deposits in the Fairbanks gold belt are dominantly fissure or fault controlled. The occurrence of gold bearing quartz veins extends northeast from Ester Dome to Pedro Dome and the Cleary Summit area.

The Yukon-Tanana Upland is on the Tanana Geoanticline, the largest of three major geoanticlines developed during the early Cretaceous orogeny.

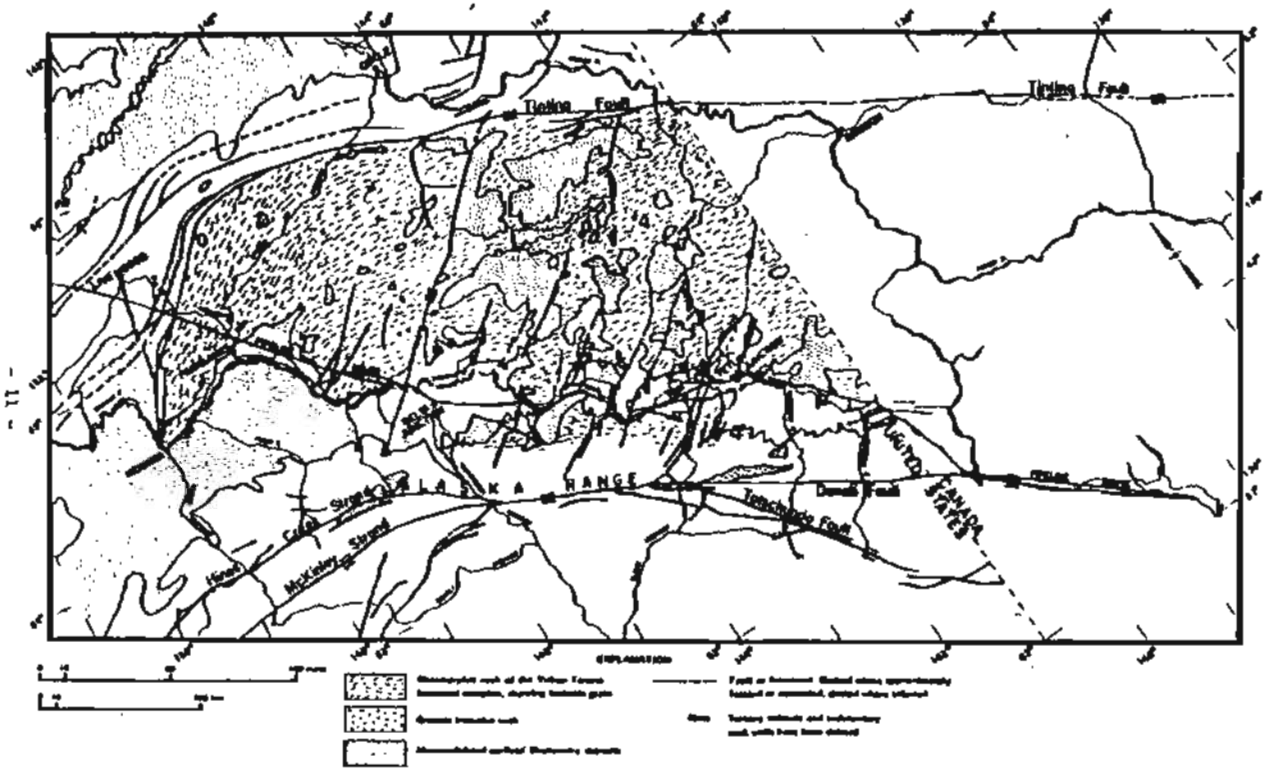

Figure 4. Geological structure map of the Yukon-Tanana Upland (Forbes, 1982).

During the Cretaceous period, detritus from the Tanana Geoanticline was deposited in the Kuskokwim Geosyncline to the north and the Alaska Range Geosyncline to the south. These troughs were uplifted and deformed during the late Cretaceous and Tertiary age.

SEISMIC REFRACTION

The first seismic refraction was introduced for oil exploration in 1923. Since then, it is widely applied as a reconnaissance tool in newly explored areas. Refraction is particularly useful where the surface of a high-wave-speed layer, such as the top of a bedrock, is a target of prospecting interest. For problems concerning the determination of the depth, dip and type of a sedimentary formation, refractive seismology can be a highly effective and economical approach for achieving this objective. Under favorable circumstances this technique can also be used to detect and estimate the throw of a subsurface structure or an irregular buried channel bottom.

THEORY

Time - Distance Relationship

Seismic waves travel down-ward to the subsurface layers from the energy source along slant paths, approach the layers at the critical angles, and return to the surface along the critical-angle paths are regarded as refraction. The physical mechanism involved in this type of wave propagation can be best illustrated using the hypothetical subsurface formations with uniform properties within each layer. The upper layer is separated from the lower by a horizontal boundary at depth z (Figure 5). The velocities of seismic waver within both media are V_0 and V_1 respectively. The seismic wave is generated at point A on the surface and a set of geophones are located at point D at a distance X from A.

When the wavefronts strike the boundary where the wave velocity changes, the energy will be refracted into the lower medium according to Snell's law:

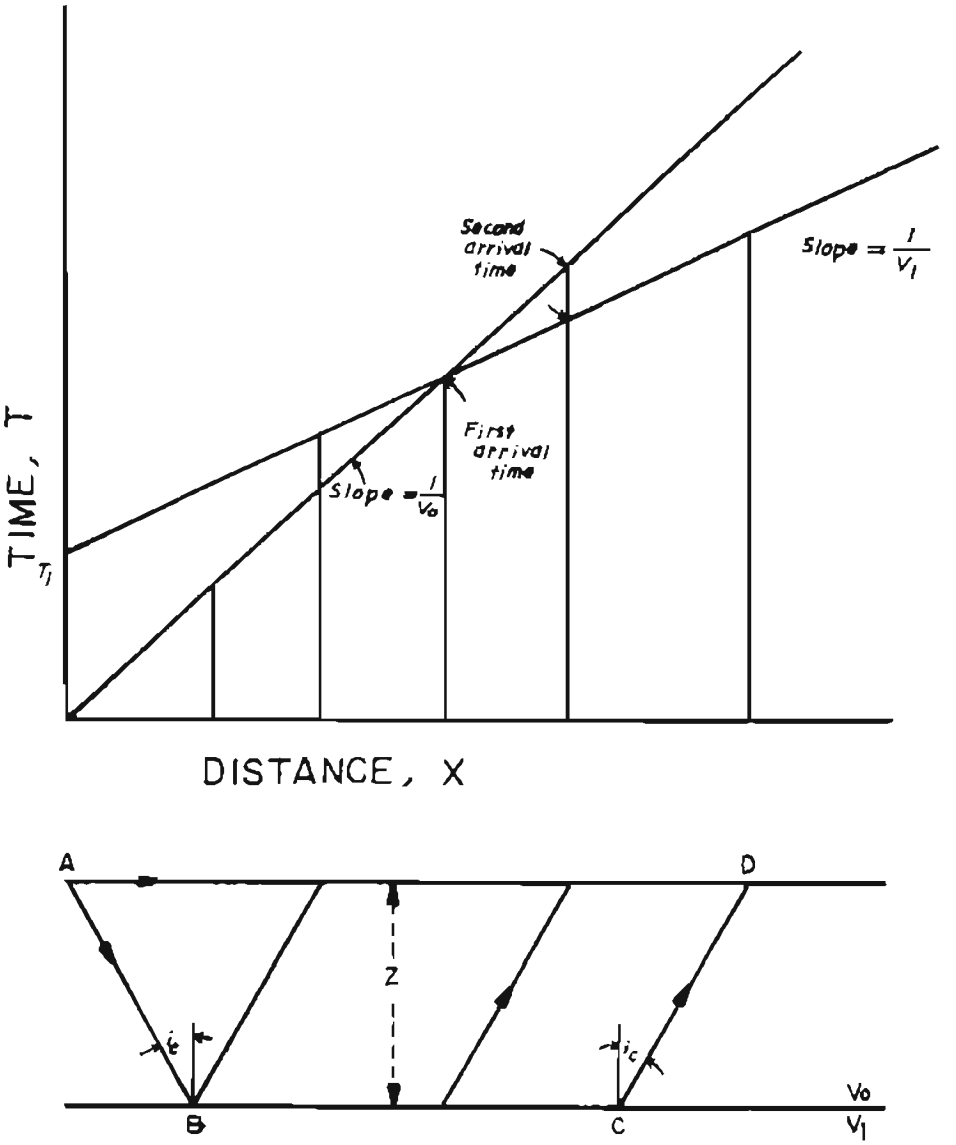

Figure 5. Seismic wave paths of the least time and time–distance curve for a two layer structure.

$$\text{Sini}_c = V_o/V_1 \qquad \text{(Eq. 1)}$$

If the geophones - energy distance is small, the first arrival wave to the geophone will be the one that travels horizontally at a speed V_0. At greater distance, the wave that takes an indirect refraction path, traveling down to, along, and up from the interface, will arrive first because of the time gained in travel through the higher-speed medium. In the case of a subsurface consisting of discrete homogeneous layers, the simplest and most useful way to interpret refraction data is to plot the first arrival time (T) versus the geophone - energy distance (X).

To determine the arrival time along the refraction path in terms of horizontal distance, the total travel-time is:

$$T = X/V_1 + [2Z(V_1^2-V_o^2)^{0.5}/(V_1\ V_o)] \qquad \text{(Eq. 2)}$$

On the T vs. X plot, slopes of the two line segments are the inversed velocities ($1/V_0$ and $1/V_1$) of top and bottom layers. The upper line intercepts the lower line at the crossover distance (X_{cross}) and the time axis at a time (T_i):

$$T_i = 2Z(V_1^2-V_o^2)^{0.5}/(V_1\ V_o) \qquad \text{(Eq. 3)}$$

The depth to the interface can be calculated from the Equation 2 or 3 or from the crossover distance. It is

$$Z = (T_i/2)[V_1V_o/(V_1^2-V_o^2)^{0.5}] \qquad \text{(Eq. 4)}$$

or $$Z = 0.5[(V_1-V_o)/(V_1 + V_o)]X_{cross} \quad \text{(Eq. 5)}$$

For cases with three or more layers, the calculations for velocity, depth to the bedrock and thickness of each stratum are similar but more complicated. The seismic microcomputer program capable of solving problems with up to ten formations was developed to perform this type of tasks.

Dipping Beds

The natural placer deposits are usually not horizontal. The dip angle ( ) of refractor can be determined from the time-distance data (Figure 6). If the perpendicular distance (Z_d) from the shot to the refractor at the end of the survey line at which one shoots downdip, the total travel time (T_d) from the energy to geophone is:

$$T_d = 2Z_d \, Cosi_c/V_o + (X/V_o) \, Sin(i_c + \theta) \quad \text{(Eq. 6)}$$

Similarly, the time (T_u) for shooting updip is

$$T_u = 2Z_u \, Cosi_c/V_o + (X/V_o) \, Sin \, (i_c - \theta) \quad \text{(Eq. 7)}$$

where the Z_u is the perpendicular distance at the end of a survey line from which the wave refracted updip.

Since the respective slopes of the upper line segments for both sets on the time - distance plot are not the same, the true velocity of the lower layer cannot be calculated directly. To obtain the velocity of the lower layer and the dip angle of the refractor, the slope (m_d) of the downdip line segment and the slope (m_u) of the updip line should be combined. It yields:

$$i_c = 0.5 \, (Sin^{-1} \, V_o \, M_d + Sin^{-1} \, V_o \, M_u) \quad \text{(Eq. 8)}$$

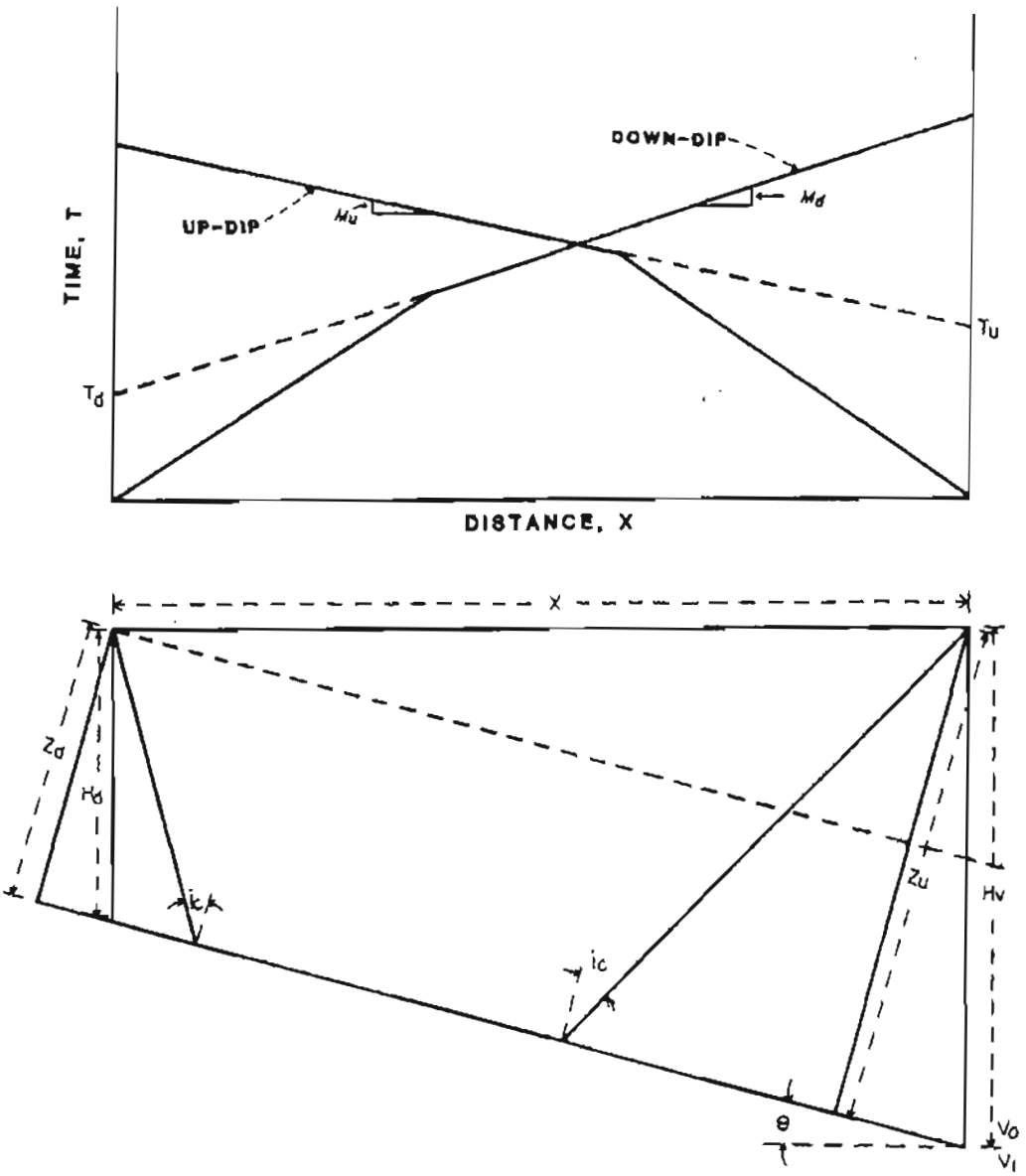

Figure 6. Seismic refraction along a dipping bed. Respective shots are at updip and downdip ends of survey line.

and the dip angle of refractor is:

$$\theta = 0.5\ (\mathrm{Sin}^{-1}\ V_o\ M_d - \mathrm{Sin}^{-1}\ V_o\ M_u) \qquad \text{(Eq. 9)}$$

With the determination of i_c, the velocity of lower formation can be computed from the Snell's low. The perpendicular distance Z_u and Z_d are calculated from the intercept time T_u and T_d:

$$Z_u = (V_o\ T_u)/(2\ \mathrm{Cos}i_c) \qquad \text{(Eq. 10)}$$

and

$$Z_d = (V_o\ T_d)/(2\ \mathrm{Cos}i_c) \qquad \text{(Eq. 11)}$$

The mathematical calculations for determining dips and depths of geological layers used in the computer program were adopted from Mota (1954). Figure 7 shows the geometry and ray paths for a n-layer case. The depth of the refractor at both shot points is given by:

$$H_n = (1/\mathrm{Cos}\,\theta_n)\left[\sum_{i=1}^{n-1} Z_{n,\,i}\ \mathrm{Cos}\ (\alpha_{n,\,i} - \theta_n + \theta_i)/\mathrm{Cos}\,\alpha_{n,i}\right] \qquad \text{(Eq. 12)}$$

and

$$h_n = (1/\mathrm{Cos}\theta_n)\left[\sum_{i=1}^{n-1} Z_{n,i}\ \mathrm{Cos}\ (\beta_{n,i} + \theta_n - \theta_i)/\mathrm{Cos}\beta_{n,i}\right] \qquad \text{(Eq. 13)}$$

The dip angle of the nth refractor is θ_n which can be determined with the angles made by the wave refracted along the previous interface and the dip angle of the (n-1)th layer. From this, the θ_n is

$$\theta_n = 0.5(\gamma_{n-1} - \alpha_{n,n-1}) + \theta_{n-1} \qquad \text{(Eq. 14)}$$

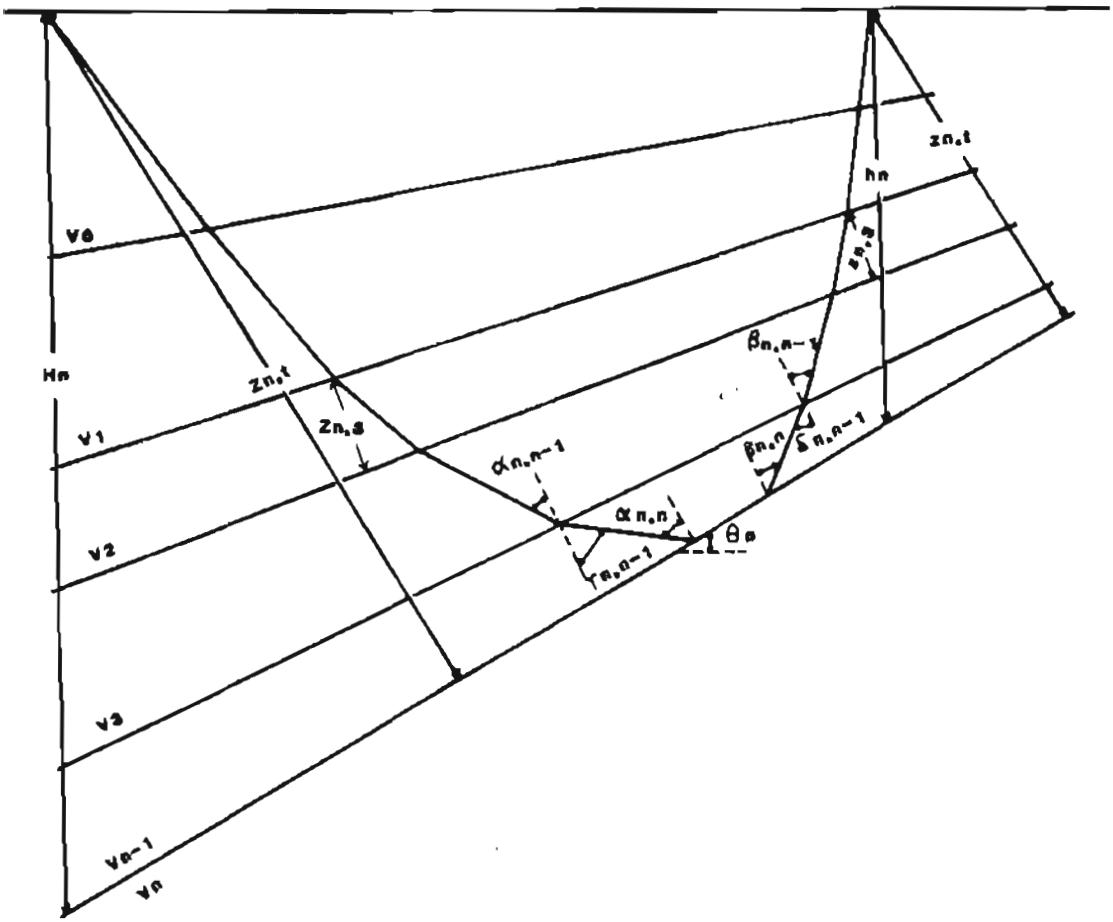

Figure 7. Refraction along the nth dipping layer (after Mota, 1954).

Thickness of the mth layers measured where the wave travels through to the nth interface is expressed as below:

$$Z^{n,m} = Z^{n-1,m} + [(Z_{n-1,1}\,\mathrm{Tan}\,\theta_{n-1,1} - Z_{n,1}\,\mathrm{Tan}\ n,1)$$
$$[\mathrm{Cos}(\theta_2-\theta_1) \ldots \mathrm{Cos}\ (\theta_{m-1} - \theta_{m-2})] + (Z_{n-1,2}\,\mathrm{Tan}_{\alpha}\ n-1,2$$
$$-Z_{n,2}\,\mathrm{Tan}_{\alpha}\ n,2)[\mathrm{Cos}(\theta_3-\theta_2) \ldots \mathrm{Cos}\ (\theta_{m-1} - \theta_{m-2})]$$
$$+\ldots+ (Z_{n-1,\,m-1}\,\mathrm{Tan}\,\alpha_{n-1,\,m-1} - Z_{n,\,m-1}\,\mathrm{Tan}_{\alpha}\ n,m-1)]\ \mathrm{Sin}\,\theta_{n-\theta\ m-1})$$

(Eq. 15)

Refraction Across a Subsurface Structure

As a subsurface structure, if a fault or buried river channel occurs along a survey line, the upper line segment of the time-distance diagram will be offset (Figures 8A and 8B). The amount of throw (Z_t) can be determined from the difference ($T_{i2}-T_{i1}$) of the intercept times corresponding to the offset lines. It is:

$$Z_t = (T_{i2} - T_{i1})[(V_1 + V_o)/(V_1-V_2)]^{0.5} \qquad \text{(Eq. 16)}$$

The value of Z_t can be positive or negative depending upon where the shot locates. It is a positive value when the shot is on the upthrown side of the structure.

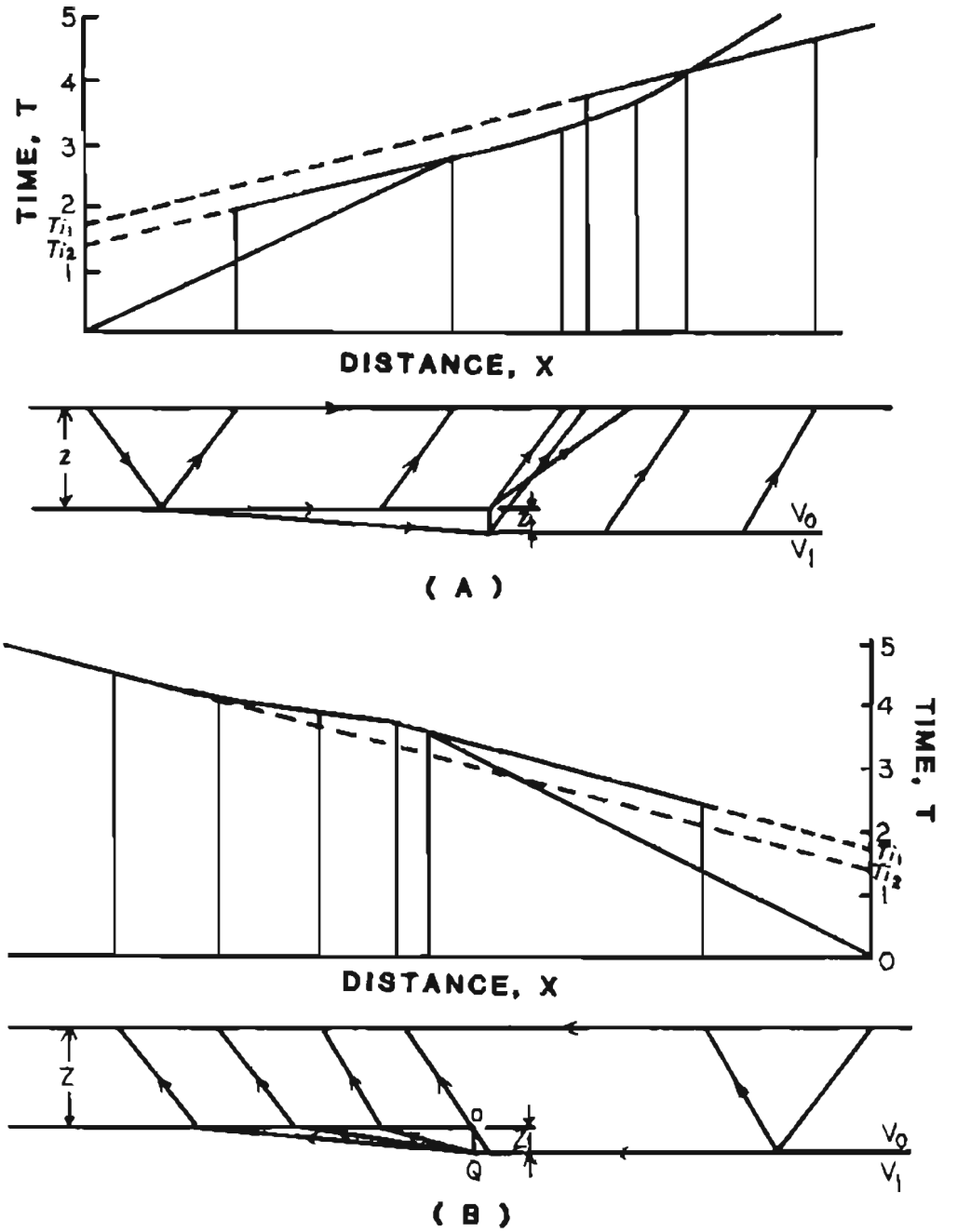

Figure 8. Refraction across a subsurface structure. (A) Shot at up-thrown side, (B) shot at down-thrown side.

Topography Correction

Refraction data must be corrected for elevation. The correction removes differences in travel times due to irregular topographic surface. The most commonly used procedure for this correction is to place both shot and geophones on the same reference plane. It is done by subtracting the times that are required for the waves to propagate from the shot or geophones to the datum plane. Figure 9 illustrates the correction procedures. The delay time associated with topographic variation (ΔT_e) is:

$$\Delta T_e = (h + g - 2d)(V_n^2 - V_o^2)^{0.5}/(V_n V_o) \qquad \text{(Eq. 17)}$$

The delay time should be subtracted from the observed travel time for each geophone in order to place both energy source and detector on the same reference plane.

ROUTINE FIELD PROCEDURES

Since the possibility exists that a prospector may use refraction seismology for determining the depth to gold bearing deposit, a brief description of the routine field survey procedures are summarized.

Before laying out and making the actual seismic survey, a certain amount of planning should be prepared, which involves the following considerations:

1. Length of survey line - The maximum survey distance should be 3 to 5 times the desired depth of investigation. For placer exploration in the Fairbanks mining district, the distance of geophone spread is recommended to be at least 200 to 600 ft. The distance varies depending upon the location of the survey.

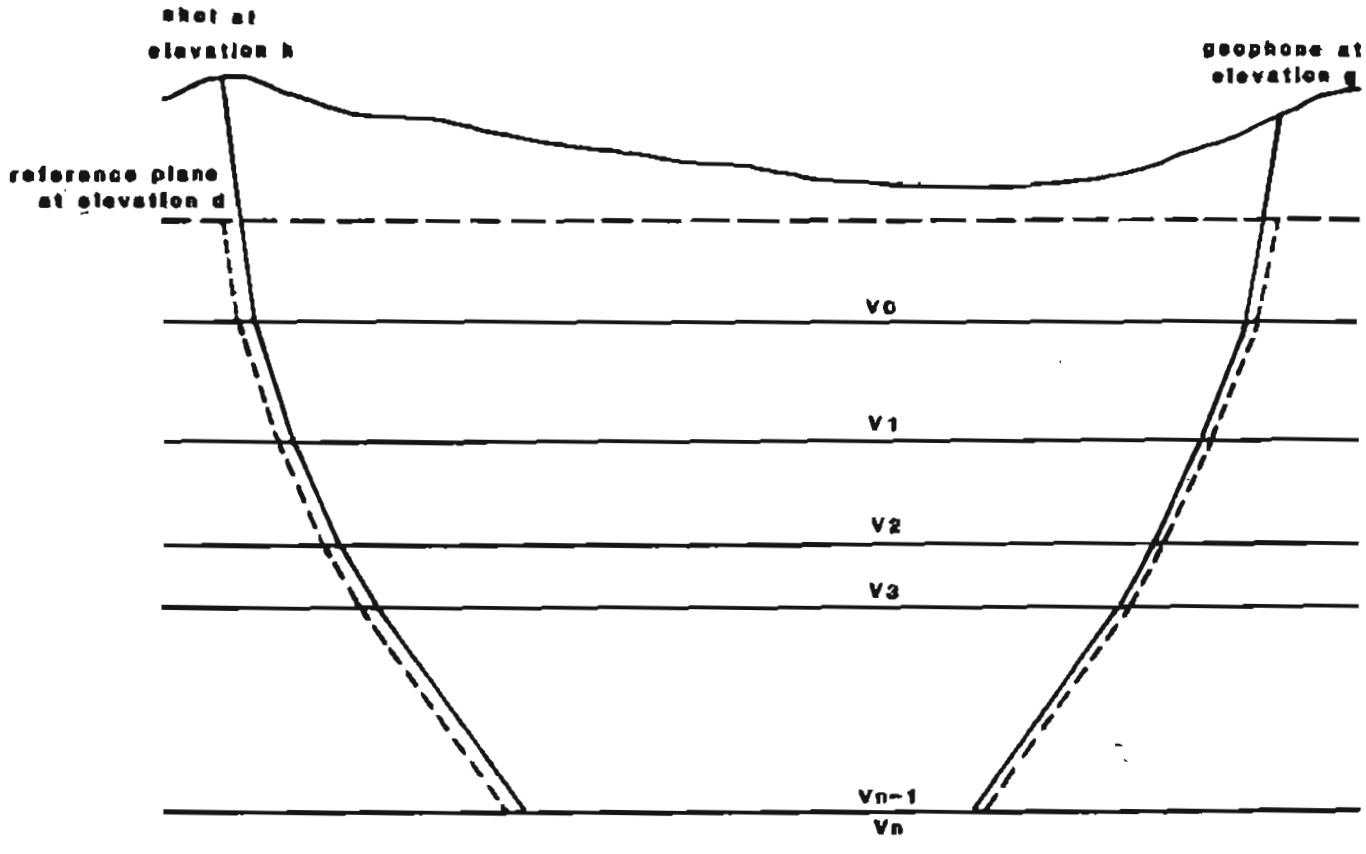

Figure 9. Correction of refraction times for elevation.

2. Location of survey line - The line should be centered at the position where depth information is required and oriented in any convenient direction. Although effects of topographic irregularities can be corrected, it is more convenient to avoid them than to process the data later.
3. Spacing of geophones - Spacing between geophones should be selected to provide sufficient quantity of data to adequately determine the velocity of each formation. When starting a traverse in an unknown area, it is adequate to separate geophone stations by about one-half the desired depth of investigation. Equal spacing is convenient but not essential. Smaller intervals can be used as the geophone is close to the shotpoint.

After laying out the survey line and the field equipment, the actual survey should proceed with care. All vibrations must be kept to a minimum as the readings are being taken. The highly sensitive transducer of the geophone will respond to footsteps, distant machinery and traffic.

MICROCOMPUTER ANALYSIS

SEISMIC, the computer program for processing the refraction data, was written in Microsoft BASIC (MBASIC) language. The MBASIC is one of the most popular software languages used in microcomputer industry. With a small modification of the SEISMIC program listed in Appendix A, it should be able to run on many different microcomputers. An example problem with the input and output information is listed in the Appendix A for illustration.

Functions of the program include calculations of wave velocity of material, thickness and depth of a subsurface formation, and dip angle of a refractor. In addition, the location of a possible subsurface structure can be estimated. The software package consists of seven major segments which include plotting routine, statistical analysis, topography correction, dip angle and thickness calculation, and input and output statements. Figure 10 illustrates the flowchart of the program. The calculation procedures used in this program are similar to those discussed in the previous section.

Since it was programmed in a user friendly mode, the prospector who uses this package should be able to run the program without difficulty. Due to the limitation of CPU memory and processing speed of a microcomputer, the user should be aware of the capacity of the program. The input-output sequence and the restrictions of the program are discussed as follows:

1. As the program is run, the first message shown on the monitor and printer is:

```
**************************
*                        *
*   SEISMIC REFRACTION   *
*                        *
**************************
```

PROBLEM —

Type the title of the study into computer. The maximum length of title is 80 characters.

2. The second information on the monitor is:

REVERSE SHOOTING (Y/N)?

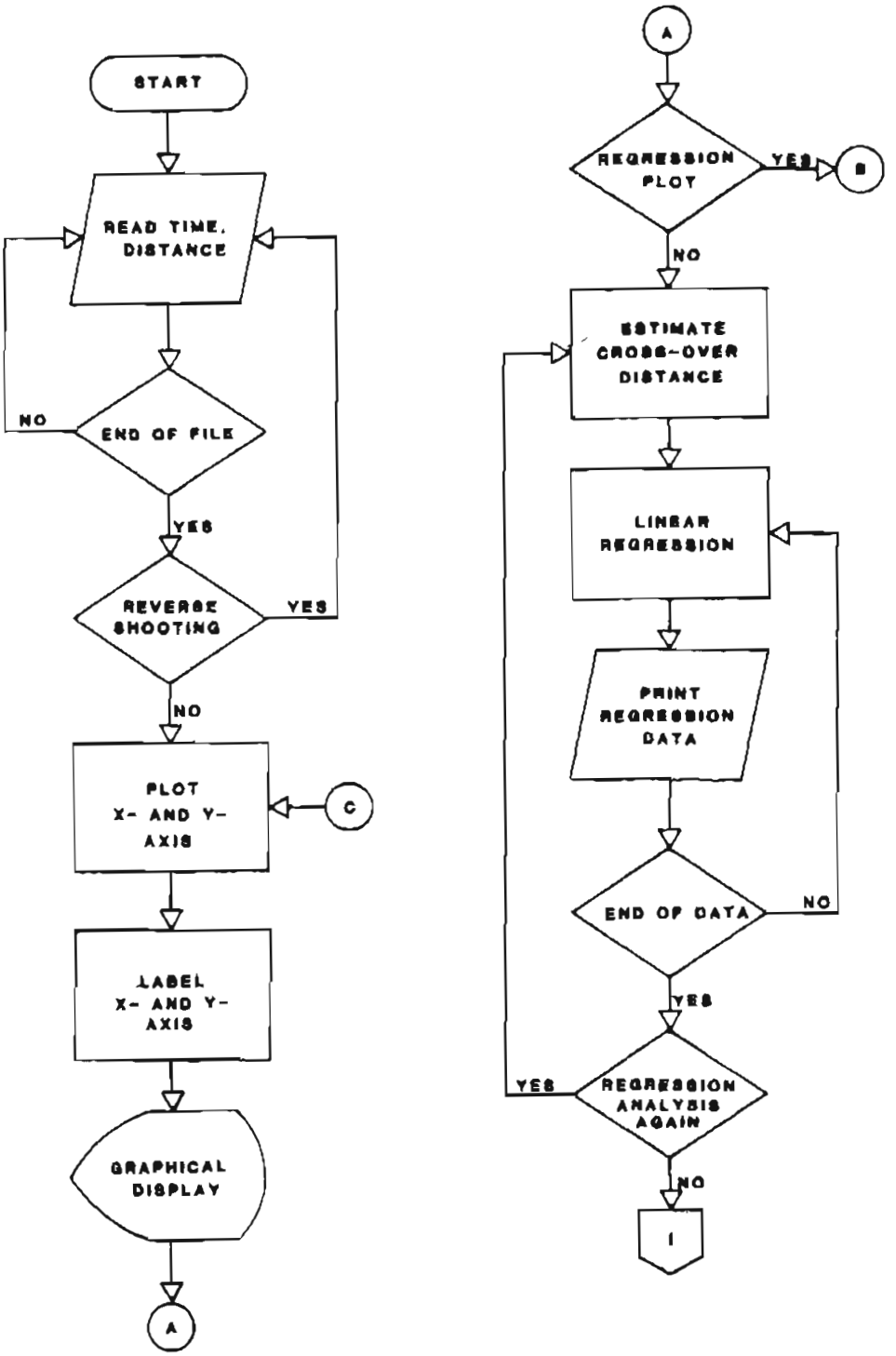

Figure 10. Flow chart of the SEISMIC microcomputer program.

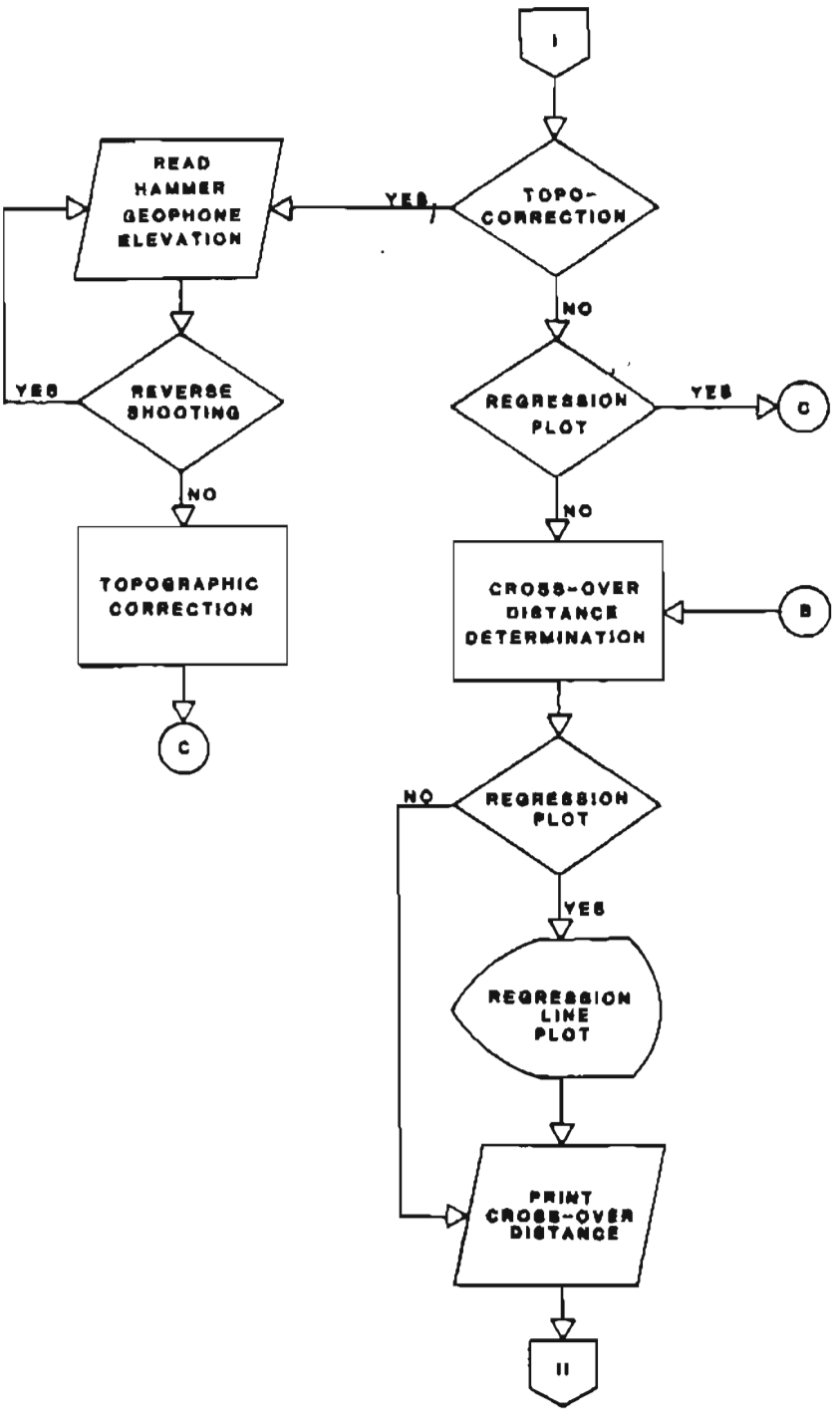

Figure 10. Flow chart of the SEISMIC microcomputer program (cont'd).

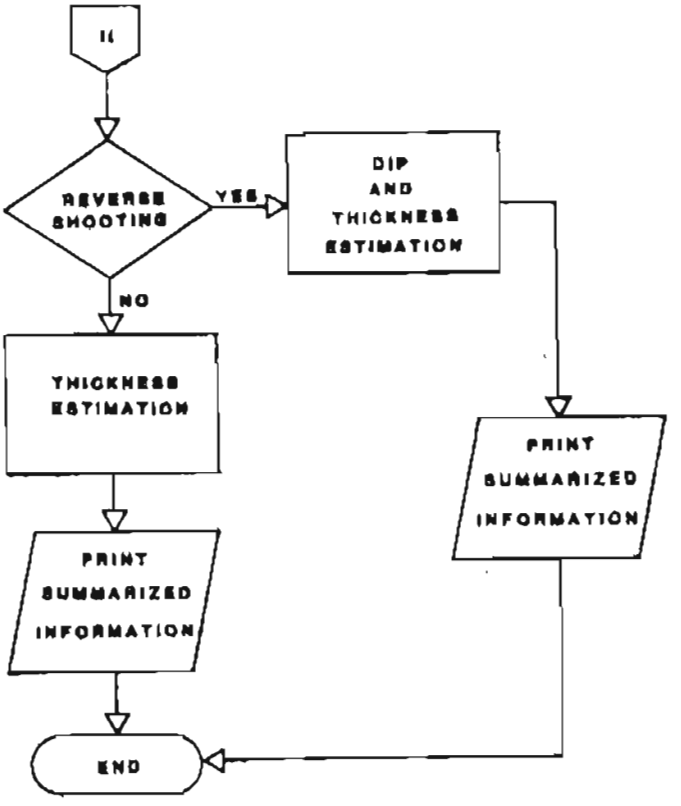

Figure 10. Flow chart of the SEISMIC microcomputer program (cont'd).

If the field work contains shotpoints at the two ends of the survey line, then type "Y" otherwise type "N".

3. The following message will be on the monitor and printer:

*** FORWARD SHOOTING ***

INPUT -1 FOR TIME AND -1 FOR DISTANCE WHEN COMPLETE

TIME (mSec) DISTANCE (Ft)

A similar message for reverse shooting will prompt if the previous question is answered as "Y".

4. The field data, travel time and shot-geophone distance, should be input according to the above instruction. The travel time in msec, should be typed in first then input the geophone-shot distance in ft. When the last set of data is typed, input -1 for both time and distance to terminate this statement. Maximum number of data points is limited to 50. However, with small change of the DIM statement in the main program the size of data points can be increased accordingly. Same input procedures are applied to the reverse shooting.

5. Upon completion of input statement, monitor and printer will show a time-distance diagram (Figures 11A and B) for one directional shooting or forward-and-reverse shooting.

6. Following the graphic display the message on monitor and printer will be:

REGRESSION ANALYSIS — TRIAL # 1

7. Then the monitor alone will indicate a clearing screen message:

TYPE-IN 26 TO CLEAR THE SCREEN

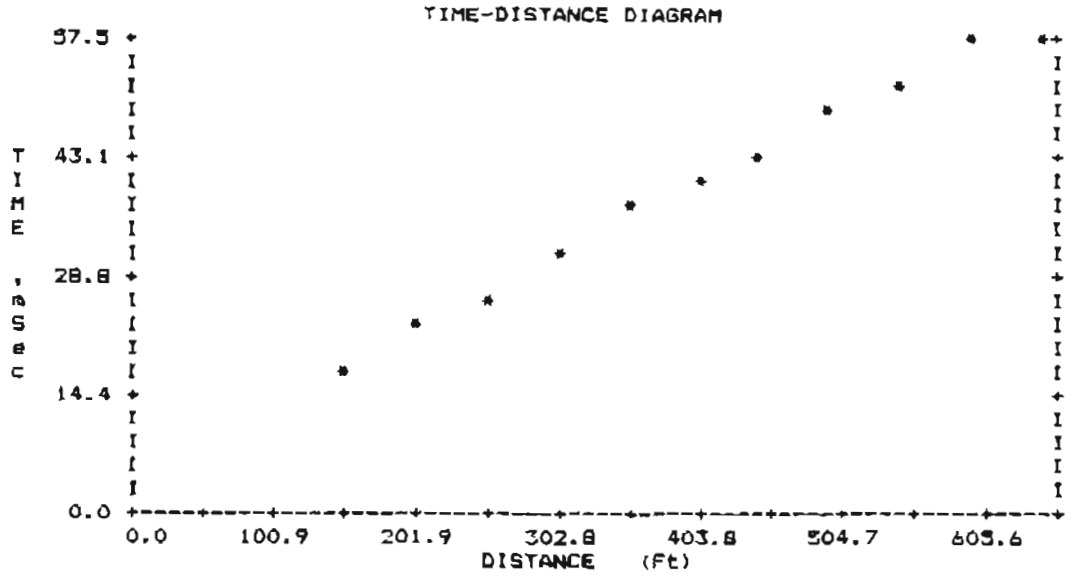

(A)

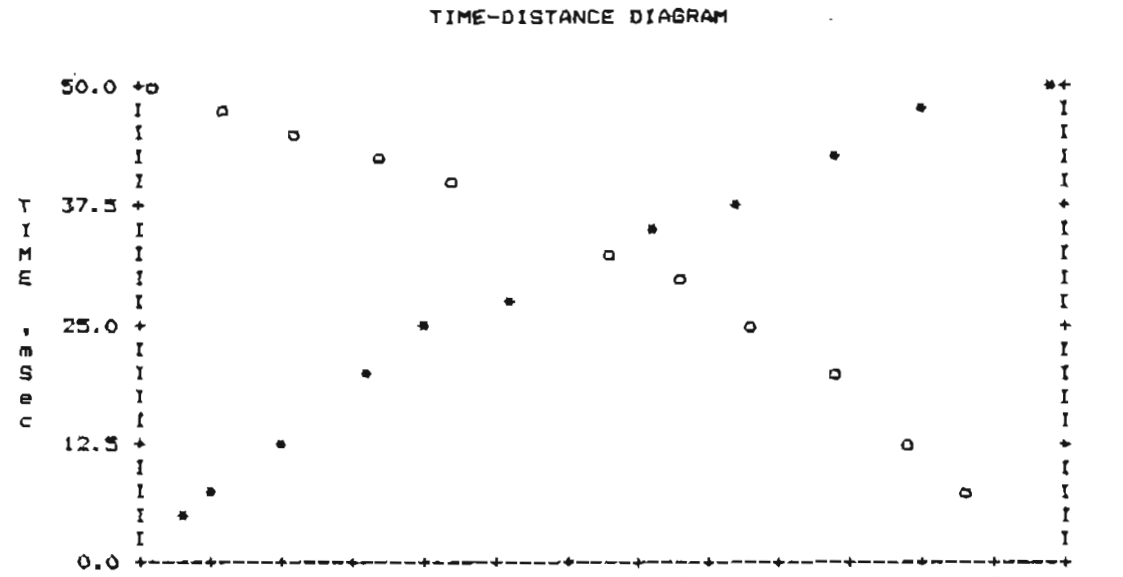

(B)

Figure 11. Computer output of the time - distance plot. (A) One directional survey, (B) two directional survey.

Input 26 will clear the monitor screen. Any number less than 127 will not affect the display. Numbers beyond 127 will cause syntax error.

8. Following the screen clearing action are several messages concerning estimations of cross-over distance:

```
ESTIMATE 1ST, 2ND, ...., 10TH CROSS-OVER DISTANCE
COMPLETE FORWARD SHOOTING FIRST
THEN REVERSE SHOOTING IF AVAILABLE


INPUT THE MAXIMUM DISTANCE WHEN FINISH
```

9. Estimate the cross-over distance (X_{cross}) from the time-distance diagram and input accordingly. Computer will repeat the following statements until the total survey distance is reached. Similar statements will be shown if reverse shooting is required.

```
INPUT CROSS-OVER DISTANCE FOR FORWARD SHOOTING

CROSS-OVER DISTANCE # 1          (Ft)
```

10. When the estimated cross-over distance is read, computer will excute the statistical routine and generate a series of output as follows:

```
*** FORWARD SHOOTING ***

REGRESSION EQUATION FOR #  1  LAYER (Y IN mSec & X IN Ft)
Y = a1 * X + b1
CORRELATION COEFFICIENT IS r1
VELOCITY (Ft/Sec) = v1
```

The values of a1, b1, r1 and v1 are computed for each line segment on the time-distance plot. The regression analysis repeats for reverse shooting if asked.

11. The regression analysis can be continued if the correlation coefficient for any line segment is not satisfied. It is done by typing-in "Y" to the following statement:

    TRY REGRESSION AGAIN (Y/N)?

    The answer "Y" will transfer the control back to step 5 and repeat steps 5 - 11 again. If the answer is "N", then computer will move to the next statement.

12. Topography correction subroutine will be activated by answering "Y" to the following statement:

    ELEVATION CORRECTION (Y/N)?

    The step 13 will be skipped if elevation correction is not desired.

13. Topography correction requires information as such:

    SELECT DATUM PLANE ELEVATION (Ft):

    FORWARD SHOOTING

    ENERGY SOURCE ELEVATION (Ft):

    INPUT GEOPHONE ELEVATION (Ft) FOR
    TOPOGRAPHIC CORRECTION
    GEOPHONE STATION:
    GEOPHONE STATION:

    Elevation of the reference plane should be properly decided for the forward shooting and the reverse shooting. There is only one datum plane needed for each analysis. Elevations of shotpoint and geophone stations should be input sequentially. If two directional shootings are conducted, similar statements will appear for inputing data for reverse

shooting. Computer will automatically return control to step 5 and generate a similar time-distance diagram as shown in Figure 11.

14. The last input statement concerns the choice of a regression line plot on the monitor. It is:

    REGRESSION LINE PLOT (Y/N)?

    Due to the size limitation of monitor screen, the resolution of line plot is inadequate. Also, this statement is only workable on the monitor screen. The hardcopy printer will generate identical diagram as shown in Figure 11.

15. After all the previous 14 steps are performed, program will determine the cross-over distance. It yields similar output as follows for the forward shooting and the reverse shooting:

    CROSS-OVER DISTANCE DETERMINATION

    *** FORWARD SHOOTING ***

    NO # 1 CROSS-OVER DISTANCE (Ft) =

    NO # 2 CROSS-OVER DISTANCE (Ft) =

16. The final information of each subsurface layer will be displayed in the following form for one directional shooting:

    *** SUMMARIZED INFORMATION ***

    LAYER # 1
    VELOCITY (Ft/Sec) =
    THICKNESS OF BED (Ft) =
    DEPTH OF BED (Ft) =

    LAYER # 2
    VELOCITY (Ft/Sec) =
    THICKNESS OF BED (Ft) =
    DEPTH OF BED (Ft) =

or as follows for two directional shooting:

```
        *** SUMMARIZED INFORMATION ***

LAYER #  1
VELOCITY (Ft/Sec) =
DIP OF NO.  1  REFRACTOR (Degree) =
THICKNESS OF BED AT STARTING POINT (Ft) =
THICKNESS OF BED AT ENDING POINT (Ft) =
DEPTH OF BED AT STARTING POINT (Ft) =
DEPTH OF BED AT ENDING POINT (Ft) =

LAYER #  2
VELOCITY (Ft/Sec) =
DIP OF NO.  2  REFRACTOR (Degree) =
THICKNESS OF BED AT STARTING POINT (Ft) =
THICKNESS OF BED AT ENDING POINT (Ft) =
DEPTH OF BED AT STARTING POINT (Ft) =
DEPTH OF BED AT ENDING POINT (Ft) =
```

Additional information such as the possible location of subsurface structure and the amount of throw will be displayed when the line segments are offset and parallel to each other. This process is automatic when two adjacent linear lines have a difference of slopes less than or equal to 0.0001. Also, a message of low velocity zone below a high velocity zone will be prompted when the slope of any given line segment on time-distance diagram is greater than that of the previous line.

CASE STUDIES

Two seismic refraction surveys were conducted in order to obtain the basic physical properties of placer deposits. One survey was performed in an area where little exploration has been done. The second field work was carried out on a site where the local geology is well understood. The discussion of these two surveys follows.

Willow Creek Survey

Placer gold mining has been quite successful in the region immediately south of the Chatanika River near Olnes, Alaska, however, little work has been done in the area north of the river. This survey was conducted in an attempt to estimate the depth to bedrock in the Willow Creek area. The site locates about one and three quarter miles north of the Chatanika River (Figure 12).

Local Geology: Detailed geology of this area is not available. The hills surrounding the site, like those in the rest of the region, are composed of Precambrian Birch Creek schist. To the south, there are Mesozoic and Tertiary granitic intrusives, some of which are gold-bearing. The source for the gold in the Olnes area is believed to have been from the south. This is not necessarily true for the sediments north of the Chatanika River.

In the valleys the schist is covered with thick layers of the Quaternary loess and gravels. Typically those deposits are sixty to seventy feet thick south of the Chatanika River.

The overall structure of the region strikes northeast-southwest. There are several large faults in the uplifted region that show thrusting toward the northwest. These thrusts are believed to be caused by the compressional forces from the south.

Survey Procedures: The refraction survey was carried out using twelve geophones at 15 meter (49.2 ft) intervals along a north-south lines. Each shot consisted of approximately 3 pounds of explosive placed in a hole about 3 feet deep. Geophones were frozen into the ground to reduce interference. A 12 channel Geometric/Nimbuk ES-1210 seismograph was used to record the seismic

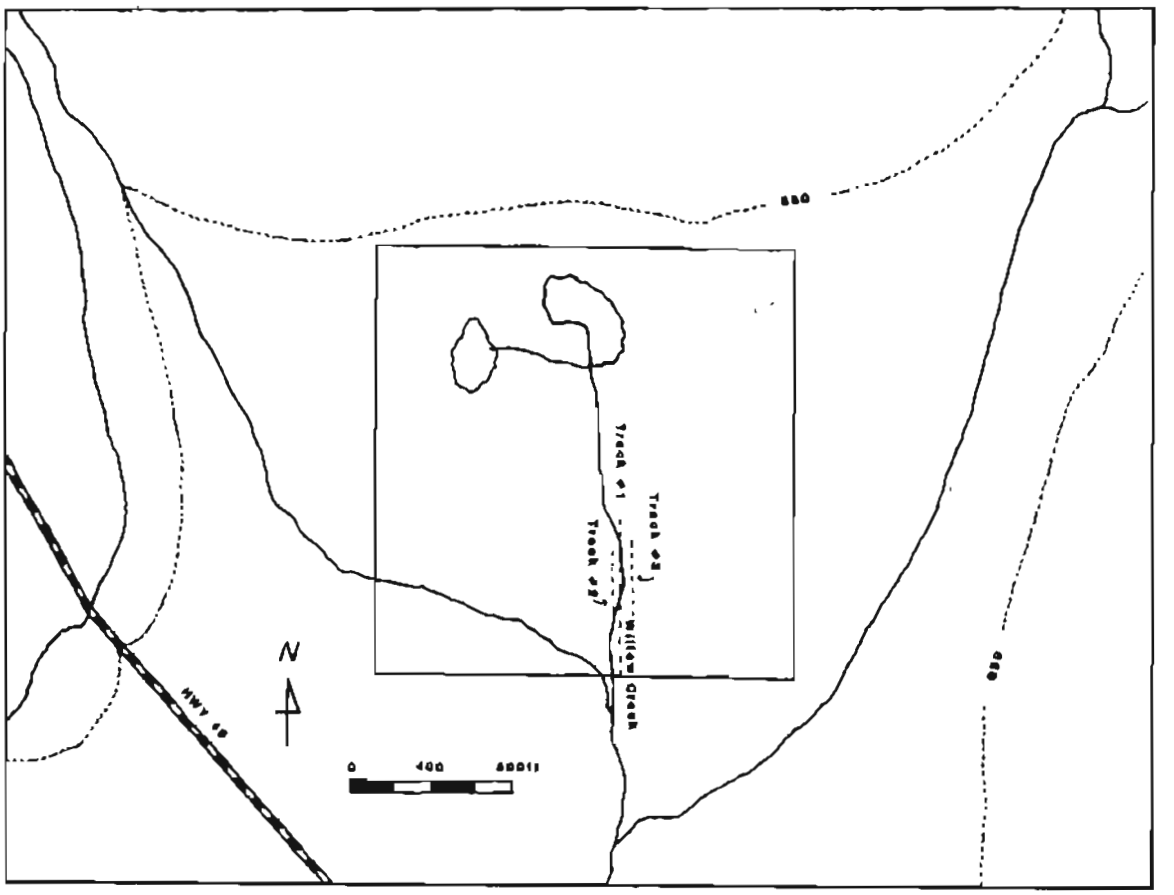

Figure 12. Map showing the site of seismic refraction survey along Willow Creek.

signals. Two directional shootings were conducted along three survey lines (Figures 12).

Results: The shootings produced records with clearly defined first arrival waves. The travel times were determined by selecting the beginning of the first downward, sharp motion peak as the starting points of the first arrival waves. Tables I through III summarize the field data which were used to calculate and interpret the possible subsurface geology of the site. The time-distance plots of those three tracks are shown in Figures 13 to 15. Table IV lists the results from the SEISMIC program. Three sets of data indicate that the bedrock dips toward south. The depth to the schist bedrock varies from one survey line to another. It ranges from approximately 88 to 134 ft. The survey line #1 (the center line) was in general located on top of the buried river channel where the depth is the greatest and the dip of the old river bed is 2.16^{o}. At the north end of the survey line the bedrock inclines slightly toward west which infers the old river channel probably bends to the east. The velocity of bedrock is in the range of about 14000 to 16000 ft/sec. The variation of bedrock velocity may depend upon the weathering of the old channel bed and the river banks.

Overlying the bedrock are layers of silt, sands and gravels with velocity of 10000 ft/sec. The near surface layer has wildly varying thickness. Data from the center survey line indicates the existence of a formation between the top layer and the bedrock. It might be caused by the deposition of the old river. Dip of the boundary between the top layer and the middle layer is 6.33^{o} toward south and it ranges from 63.0 to 68.0 feet in thickness.

Table I. Summary of the time-distance measurements along track 1 at the Willow Creek site.

Southward Shooting		Northward Shooting	
Time (mSec)	Distance (ft)	Time (mSec)	Distance (ft)
15.0	164.0	21.5	229.7
20.63	213.3	26.5	278.9
25.0	264.5	31.25	328.1
30.5	311.7	36.0	377.3
35.0	360.9	39.75	426.5
37.63	410.1	44.0	475.7
42.5	459.3	48.25	524.9
46.25	508.5	51.5	574.1
50.0	557.7	56.0	623.3
55.0	606.9	61.0	672.5
57.5	656.1	63.5	721.7
—	—	66.25	770.9

Table II. Summary of the time-distance measurements along track 2 at the Willow Creek site.

Southward Shooting		Northward Shooting	
Time (mSec)	Distance (ft)	Time (mSec)	Distance (ft)
5.0	53.0	5.5	54.3
8.75	84.7	9.0	87.4
13.75	128.0	13.0	131.0
17.5	174.4	18.5	177.6
21.25	222.1	22.0	225.3
26.25	270.3	27.5	273.5
31.0	318.8	32.0	322.0
35.0	367.5	36.0	370.8
40.0	416.3	41.0	419.6
45.0	465.2	45.5	468.5
47.5	514.2	48.25	517.5
50.62	563.2	51.5	566.5

Table III. Summary of the time-distance measurements along track 3 at the Willow Creek site.

Southward Shooting (S5)		Northward Shooting (S6)	
Time (mSec)	Distance (ft)	Time (mSec)	Distance (ft)
5.0	53.0	5.7	54.3
8.75	84.7	9.5	87.4
11.88	128.0	13.25	131.0
19.38	174.4	18.5	177.6
22.5	222.1	22.5	225.3
27.5	270.3	28.0	273.5
30.0	318.8	32.25	322.0
35.0	367.5	36.5	370.8
40.0	416.3	41.5	419.6
43.75	465.2	44.5	468.5
46.25	514.2	48.0	517.5
50.0	563.2	51.0	566.5

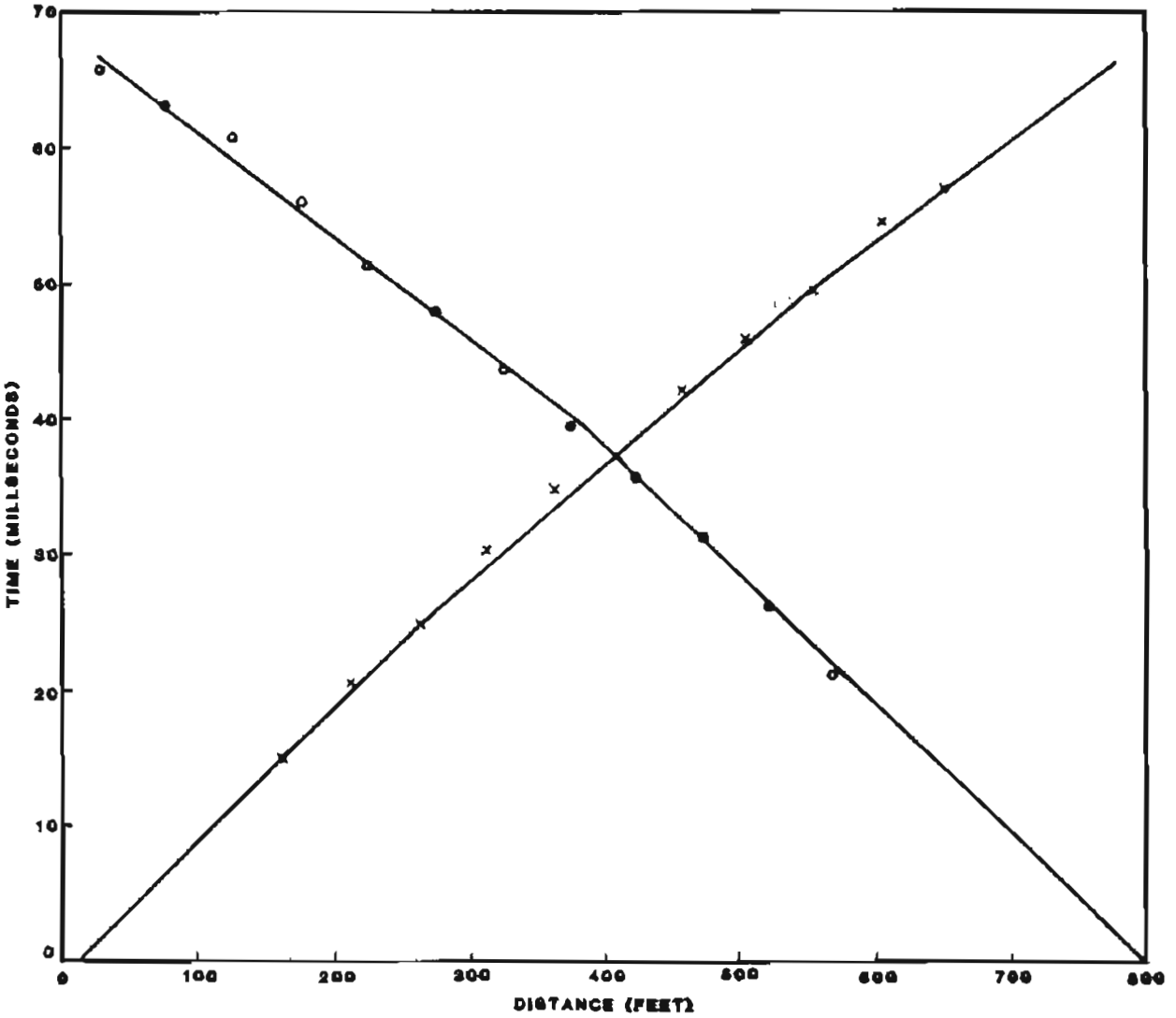

Figure 13. Time - distance diagram of the track 1 at the Willow Creek site.

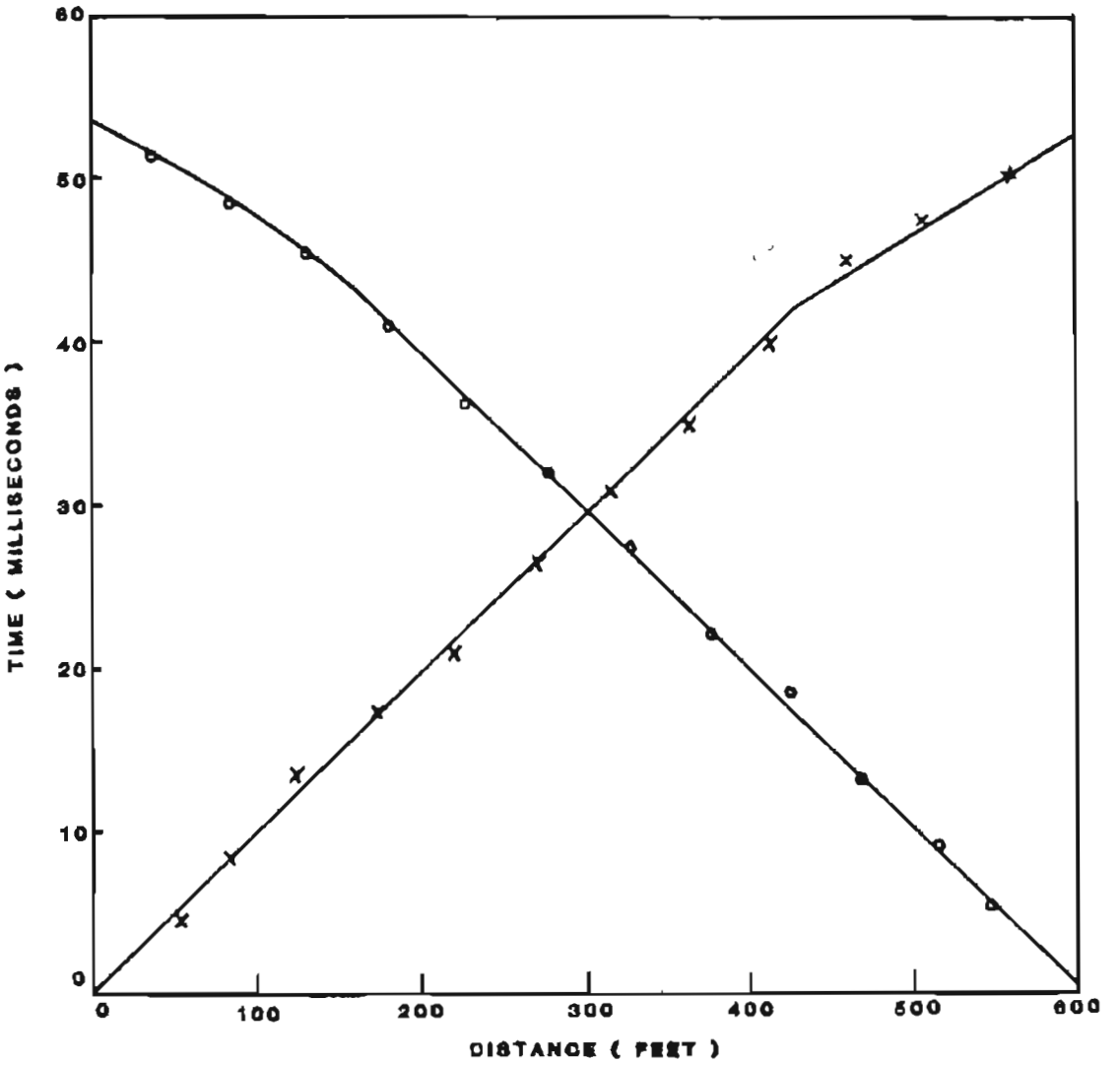

Figure 14. Time - distance diagram of the track 2 at the Willow Creek site.

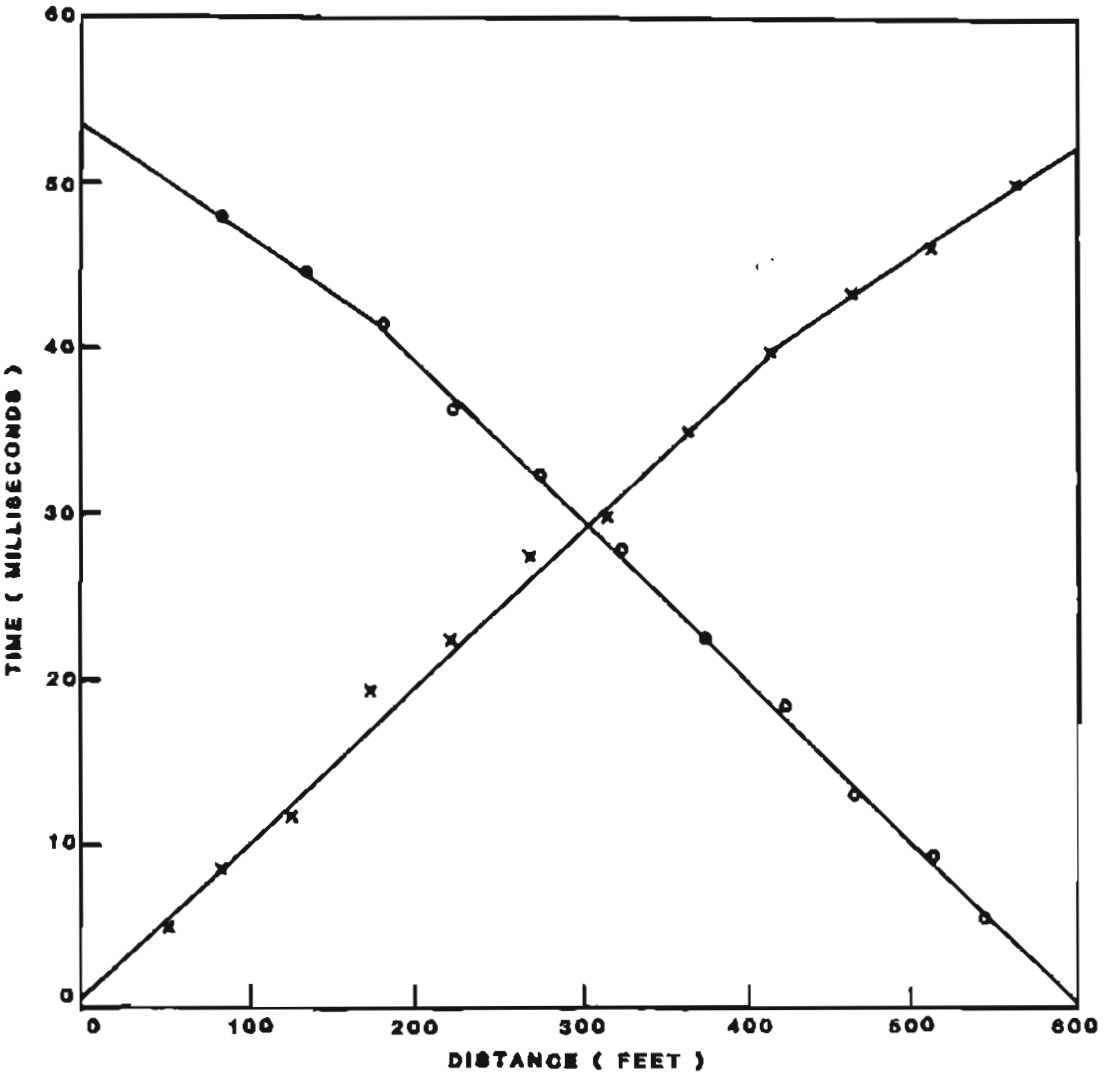

Figure 15. Time - distance of the track 3 at the Willow Creek site.

Table IV. Results of seismic survey at the Willow Creek site.

	Velocity (ft/sec)	Dip	Thickness (N-S, ft)	Depth (N-S, ft)
Set I (Max. spread - 770.9 ft.):				
Layer #1	10284	6.33°S	18.4- 76.7	18.5- 77.1
Layer #2	12135	2.16°S	67.7- 63.2	87.7-134.1
Layer #3	13854	———	———	———
Set II (Max. spread - 566.5 ft.):				
Layer #1	10448	0.98°S	101.7-115.4	101.7-115.4
Layer #2	16011	———	———	———
Set III (Max. spread - 566.5 ft.)				
Layer #1	10385	0.41°S	89.0- 99.9	88.0- 99.9
Layer #2	15184	———	———	———

USA CRREL Tunnel Survey

Placer gold mining was quite active along goldstream at Fox, Alaska. After World War II the industry declined and there is currently no major operation around. The U.S. Army Cold Region Research and Engineering Laboratory (CRREL) permafrost tunnel was cut into a near vertical silt escarpment formed by the old placer operations (Figure 16). Since the excavation several researchers (Sellman, 1967 and Pettibone and Waddell, 1969) have performed a series of studies in the tunnel. The geology of the area is well understood.

Local Geology: The material and types of ground ice are common to many permafrost areas. An idealized geological cross-section of the area is shown in Figure 17 to illustrate the sedimentary formation.

Silt is the dominant constituent of the late pleistocene deposits in the area. The silt sections are as much as 55 to 60 ft thick. Silt samples from the tunnel indicate that 68 percent of the material is within the silt size range. The bulk density of the silt ranges from 78 to 115 pcf and averages 92 pcf, with moisture content between 32 and 139 percent by dry weight. The silt contains a massive ice wedge and small ice lenses. The volume of ground ice accounts 53 to 80 percent.

The early Wisconsin gravels were stream deposits with imbrication of the pebbles, cobbles and sands. Sand and silt lenses of Illinoian age are common in the upper part of the stratified gravels. The average thickness of the gold-bearing formation in the site is around 13 ft. Moisture contents of the gravels range from 8.9 to 10.3 percent by dry weight. Particle size analysis showed that 55 percent of the material is in the gravel range. Although the

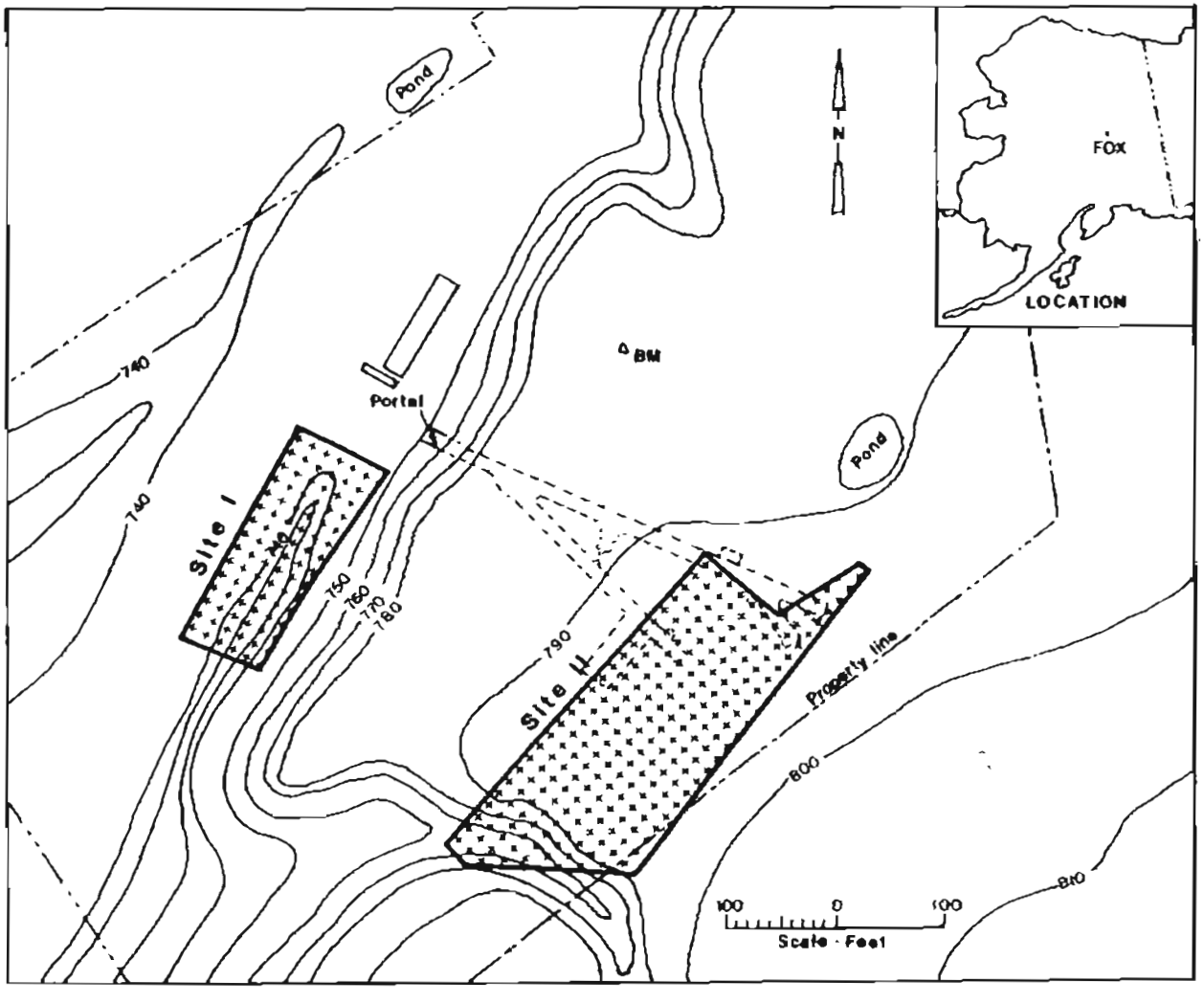

Figure 16. Map showing the seismic survey sites at USA CRREL permafrost tunnel, Fox, Alaska.

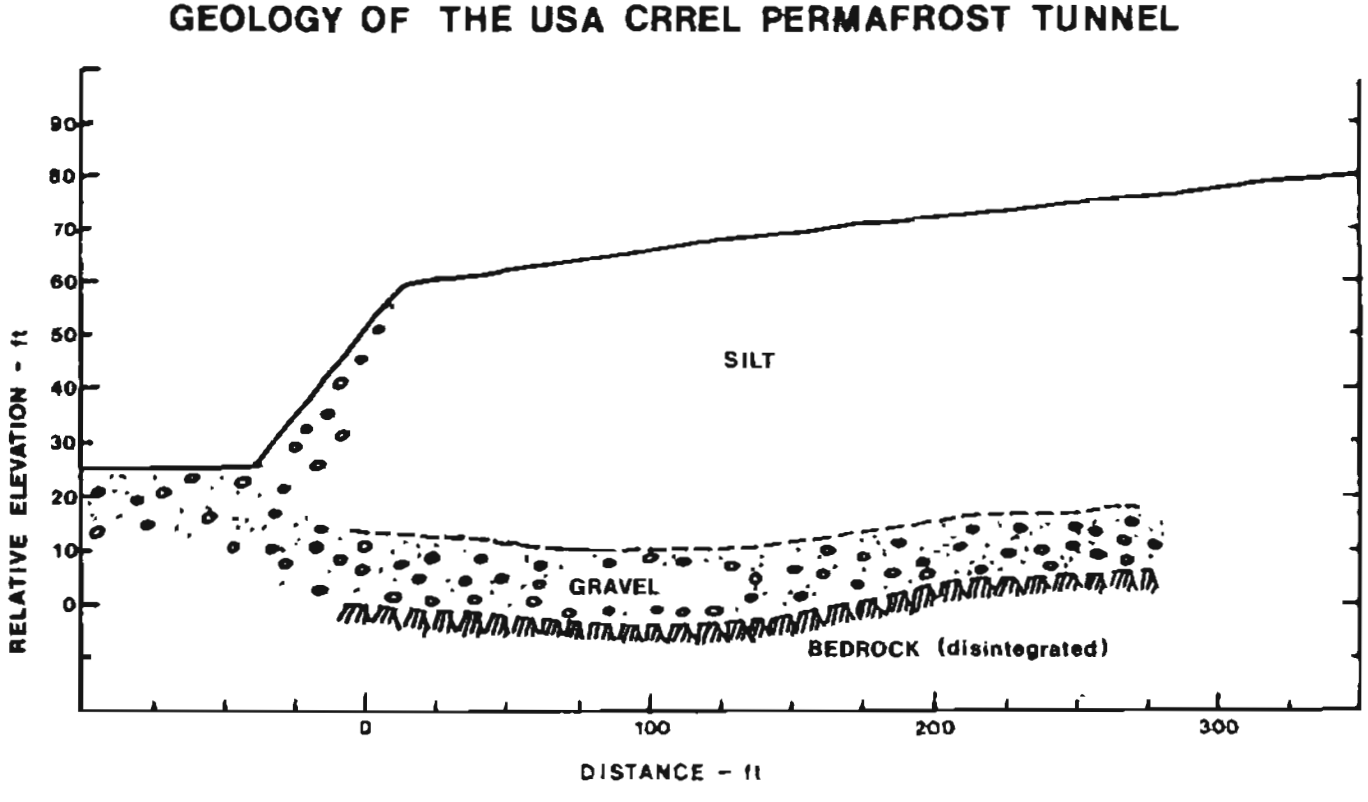

Figure 17. Geology of the USA CRREL permafrost tunnel.

gravel, similar to the silt, is bonded with ice, it does not contain massive ground ice.

The bedrock in the area is the same as that in the Willow Creek area. The Precambrian schist is a gray to brownish quartz mica schist. The gravel-bedrock contact is very irregular. The top surface of the bedrock is highly altered and forms a clay layer. Placer gold usually occurs at this altered zone. Moisture contents of the decomposed bedrock range from 6.5 to 19.9 percent by dry weight and average 11.7 percent.

Survey Procedures: The surveys were conducted at two sites. Site I, near the escarpment, is a deposit of old tailings overlying the schist bedrock. Two 200 ft. survey lines in the northeast-southwest direction and one 100 ft. track perpendicular to the NE-SW lines were superimposed on the ground surface. Unlike site I, site II locates in the permafrost zone. Four 300 ft. survey lines were run along the northeast direction with varied geophone interval depending upon the distance from two end points. The 5- and 10- ft. spacings were used as the survey approached the ends of each survey line. The tundra at site II was stripped to the base of the active layer and the geophones were placed directly in contact with the frozen silt.

A two channel soil test MD-9 signal enhancement seismograph was used with a 15 lb. tamper and one geophone integrator. The geophone intergrator amplifies the arrival waves and reduces noise interference through a set of four geophones. The integrator was useful when the shot and geophone distance were greater than 200 ft.

Results: Data from Site I reveal three subsurface formations (Figure 18). The near-surface layer with velocity of about 1000 ft/sec is composed of sands and

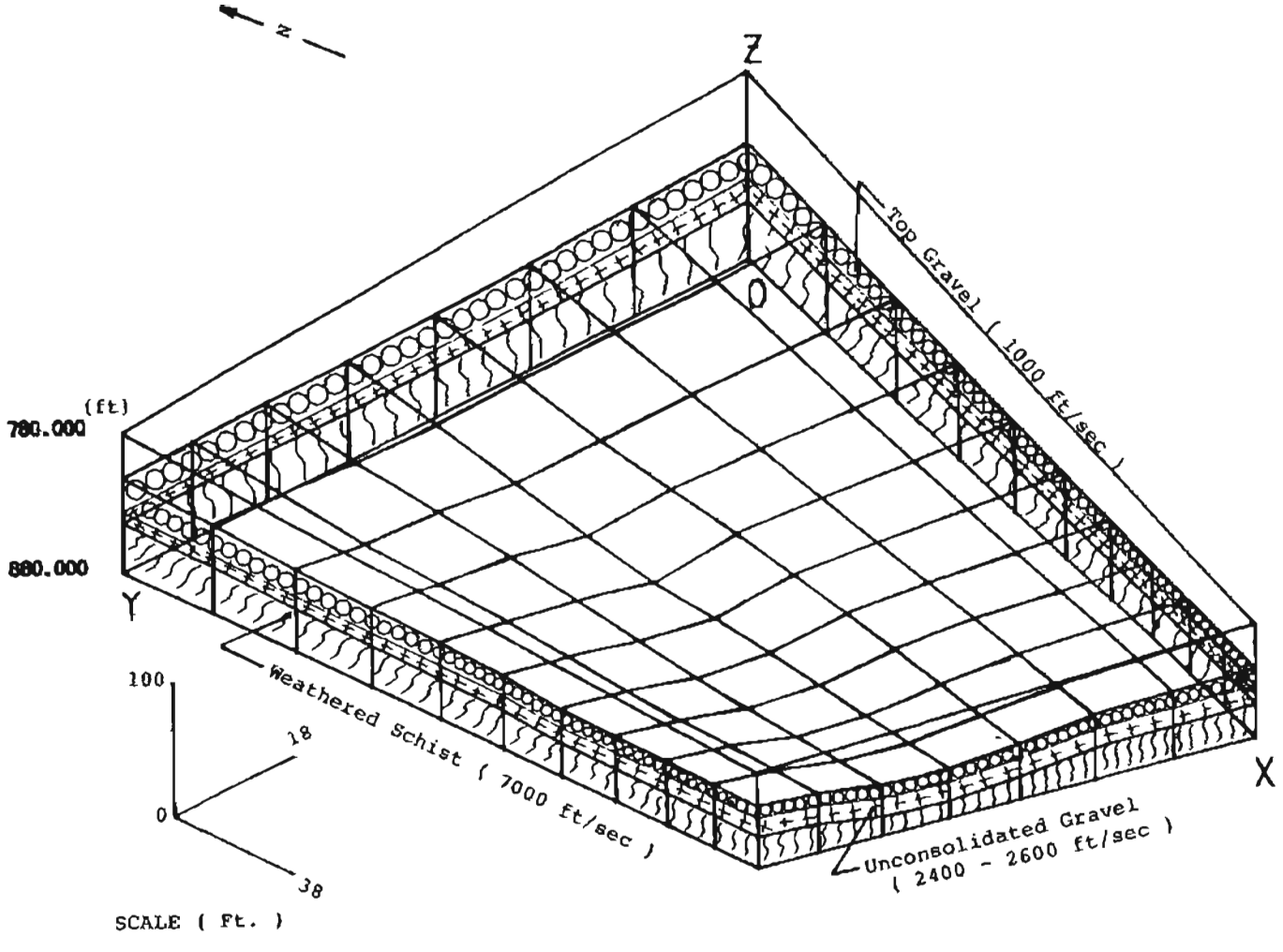

Figure 18. Subsurface layering structure at Site I, USA CRREL permafrost tunnel.

gravels. The low velocity indicates that the material is loosely compacted. The thickness of the top sand-gravel layer ranges from approximately 10 to 25 ft., with dip of 4.2°S.

The middle layer has a velocity ranging from 2400 to 2600 ft/sec. The difference between the top two layers is small, however, it is significant enough to separate them. The thickness of the layer is in a range of 6 to 21 ft. The relatively higher velocity might be caused by the higher moisture content, colder temperature and the consolidation effect. It inclines toward south, which might contribute to the thickening of the layer at the south end.

Underlying the unconsolidated gravels is highly weathered schist. Velocity of the schist bedrock is 7000 ft/sec. Compared to the bedrock velocity observed at Willow Creek, it is about one half of that speed. It is probably caused by the old dredging operation, which fractured and thawed the frozen bedrock. Depth to the weathered bedrock is approximately 31 ft.

Using the records produced from site V, it was somewhat difficult to determine the exact position of velocity breaks. It is probably caused by the presence of ice wedges and the underground openings. Velocity of the upper layer, the frozen silts, ranges from 7500 to 11000 ft/sec. The depth to bedrock from the seismic data was not determine due to the insufficient survey length.

ELECTRICAL RESISTIVITY

The electrical resistivity method for subsurface study was first used by Schlumberger in France in 1912. Since then, the method has proved to be among the most effective geophysical means for shallow subsurface investigation. The major advantage of resistivity survey is its simplicity. The method is more frequently used in searching for metals and minerals than it is in exploring for petroleum.

THEORY

Electrical resistivity prospecting makes use of the fundamental property of rock: the resistivity controls the amount of current that passes through the rock when a specific electric potential difference is applied. Field measurements of the properties of subsurface formations afford an opportunity for distinguishing one type from another and determining depth to the layer.

The resistivity of a material is defined as the resistance (R) of a cylinder with a cross section of unit area and the unit length. If a block of conductive material has a length L and a cross sectional area A, then the resistivity, ρ, is expressed as follows:

$$\rho = RA/L \qquad \text{(Eq. 18)}$$

The general units of resistivity are ohm-feet or ohm-meter. This property is independent of the volume of material whereas resistance depends upon the shape and the size of the material.

Resistivity survey is generally carried out, using four electrodes shown in Figure 19. A current (I) is induced between the two outer electrodes. When current flows through the formations, a potential difference (V) is

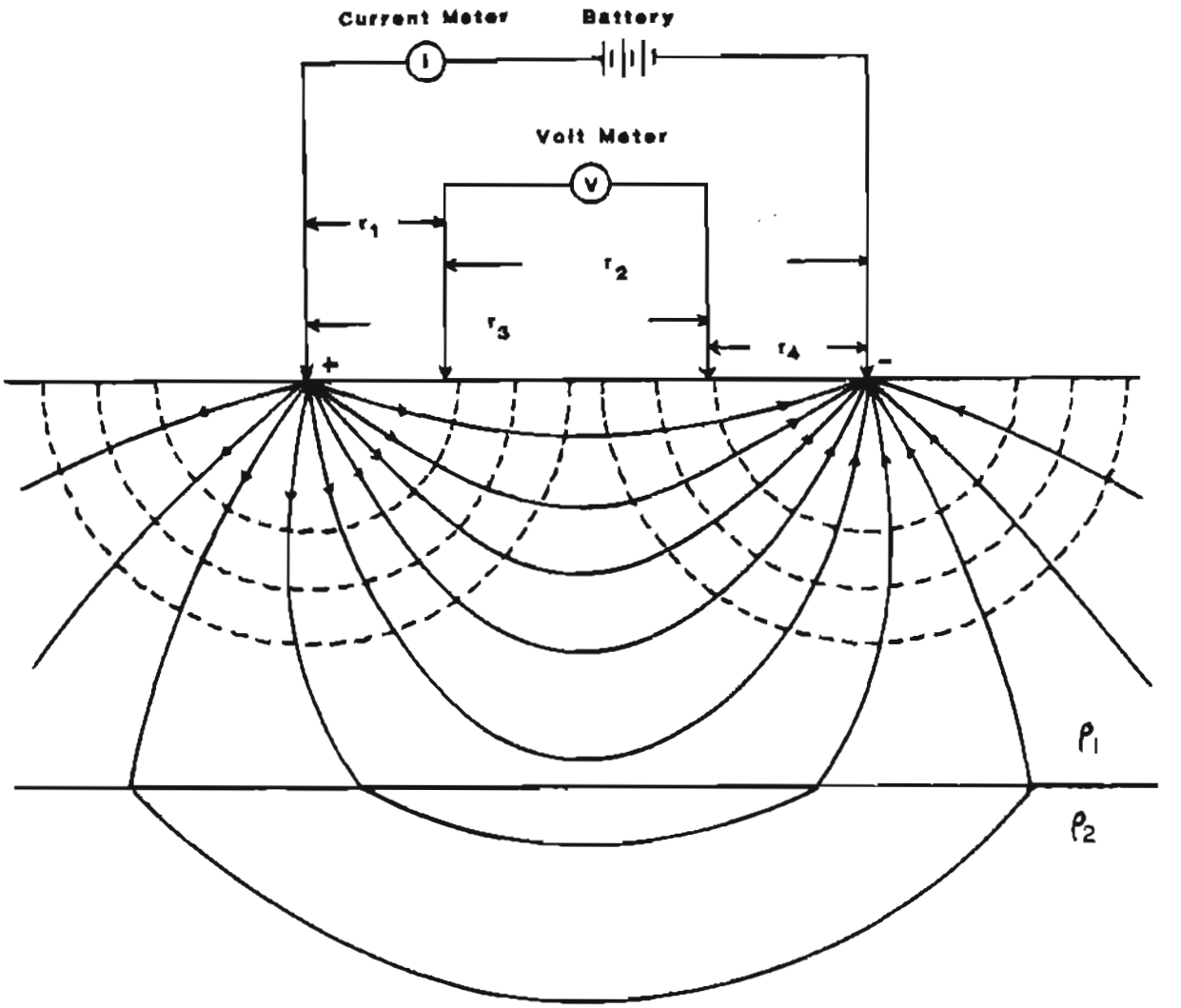

Figure 19. Vertical cross-section of the earth showing the electric current lines (solid lines) and the equipotential lines (dashed lines).

developed between any two points in the material. This potential difference may be measured by a voltmeter attached to the inner electrodes. This arrangement is, in effect, a field application of Ohm's law:

$$R = V/I \qquad \text{(Eq. 19)}$$

The current flowing into the formation spreads out vertically and horizontally. Hemispherical equipotential surfaces develop if the material is homogeneous. The volume of material through which the current passes is proportional to the distance between two current electrodes. It indicates that the penetration depth of the current is proportional to the two current electrodes distance. Thus, it is possible to measure the resistance of a volume of earth proportional to the electrode distance. The potential difference measured by the voltmeter between two potential electrodes is:

$$V = (I\rho/2\pi)[(1/r_1-1/r_2)-(1/r_3-1/r_4)] \qquad \text{(Eq. 20)}$$

This is the basic equation which gives the resistivity in terms of potential difference, current and electrode spacing. Since there is some variation in the results as the electrode arrangement is changed, interpretation depends upon the electrode array used in the field. A number of different configuration of current and potential electrode exists. In all arrangements, the electrodes are laid out along a line with the current probes generally placed on the outside of the potential probes. In the study, the Schlumberger and Wenner method were used.

Schlumberger Configuration

The Schlumberger array uses four electrodes. The two potential electrodes are closely spaced and located midway between the two widely spaced current electrodes (Figure 20). The arrangement measures approximately the potential gradient at the midpoint of the spread. The advantages of this method is that only the current electrodes are moved. The potential electrodes remain in their original positions as long as the distance between the two inner probes are less than two-tenths the distance between the inner and outer probes. For this array, Equation 20 can be rearranged and becomes:

$$\rho_a = \pi R[(ra^2-b^2)/4b] \approx \pi R\, a^2/b \qquad \text{(Eq. 21)}$$

The measurement (ρa) produced in a survey is known as apparent resistivity. It is neither the true resistivity of the layer nor the average resistivity, but is an idealized value which can be used for survey data interpretation.

Wenner Configuration

The Wenner array uses four electrodes equally spaced along a survey line. In the array, the outer probes serve as the current electrodes and the two inner probes are potential electrodes (Figure 21). From this arrangement, the Equation 20 becomes:

$$\rho_a = 2\pi aR \qquad \text{(Eq. 22)}$$

The apparent resistivity determined from the above equation is assigned to a location midway of the survey spread.

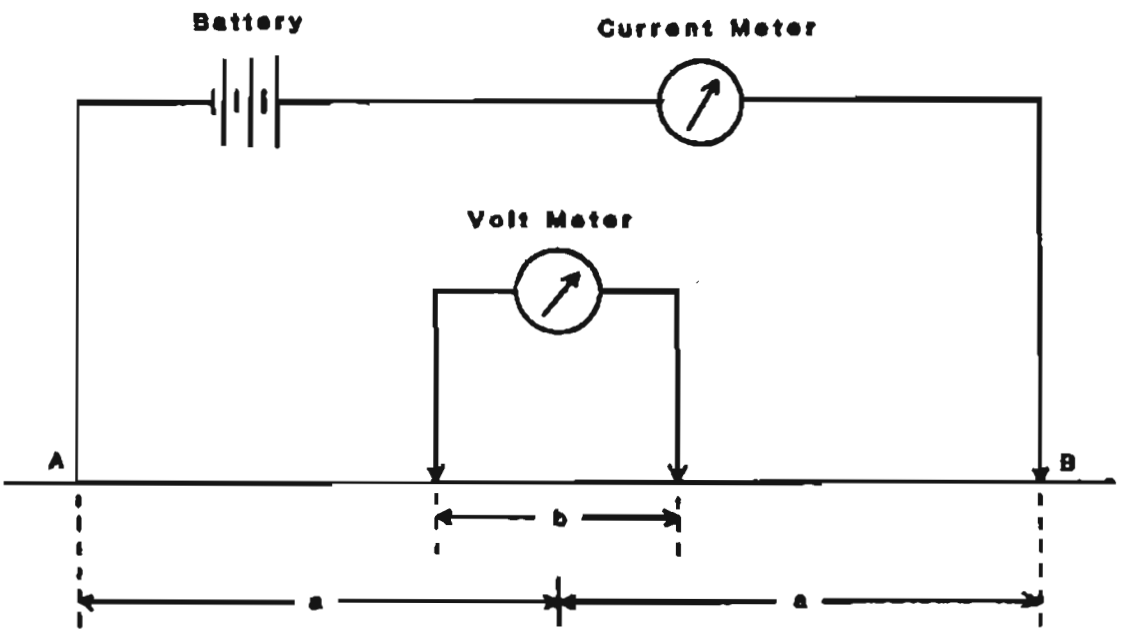

Figure 20. The Schlumberger electrode configuration.

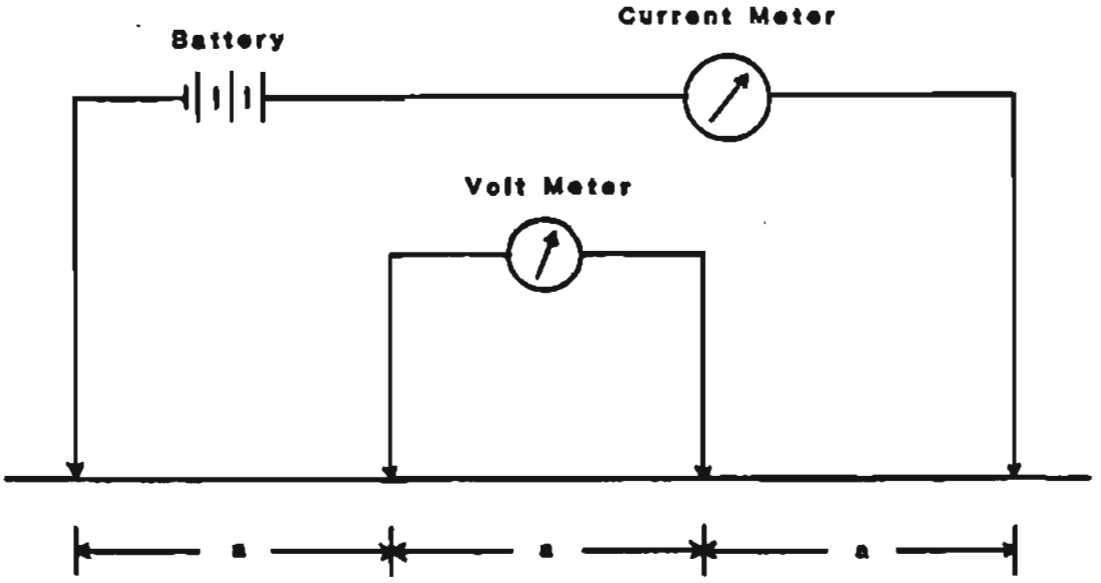

Figure 21. The Wenner electrode configuration.

Vertical Electrical Sounding (VES)

The electrical sounding will produce different apparent resistivity readings while different subsurface conditions exist. The interpretation of VES curves is usually made by curve-matching techniques in which a set of theoretical curves is used in conjunction with the field data. The theoretical curves are computed for a particular layering structure. If a match can be obtained, then the subsurface structure is assumed to be identical with the theoretical structure. Although the principle of this method is straightforward, it requires a great deal of practice and can be frustrating to the inexperience interpreter.

The direct interpretation of VES curves has attracted the attention of many researchers for the past half century. This method has gained wide acceptance since the development of computer. A digital computer can process large numbers of VES curves in very short periods of time and fit them to certain theoretical layering conditions.

For a horizontally stratified, laterally homogeneous, and isotopic subsurface layers, the Schlumberger apparent resistivity is calculated in two steps. The first step consists of the computation of the total kernel function $T(h,\rho,r)$ for an n-layer model:

$$T_i\ (h,\rho,\lambda) = (1-\partial_i e^{-2\lambda h_i})/(1+\partial_i e^{-2\lambda hi}) \qquad \text{(Eq. 23)}$$

$$\partial_i = (\rho_i - \rho_{i+1}\ \partial_{i+1})/(\rho_i + \rho_{i+1}\ \partial_{i+1}) \qquad \text{(Eq. 24)}$$

$$T_{n-1} = (1-\partial_{n-1} e^{-2\lambda h_{n-1}})/(1+\partial_{n-1}\ e^{-2\lambda h_{n-1}}) \qquad \text{(Eq. 25)}$$

$$\partial_{n-1} = (\rho_{n-1} - \rho_n)/(\rho_{n-1} + \rho_n) \qquad \text{(Eq. 26)}$$

where ρ_i and h_i are the resisitivity and thickness of the ith layer, and λ is the integration variable.

The second step is to convolve the inverse filter coefficients with the derived total kernel function. The convolution is made for six apparent resistivity values per logarithmic cycle.

ROUTINE FIELD PROCEDURES

There are two basic field procedures used: electrical profiling and electrical sounding. Electrical profiling requires constant electrode separation throughout the survey. This method is normally applied in a area where a rapid survey is needed. It is particularly suited for prospecting for ore bodies and identifying dipping structures.

During the profiling survey, a suitable electrode spacing is chosen. Since the depth of current penetration is related to the electrode distance, the depth of investigation essentially will be constant for all stations. As the survey proceeds, the changes in subsurface layers above certain depth will be reflected by the readings. The lateral variations may be constructed as map which shows a series of equipotential lines.

Electrical sounding is designed to provide information on the variation in subsurface conditions with depth. Field procedure requires that the center of the electrode spread remains at the same location while the electrode spacing is changed from one reading to another. The depth of penetration of this procedure is generally equal to the electrode spacing. This method is

valuable for detecting the sequence of subsurface layers for placer exploration.

Regardless of the types of survey procedures, the choice of electrode spacing should be careful for several reasons. Spacing which is too wide will make it difficult to obtain reliable field curves. Too small a spacing will require unnecessary field time. For shallow placer exploration, the electrode spacing can be spared with equal intervals on a linear scale. The largest electrode separation should be at least 3 times the maximum depth of interest. The smallest separation should be less than one-half the minimum depth at which a change in material property is expected.

MICROCOMPUTER ANALYSIS

The computer software "RESISTIVITY" and an example problem are listed in Appendix B. The RESISTIVITY was written in Microsoft BASIC. It consists of four subroutines including spacing, kernel, conves, and least square analysis. A flow chart of the program is shown in Figure 22. This software was programmed only for the Schlumberger sounding survey. It calculates the depth and resistivity of a subsurface structure by fitting the field data to a set of theoretical conditions. A theoretical model with the least deviation from the observed measurements is selected as the most probable field condition. The step-by-step input and output statements are discussed as follows:

1. When the program is run, the first message shown on the monitor and printer is:

```
**********************************************
*                                            *
*    RESISTIVITY --- SCHLUMBERGER SOUNDING   *
*                                            *
**********************************************
```

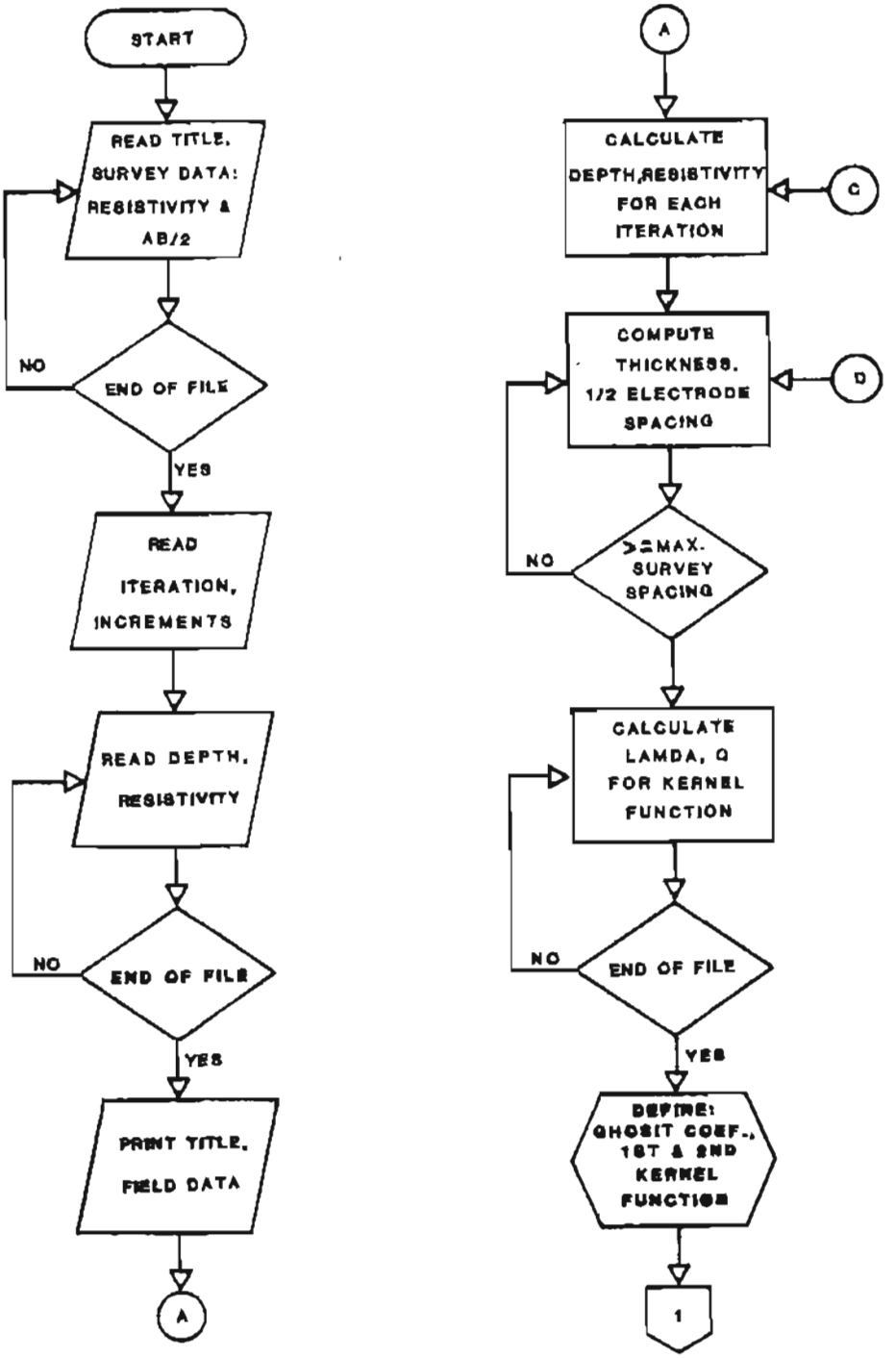

Figure 22. Flow chart of the RESISTIVITY microcomputer program.

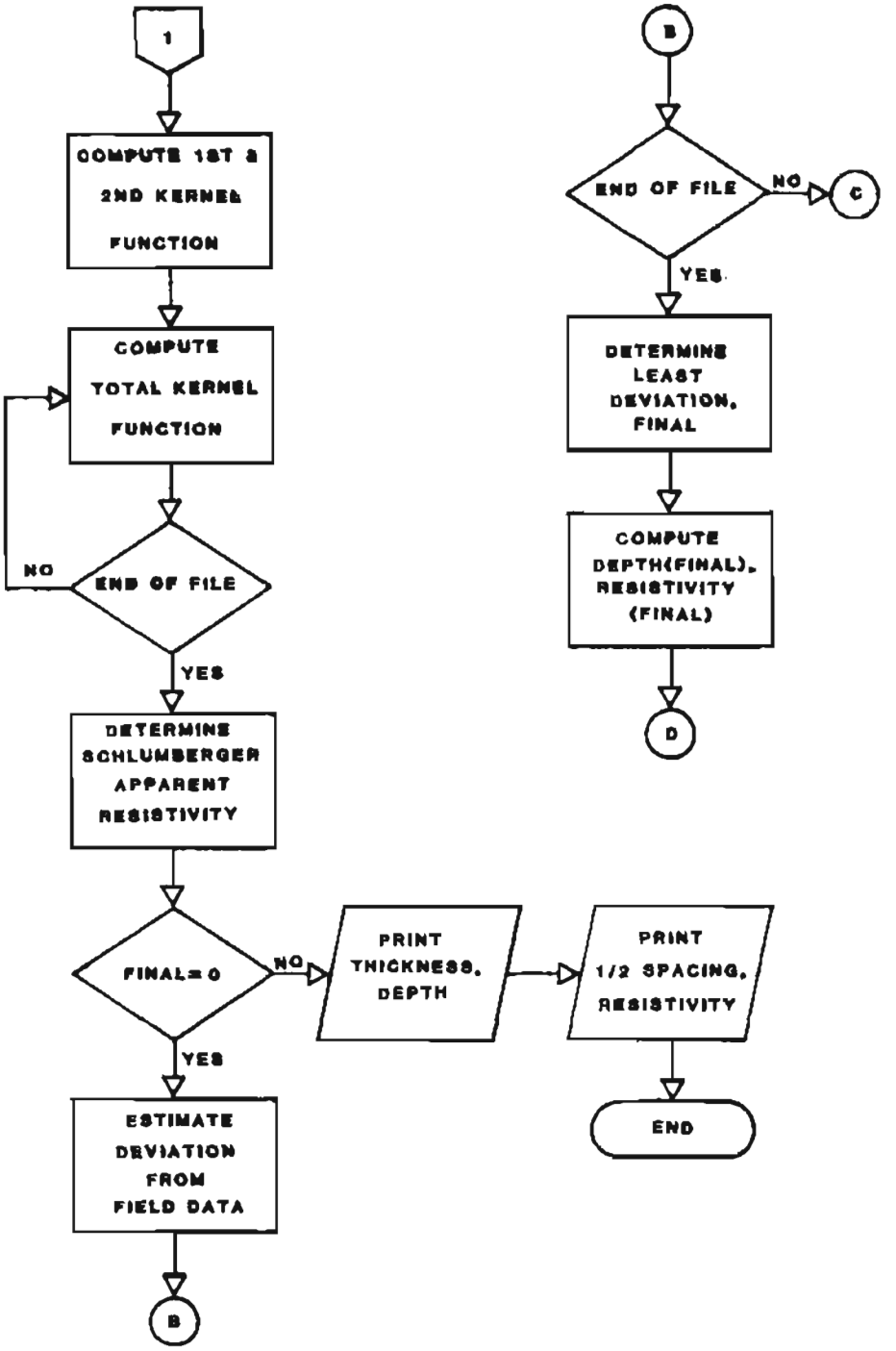

Figure 22. Flow chart of the RESISTIVITY microcomputer program (cont'd).

TITLE —

Type in the title of the study. The length of the title cannot be more than 80 characters. A comma symbol is not acceptable and will cause a syntax error.

2. The second statement on the screen and printer are:

```
INPUT APPARENT RESISTIVITY (Ohm-Ft), 1/2 ELECTRODE SPACING (Ft):
INPUT -1 FOR RESISTIVITY AND SPACING WHEN COMPLETE
```

3. The next statement requires a set of field data be typed, and it follows:

```
RESISTIVITY                    1/2 SPACING
```

Input the field measured apparent resistivity and one-half current electrode spacing. When all the data are read, type -1 for both readings to stop this statement. The maximum number of field data is limited to 50. The dimension of the data set can be increased by changing the DIM statement in the main program.

4. After the field data are read, the computer will ask information concerning iteration:

```
ITERATION (Y/N)?
```

If the answer is "Y", the computer will proceed to next statement and 10 iterations will be conducted for each theoretical subsurface condition. If the answer is "N", the computer will stop the execution.

5. The program can handle iteration with increasing magnitude (up) or iteration with decreasing magnitude (DOWN):

```
ITERATION UPWARD OR DOWNWARD (UP/DOWN)?
```

By typing-in "DOWN", the iteration will be processed downward.

6. Increments for depth and resistivity of the assumed theoretical condition will be asked by the following statement:

INCREMENTS FOR DEPTH AND RESISTIVITY:

The values of the increments can be positive, negative or zero. For a quick analysis a larger increment is suggested to cover wider range of the subsurface conditions. For example, a value of 0.1 for the depth parameter calculates ten subsurface conditions with an increment of 0.1 times of the original depth. Similar process is applied to the iteration of the resistivity values.

7. The following statements require information concerning the theoretical layering condition:

TOTAL NUMBER OF SUBSURFACE LAYERS:
DEPTH (Ft) AND RESISTIVITY (Ohm-Ft):

The values of depth and resistivity should be input as many as the number of the subsurface layers. Since the program assumes the last layer extends infinitely, therefore, a huge number such as "999999" must be used for the depth to the last formation.

8. The output from the program are:

THICKNESS (Ft)	DEPTH (Ft)	RESISTIVITY (OHM-FT)
....	....	.....

1/2 SPACING (Ft)	RESISTIVITY (Ohm-Ft)
....	.....

LEAST SQUARE ROOT OF DEVIATION: .....
AT ITERATION

The first table shows thickness, depth and resistivity of the subsurface structure which has the least deviation from the field measurement after 10 iterations. The second table summarizes the simulated Schlumberger sounding data based upon the condition indicated in the first table. The third output indicates the deviation from the true sounding curve. If the deviation is large, the steps 4 through 8 should be repeated until the condition is acceptable.

CASE STUDIES

Two sites were selected for electrical resistivity surveys. One investigation was conducted at the USA CRREL permafrost tunnel where the geologic setting is known. The other survey was performed along Chatham Creek where the VLF-EM survey was previously performed by one of the field assistants.

Chatham Creek Survey

The gold deposit near the head of Chatham Creek (Figure 23), was initially mined in 1911. Excavation was terminated when the eastern extension of the gold-bearing quartz vein was lost. A resistivity profiling survey was designed to provide data on the structural configuration of the deposit and to evaluate the performance of the method.

Local Geology: The geology in the Fairbanks Mining district is composed of three distinct terranes. They are the Chatanika, Fairbanks and Cleary

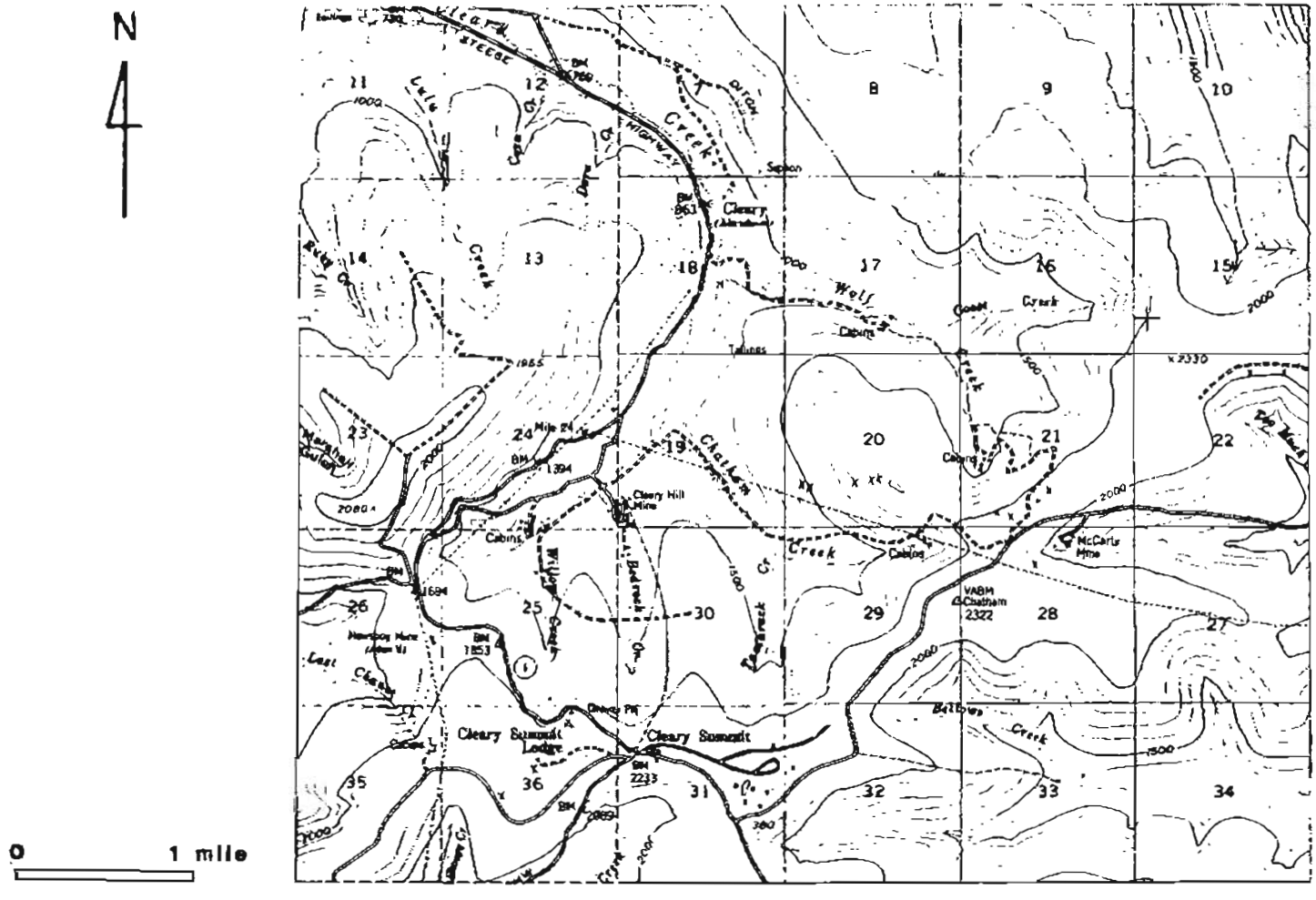

Figure 23. Map showing the location of resistivity profiling survey along Chatham Creek.

Sequence (Metz, 1982). The southern boundary of the Chatanika Terrain is located near the northern limb of the Cleary Anticline. Rocks in this unit are highly metamorphosed. Minor precious metals occur in this unit.

The Chatanika terrane is unconformably separated from the Fairbanks schist unit, and within the Fairbanks schist is the Cleary Sequence. Both units exhibit greenschist grade metamorphism. The Cleary Sequence hosts most of the precious metal occurrence in the district. It is a felsic metavolcanic package with intercallated metachert and metamorphosed pelitic sediments. The Fairbanks schist is composed of intercallated metamorphosed pelitic, argillaceous, and arkosic sediments.

The lode gold and indirectly the placer gold deposits in the district were derived from the precious metals deposited in the Cleary Sequence. Regional deformation remobilized minerals into shear zones and resulting gold-bearing quartz vein. Pedro, Gilmore and possibly Ester Domes are a result of this type of intrusive activity.

A second deformation associated with the stibnite deposits, struck in a NE-SW direction. In many locations, it crosscut and offset the earlier NW-SW striking gold deposits.

Survey Procedures: A grid covering the site was surveyed with a electric resistivity unit. Grid stations were set up on 50 foot spacing along lines spaced 200 feet apart. A soil test R-60 D.C. resistivity meter was used. Two copper-clad pusher electrodes were used as current probes and two porous pots were used as potential electrodes. Solution of $CuSO_4$ was added to the two potential electrodes to prevent polarization effects. Schlumberger profiling

survey was conducted in the field with 10 feet of the inner electrode spacing and 60 to 70 feet of the potential and current electrode distance.

Results: The profiling data are listed in Table V. Plots of the resistivity and the VLF data are shown in Figures 24A through 24E. Two sets of anomalies with low resistivity and high VLF response were detected in the survey area. The first low resistivity occurs about 100 ft. from the base line. It coincides with the known gold-bearing vein. The second anomaly locates approximately 450 ft. away from the base line. This low resistivity structure strikes NW-SE, which parallels to the Chathan vein. Compared to the VLF curve, there is general agreement between the high response of VLF and the low resistivity of the electric profiling.

USA CRREL Tunnel Survey

The USA CRREl permafrost tunnel was also used to evaluate performance of the resistivity method. General geology of the area is described in the previous chapter. At the site, there are three distinct layers: frozen silts, gold bearing gravels and the bedrock schist.

Survey Procedures: The resistivity sounding surveys were conducted at two sites (Figure 25). One track was placed in an area (site I) where frozen silts and gravels were removed by old dredging. Another four lines were placed on top of the hill, where the permafrost exists. On site I, Schlumberger and Wenner sounding techniques were applied. The maximum spread was about 600 ft. for the Schlumberger survey. The potential electrode separation was maintained at 10 ft. apart and the current electrode was moved outward with an increment of 15 ft. The electrode spacing for the Wenner

Table V. Apparent resistivity data of profiling survey at the Chatham Creek site.

Distance from Baseline (ft)	Apparent Resistivity (ohm-ft) Track A	Track B	Track C	Track D	Track E
0	8,890	9,444	18,604	16,900	5,773
50	15,315	8,927	12,841	26,211	6,482
100	12,850	15,356	11,742	28,461	13,288
150	25,190	10,543	12,005	28,395	14,856
200	21,058	25,701	15,499	19,119	29,834
250	17,748	34,429	17,013	18,378	14,487
300	14,090	15,239	29,935	11,712	11,122
350	9,189	11,366	18,531	22,973	10,108
400	9,700	8,333	7,581	16,799	15,622
450	13,459	7,373	6,739	13,559	13,018
500	12,539	6,179	3,693	12,534	6,261

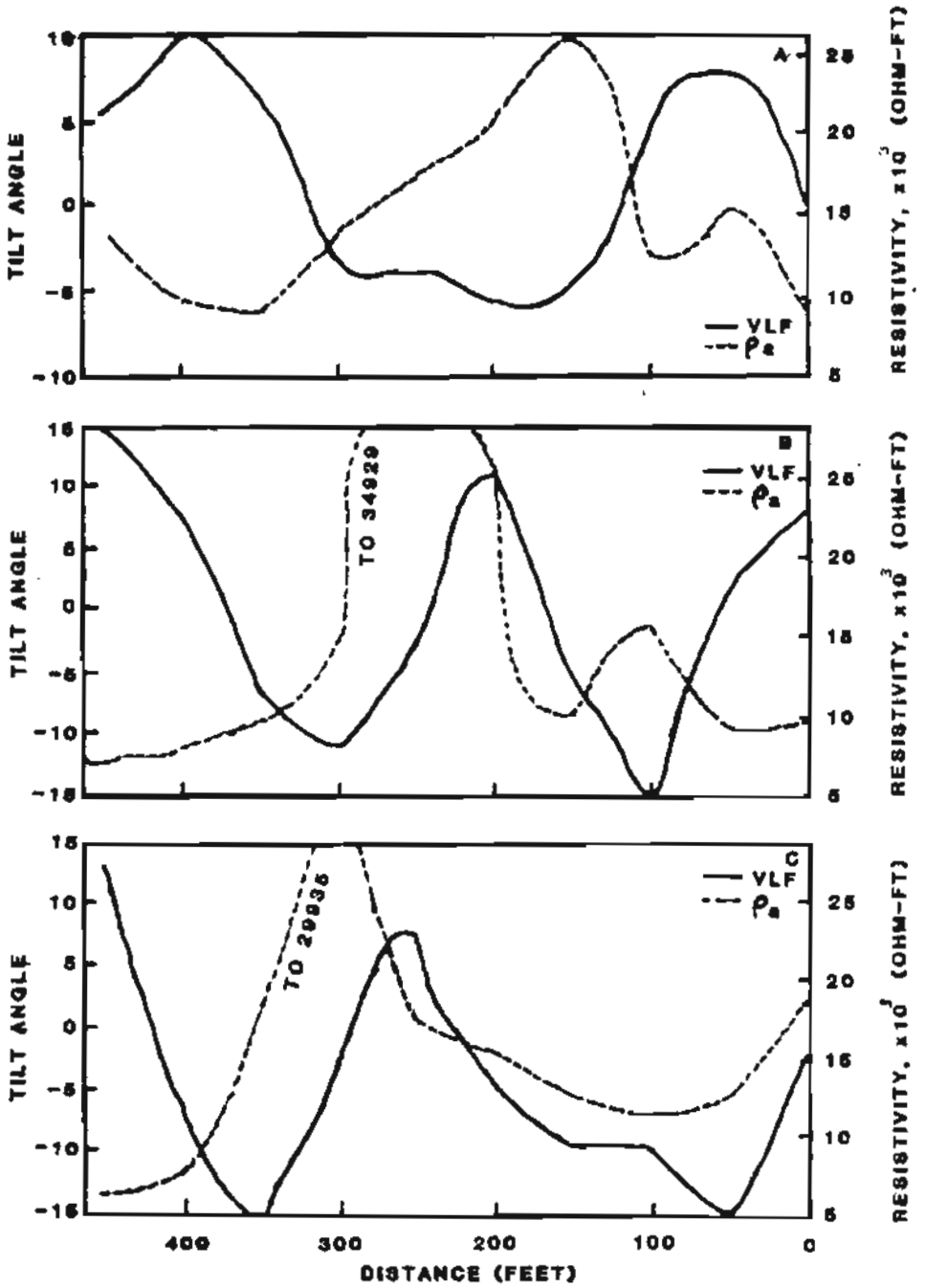

Figure 24. Profiling measurements and VLF data of the Chatham Creek site. (A) Track A, (B) track b, (C) track c.

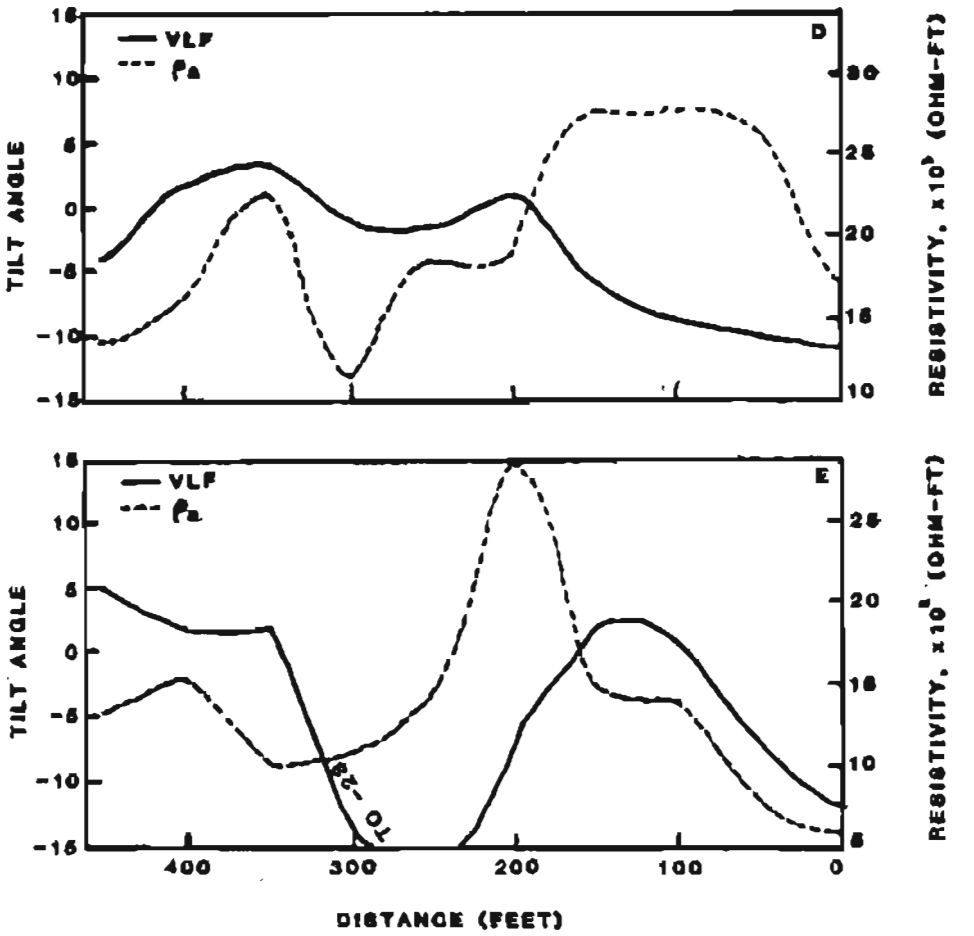

Figure 24. Profiling measurments and VLF data of the Chatham Creek site. (D) Track D, (E) track E (cont'd).

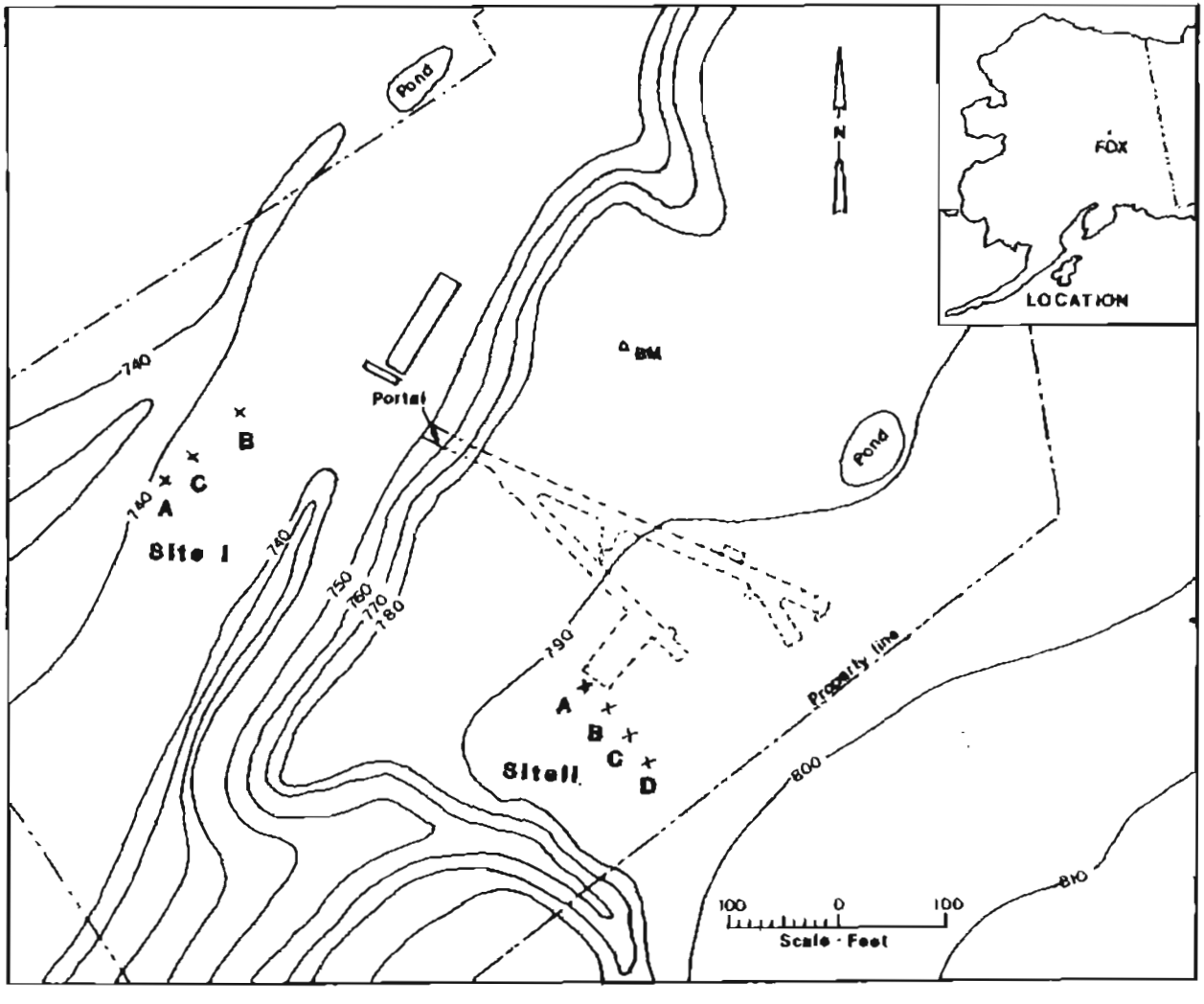

Figure 25. Map showing the resistivity survey sites at USA CRREL permafrost tunnel, Fox, Alaska.

survey was maintained at a constant interval of 15 feet. On the second site, the Schlumberger method was used along the four tracks. The inner electrode spacing was maintained at 10 ft. throughout the survey. The current electrode spacing was increased by 15 feet after each rending. Due to the terrain of the second site, the maximum spread was restricted to 300 ft.

Results: Three stations on site I were surveyed. The field resistivity measurements and one-half the current electrode spacings are listed in Tables VI and VII. The field resistivity curves and the computer simulated vertical electric sounding curves are plotted in Figure 26 to 28.

Results of the computer simulation (Table VIII) indicate that three subsurface layers exist at the site. The near-surface layer has resistivity in a range of 5000 to 23000 ohm-ft with the thickness of about 2.5 to 5.5 ft. The relatively low resistivity may be caused by the percolation of melting ice on the ground during survey. The second layer underlying the low resistivity zone has resistivity of 150000 to 225000 ohm-ft. Thickness of the middle layer is about 9 to 16 ft. The bottom is a layer with very high conductivity. Thickness of the third layer cannot be determined because of the relatively short survey spread. The high conductivity of the bottom layer is probably due to the weathering which altered the schist and formed a clay zone at the top of the bedrock.

Field measurements and the VES curves of site II are plotted in Figures 29 to 32 and the simulated subsurface layering structures are tabulated in Table IX. Due to the restriction of topography at site, there were not enough data points to identify the frozen gravel-bedrock contact, however, survey results indicate that there are two subsurface layers. The top layer is

Table VI. Field VES Schlumberger measurements of station A, B and C at site I, USA CRREL permafrost tunnel.

Station A		Station B		Station C	
AB/2 (ft)	Resistivity (ohm/ft)	AB/2 (ft)	Resistivity (Ohm/ft)	AB/2 (ft)	Resistivity (Ohm/ft)
15.5	37,000	22	28,000	22	30,000
31	70,000	37	39,000	37	44,000
46	90,000	52	40,000	52	38,000
61.5	74,000	67	36,000	67	30,000
76	64,000	82	28,000	82	26,500
92	40,000	97	21,000	97	17,000
107	26,000	112	16,000	112	12,500
122	18,000	127	12,000	127	8,700
137	11,000	142	7,800	142	6,700
152	8,800	157	4,600	157	5,000
167	6,500	172	2,850	172	3,800
182	5,000	187	2,150	187	2,800
197	3,800	202	1,950	202	2,000
212	2,950	217	1,600		
227	2,150				
242	1,980				
257	1,700				
272	1,680				
287	1,700				
302	1,600				

Table VII. Field Wenner VES measurements of station A at site I, USA CRREL permafrost tunnel

A Spacing (ft)	Apparent Resistivity (ohm-ft)
10	38,863
20	72,393
30	95,567
40	78,298
50	59,811
60	46,056
70	31,067
80	22,057
90	16,294
100	12,799
110	9,928
120	9,704
130	6,918
140	5,704
150	4,635
160	3,120
170	2,185
180	2,084
190	1,940
200	1,679

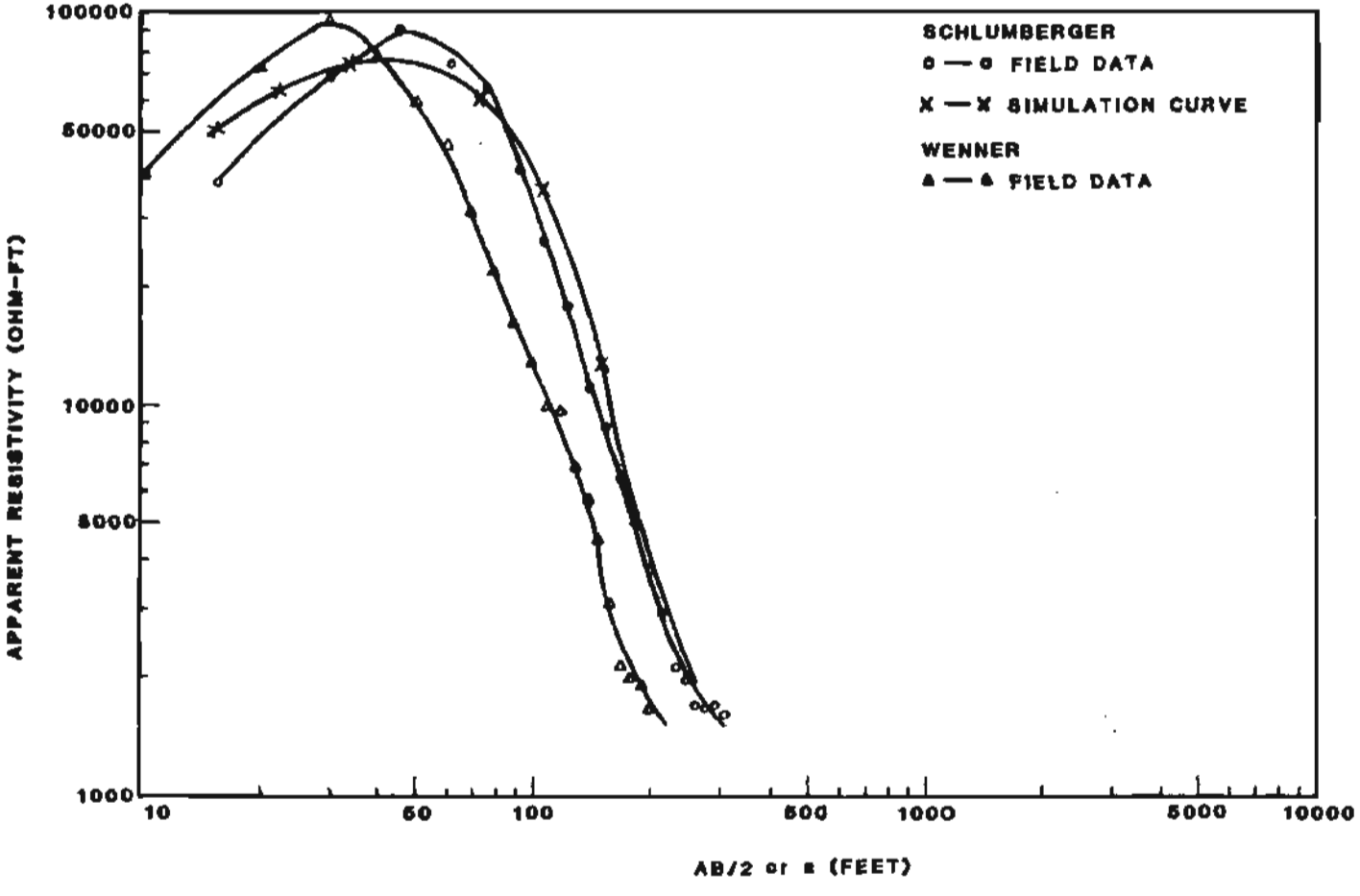

Figure 26. Diagram of theoretical Schlumberger curves and field Wenner and Schlumberger sounding measurements at station A on site I, USA CRREL permafrost tunnel.

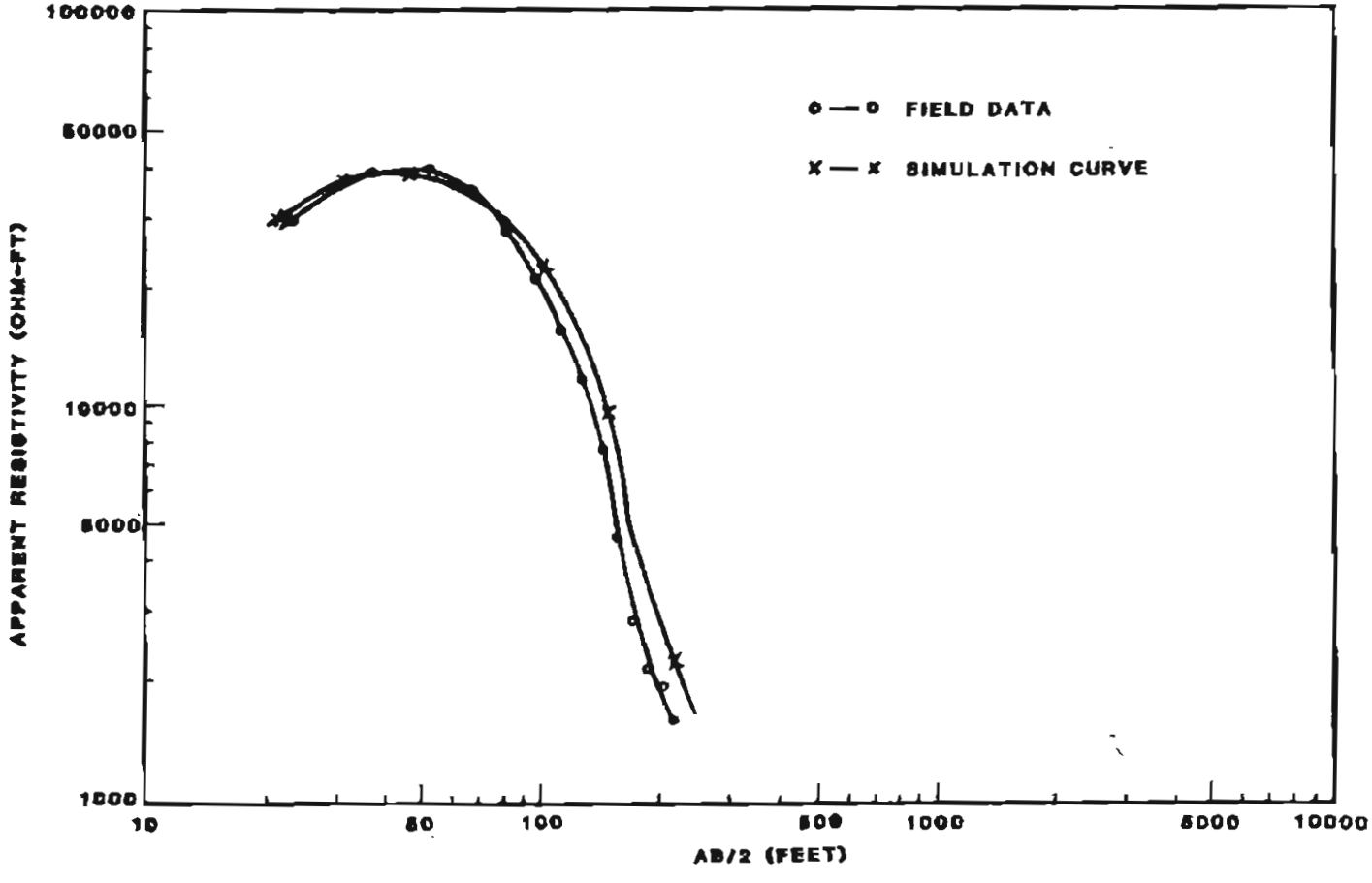

Figure 27. Diagram of theoretical and field Schlumberger VES curves at station B on site I, USA CRREL permafrost tunnel.

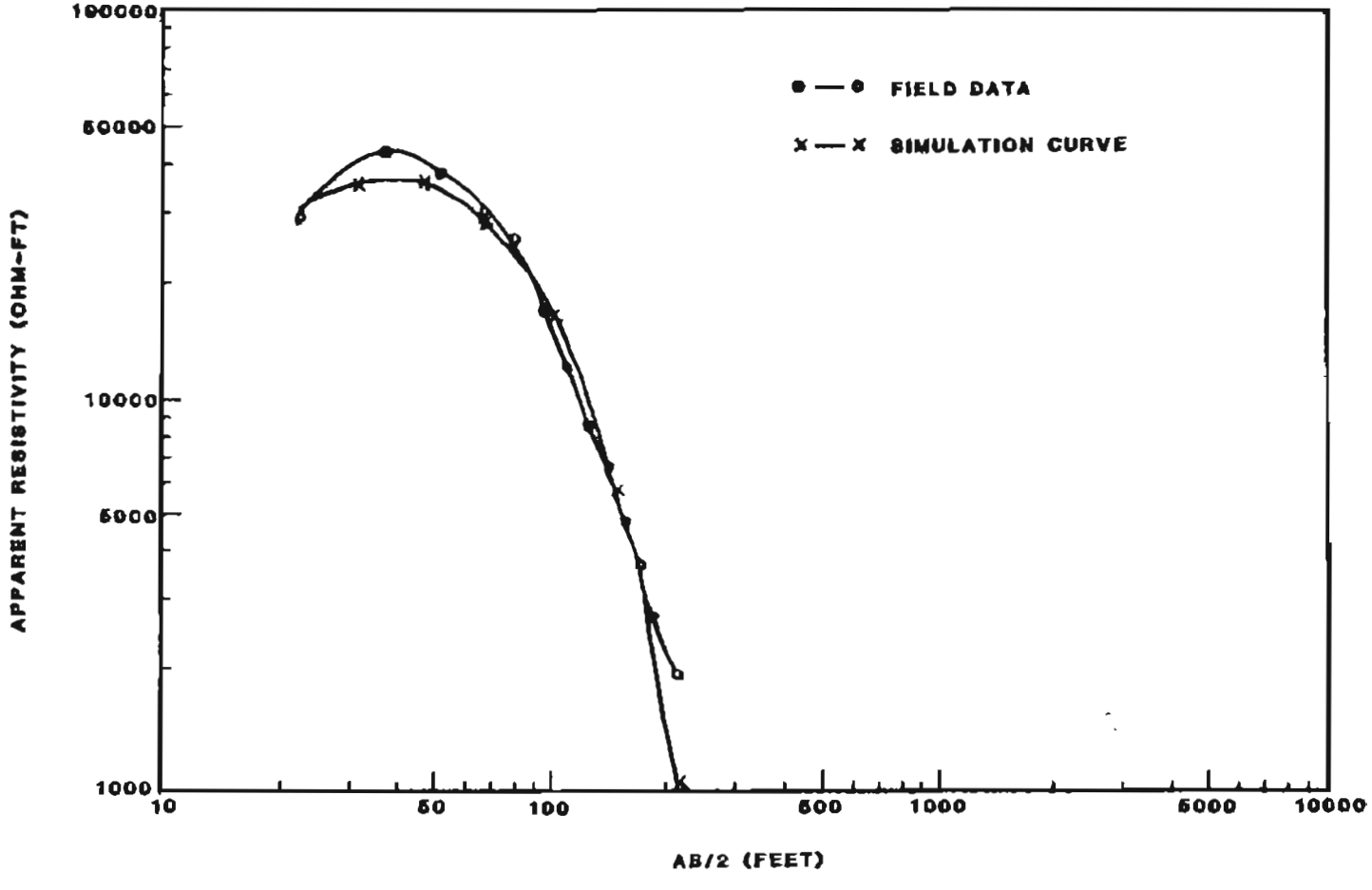

Figure 28. Diagram of theoretical and field Schlumberger VES curves at station C on site I, USA CRREL permafrost tunnel.

Table VIII. Results of electric resistivity surveys at site I, USA CRREL permafrost tunnel.

Thickness (ft)	Depth (ft)	Resistivity (ohm-ft)
Station A:		
5.4	5.4	22,655
16.2	21.6	226,550
—	—	566
Station B:		
5.6	5.6	10,439
13.4	19.0	153,519
—	—	110
Station C:		
2.4	2.4	5,000
8.8	11.2	200,000
—	—	100

Table IX. Results of electric resistivity surveys at site II, USA CRREL permafrost tunnel.

Thickness (ft)	Depth (ft)	Resistivity (ohm-ft)
Station A:		
60.5	60.5	38,885
—	—	5,000
Station B:		
50.0	50.0	35,443
—	—	5,933
Station C:		
55.0	55.0	33,750
—	—	9,000
Station D:		
54.0	54.0	33,000
—	—	8,800

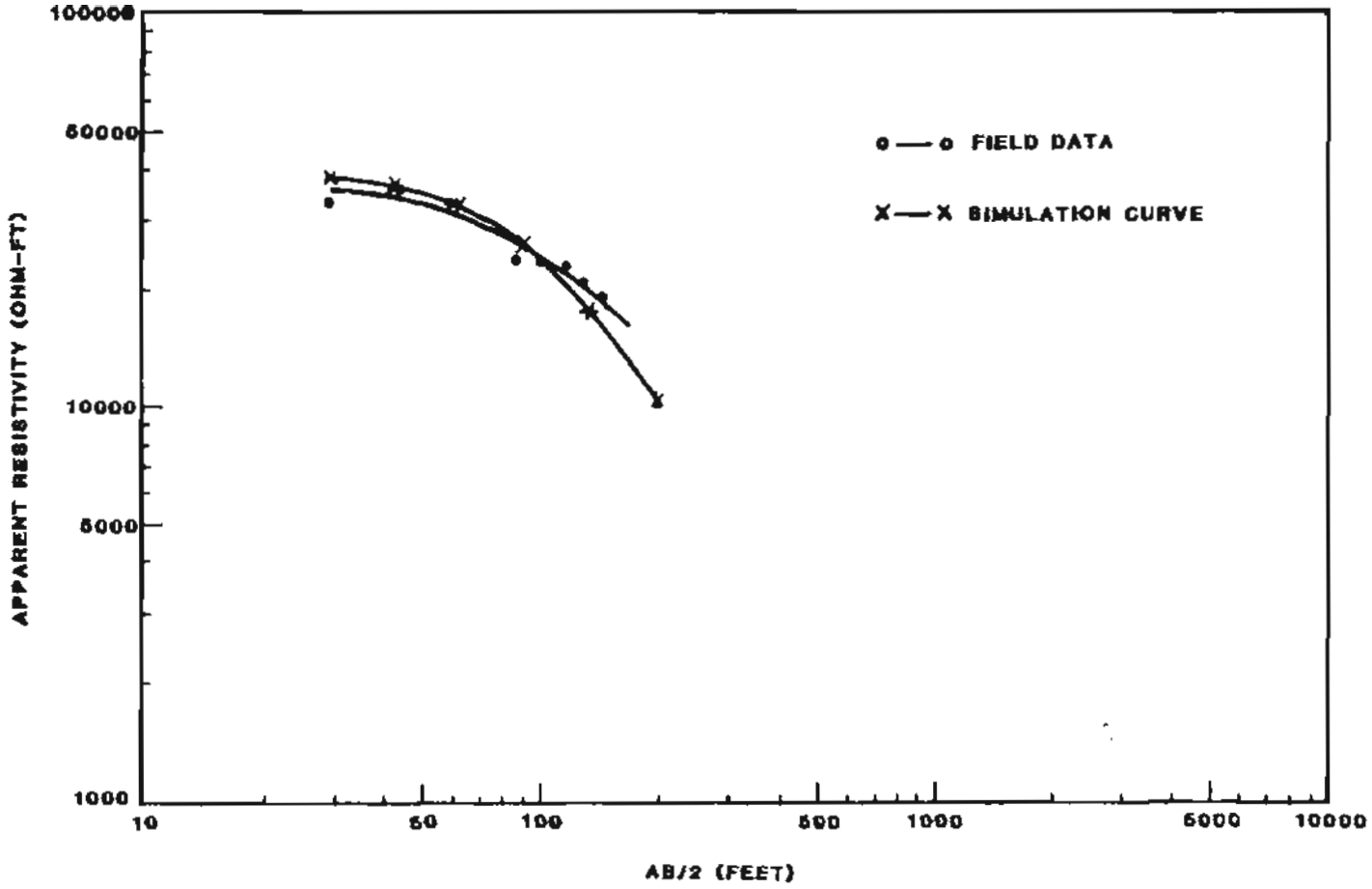

Figure 29. Diagram of theoretical and field Schlumberger VES curves at station A on site II, USA CRREL permafrost tunnel.

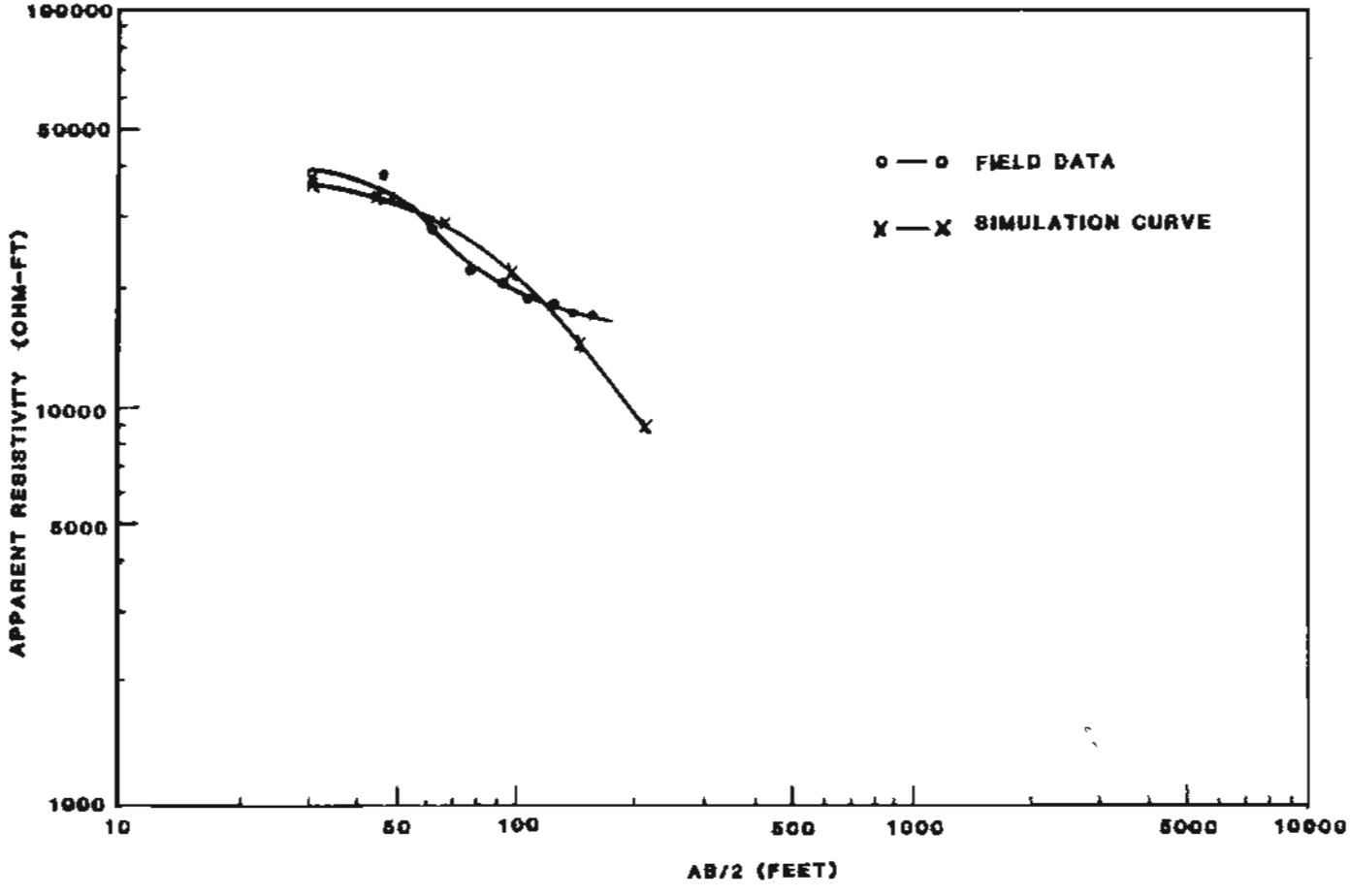

Figure 30. Diagram of theoretical and field Schlumberger VES curves at station B on site II, USA CRREL permafrost tunnel.

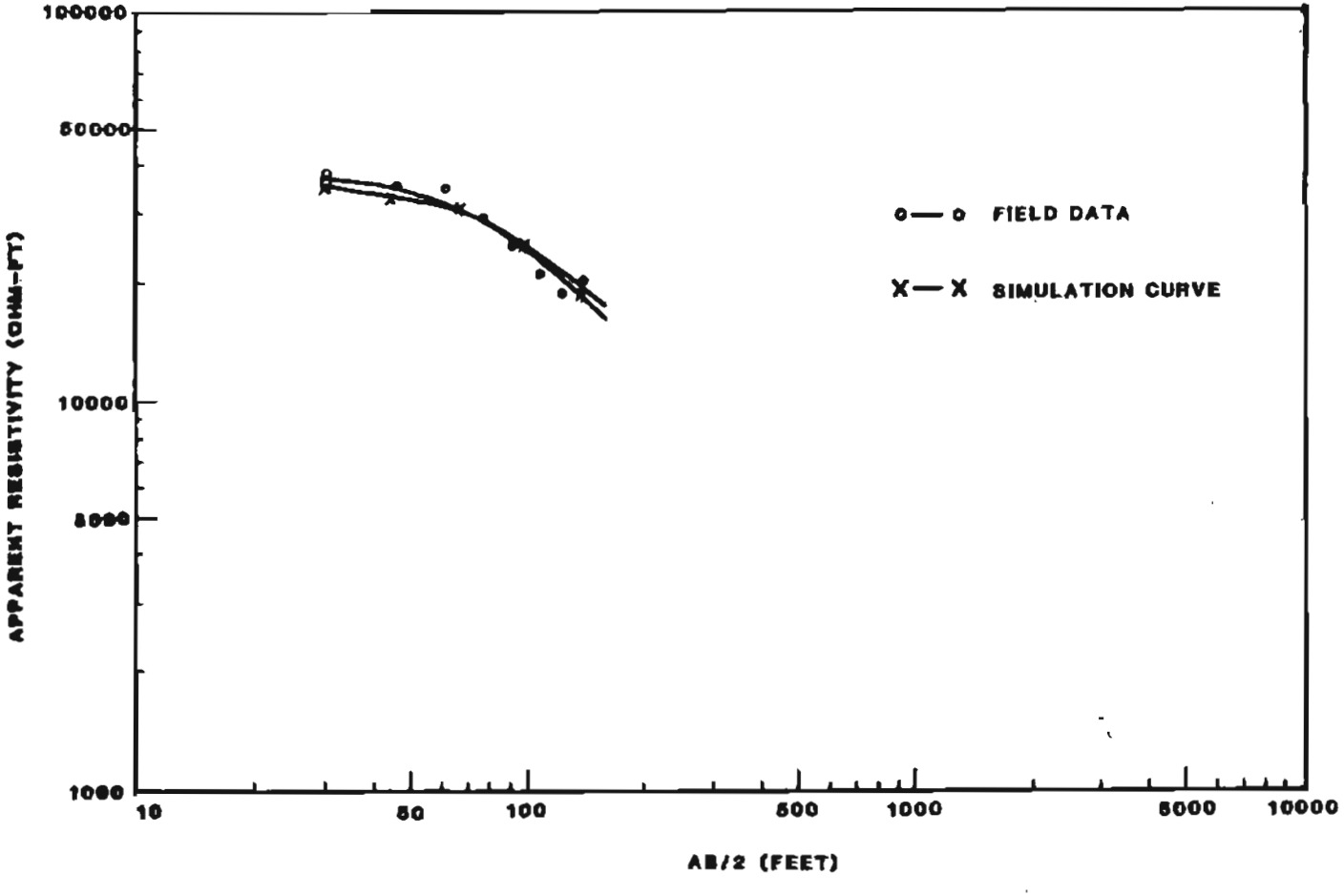

Figure 31. Diagram of theoretical and field Schlumberger VES curves at station C on site II, USA CRREL permafrost tunnel.

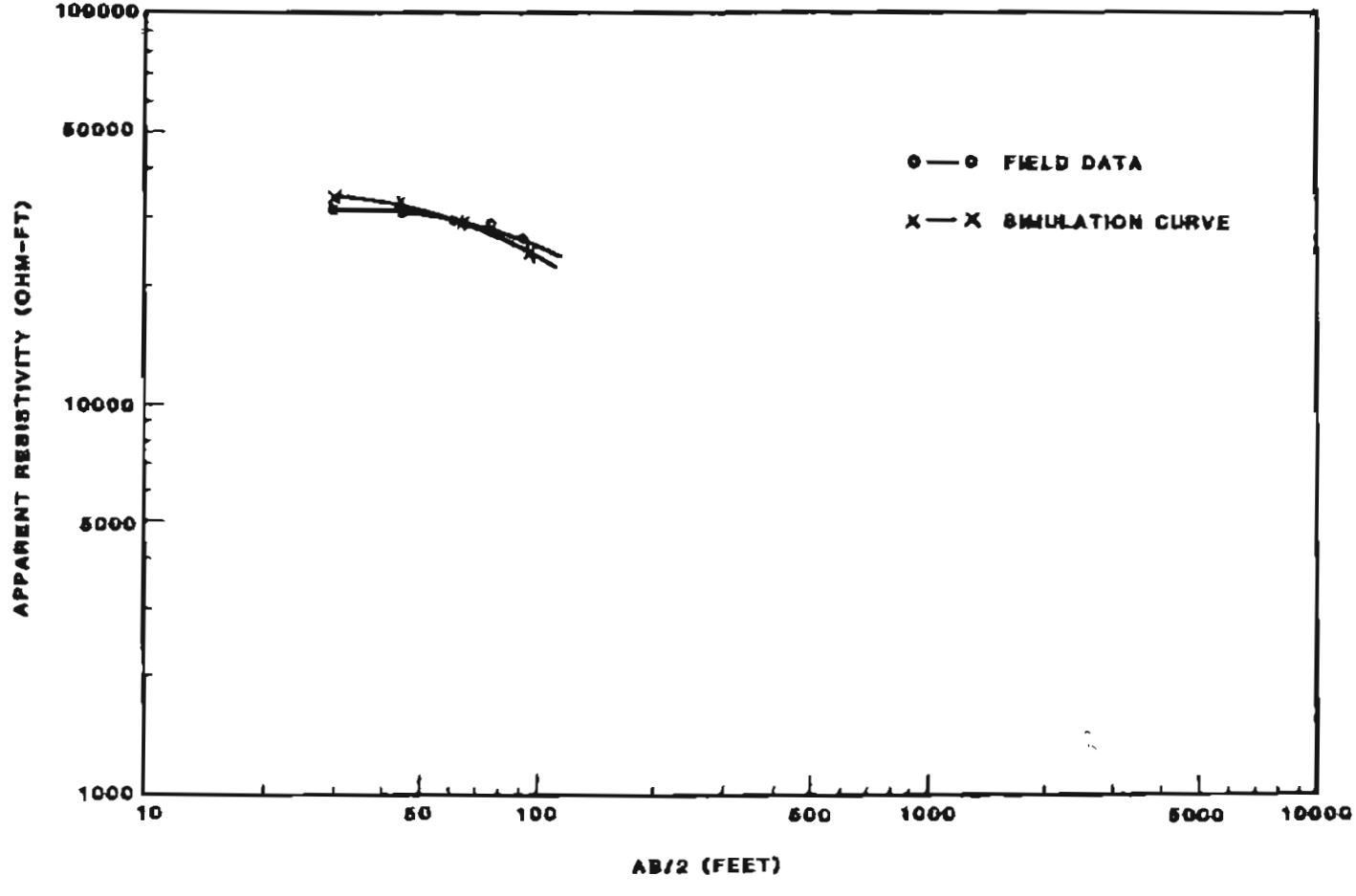

Figure 32. Diagram of theoretical and field Schlumberger VES curves at station D on site II, USA CRREL permafrost tunnel.

composed of a material with resistivity ranging from 33000 to about 39000 ohm-ft. Thickness of the near-surface layer is in a range of 50 to 60.5 ft. Compared with the drilling information at the site, the resistivity sounding technique produced fairly consistent results. Underlying the top unit is a layer with relatively low resistivity. The apparent resistivity ranges from 5000 to 9000 ohm-ft.

DISCUSSION AND CONCLUSIONS

Observations from the field surveys show that both seismic refraction and electric resistivity methods can quickly detect subsurface structure with certain accuracy. Ground condition such as distribution of permafrost or irregularity of bedding will introduce deviation from the true subsurface configuration. Data interpretation is probably the most important factor which influences the success of an exploration. Computer programs, SEISMIC and RESISTIVITY, are convenient for processing large amounts of data in a very short period of time so that the prospector may have at his disposal a basic solution. The information provided by the computer, however, should not be used without careful consideration. The computer determines the best fitting model to the observed data, but may sometimes overlook a certain layering distribution.

The Willow Creek survey shows that depth to the bedrock in the immediate area is between 88 to 134 ft. and surface of the schist dips slightly toward south. Drilling in the vicinity of the Willow Creek indicates that the depth to the Precambrian schist is approximately 150 to 160 feet. The discrepancy may be due to the irregular old river bottom or the existence of frozen ground. The velocity difference between frozen sand and gravels and frozen schist bedrock is not large. Frozen sands and gravels have velocity ranging from about 10000 to 12000 ft/sec. The seismic velocity of the bedrock is approximately 14000 to 15000 ft/sec. Such a small variation made it difficult to determine the depth of the true gravel-bedrock contact.

An investigation performed on an unfrozen site during the USA CRREL tunnel survey revealed much clear information. The velocity of the top

unconsolidated gravel ranges from 2400 to 2600 ft/sec and is 7000 ft/sec for the weathered schist. The large difference showed a sharp break on the time-distance diagram. Compared with the geological data collected by the previous study in this area, the seismic survey produced very consistent depth information. The bedrock depth estimated from the survey is about 30 feet and the depth from the geological study is about 26 feet plus. Schlumberger and Wenner methods were tested and data showed that both arrays generated very similar results.

Vertical sounding and profiling techniques were also carried out for different purposes. Schlumberger profiling technique was used to detect the distribution of a possible gold-bearing quartz vein along the Chatham Creek. Survey with AB/2 distance of 60 to 70 feet and B spacing of 10 ft. successfully identified a known vein deposit and an additional potential vein. Resistivity data also shows a similar pattern which was previously detected by VLF method.

Schlumberger vertical sounding technique was used during the USA CRREL tunnel survey. Data indicates that depth to the bedrock at site I ranges from 11 to 22 ft. The measurement is smaller than the true geologic setting in the area. This is probably due to the interpretation process. The RESISTIVITY program simulates a vertical sounding curve based upon the theoretical subsurface configuration. Three parameters, number of layers, depth and resistivity, must be defined before the computation begins. Any combination of these three parameters with the least deviation from the field data during an attempt will be selected. Nevertheless, this best fitting model may not truly represent the field layering arrangement. By changing the theoretical subsurface configuration such as subdividing one layer into several sublayers,

the best fitting model will be changed accordingly. Therefore, direct interpretation of the vertical resistivity sounding data should be made in conjunction with other information.

Vertical resistivity sounding was also conducted at site II. Four tracks were investigated and data indicate that the depth to the second layer ranges from 50 to 61 ft. This measurement is very consistent to the drilling data.

From this performance evaluation study the advantages and disadvantages of the both geophysical exploration methods are summarized as follows:

1. The seismic refraction proves itself a good method for determining the depth of gold deposit in permafrost free area. Survey conducted in frozen ground may not be able to accurately detect the gravel-bedrock contact because of the small variation between the gravel and bedrock velocity.
2. The SEISMIC computer program processes data without relying on any preassumed condition. Prospectors with little experience can easily interpret the field data and obtain the summarized results.
3. The Schlumberger array and Wenner arrangement produce very consistent results. In the field Schlumberger method seems easier to use because only the current electrodes are moved.
4. The profiling technique can successfully obtain subsurface geology of an area where the horizontal variation is large. Gold-bearing quartz vein deposit are detected using this method.
5. The vertical resistivity sounding technique produces results with some deviation. The limitations of the sounding method primarily lie in the limited accuracy of computing vertical electric sounding

curves by convolution and using Ghosh's inverse filter coefficients and the predefined layering information.

6. The RESISTIVITY program processes ten sounding curves covering three logarithmic cycles in about 2 minutes on a microcomputer. This makes the method very suitable for the processing of large numbers of field data. Due to the limited accuracy of the theory used, the resistivity method should be used in conjunction with other information.

REFERENCES

Anderson. L. A. and Johnson. G. R., Application of magnetic and electrical resistivity methods to placer investigations in the Fairbanks district, Alaska, U.S. Geol. Survey, Prof. Paper 700-C, pp C107-113, 1970.

_____, Induced polarization and resistivity surveys on Cleary Summit, Alaska, U.S. Geol. Survey, Prof. Paper 700-D, pp. D125-128, 1970.

Balen, M. D., personal communication, 1984.

Brown, J. M., Bedrock geology and ore deposits of the Pedro Dome area, Fairbanks mining district, Alaska, unpublished M.S. Thesis, Univ. of Alaska, Fairbanks, 137 p., 1962.

Eakins, G. R. and others, Alaska's mineral industry, 1982, Alaska Division of Geol. & Geophy. Surveys, Special Report 31, 1983.

Forbes, R. B., Bedrock geology and petrology of the Fairbanks mining district, Alaska, Alaska Division of Geol. & Geophy. Surveys, Open-file Report 169, 1982.

Metz, P. A., Bedrock geology of the Fairbanks mining district, Northeast sector, Alaska Division of Geol. & Geophy. Surveys, AOF-154, 1979.

Mota, L., Determination of dips and depths of geological layers by the seismic refraction method, Geophysics, v. 19, pp. 242-254, 1954.

Sellmann, P. V., Geology of the USA CRREL permafrost tunnel, Fairbanks. Alaska, USA CRREL Technical Report TR 199, 1967.

Wescott, E. M., Evaluation of geophysical methods in the Fairbanks mining district, Alaska, Division of Geol. & Geophy. Surveys, Open-file Report 171, 1982.

Zohdy, A. A. R., A computer program for the calculation of Schlumberger sounding curves by convolution, NTIS PB-232056, 1974.

APPENDIX A

SEISMIC program and the example problem

```
1000 REM ***********************************************
1010 REM ***                                             ***
1020 REM *** SEISMIC REFRACTION INTERPRETATION           ***
1030 REM ***                                             ***
1040 REM *** PROGRAMMED BY SCOTT L. HUANG  7/10/83       ***
1050 REM ***                                             ***
1060 REM *** THE SEISMIC PROGRAM CAN CALCULATE THE       ***
1070 REM *** WAVE VELOCITY, THICKNESS, DIP ANGLE         ***
1080 REM *** AND DEPTH OF THE REFRACTOR.  THE SUB-       ***
1090 REM *** SURFACE STRUCTURE CAN BE ESTIMATED,         ***
1100 REM *** HOWEVER, THE ACCURACY IS DEPENDENT ON       ***
1110 REM *** THE ASSUMPTION MADE.  MAXIMUM DATA          ***
1120 REM *** POINT FOR THE PROGRAM IS 50 SETS FOR        ***
1130 REM *** EACH DIRECTION OF SHOOTING.  TOPOGRA-       ***
1140 REM *** PHIC CORRECTION CAN BE APPLIED.             ***
1150 REM ***********************************************
1160 PRINT TAB(27);"*************************"
1170 PRINT TAB(27);"*                       *"
1180 PRINT TAB(27);"*   SEISMIC REFRACTION  *"
1190 PRINT TAB(27);"*                       *"
1200 PRINT TAB(27);"*************************"
1210 LPRINT TAB(27);"*************************"
1220 LPRINT TAB(27);"*                       *"
1230 LPRINT TAB(27);"*   SEISMIC REFRACTION  *"
1240 LPRINT TAB(27);"*                       *"
1250 LPRINT TAB(27);"*************************"
1260 PRINT:PRINT:LPRINT:LPRINT
1270 INPUT "TITLE OF THE PROBLEM: ";TIT$
1280 LPRINT "PROBLEM -- ";TIT$
1290 DIM X(2,50),Y(2,50),TX(50),TY(50)
1300 DIM SY(2,50),SX(2,50),SYM$(66),X1$(21)
1310 DIM XD(2,10),A(2,10),B(2,10),V(2,10),R(2,10),M(2)
1320 DIM HS(2,50),THK(10),VA(10),INC(10),DIP(10)
1330 DIM APH(10,10),BET(10,10),GAM(10,10),DEL(10,10)
1340 DIM Z1(10,10),Z2(10,10),H1(10),H2(10)
1350 PRINT "REVERSE SHOOTING (Y/N) ";: INPUT "  ";RS$
1360 IF RS$="Y" THEN RX=2 ELSE RX=1
1370 REM *************************
1380 REM *** ENTER SURVEY DATA ***
1390 REM *************************
1400 FOR J=1 TO RX
1410 I=1
1420 PRINT: PRINT: PRINT:
1430 PRINT:LPRINT:LPRINT
1440 IF J=1 THEN PRINT "*** FORWARD SHOOTING ***"
1450 IF J=1 THEN LPRINT TAB(10);"*** FORWARD SHOOTING ***":LPRINT:LPRINT
1460 IF J=2 THEN PRINT "*** REVERSE SHOOTING ***"
1470 IF J=2 THEN LPRINT TAB(10);"*** REVERSE SHOOTING ***":LPRINT:LPRINT
1480 PRINT "INPUT -1 FOR TIME AND -1 FOR DISTANCE WHEN COMPLETE"
1490 LPRINT "INPUT -1 FOR TIME AND -1 FOR DISTANCE WHEN COMPLETE"
1500 PRINT:LPRINT:PRINT:LPRINT
1510 PRINT TAB(15);"TIME (mSec)";TAB(35);"DISTANCE (Ft)"
1520 LPRINT TAB(15);"TIME (mSec)";TAB(35);"DISTANCE (Ft)"
1530 INPUT Y(J,I),X(J,I)
1540 IF Y(J,I) <0 THEN 1600
1550 PRINT TAB(17);USING"####.##";Y(J,I);
1560 PRINT TAB(38);USING"####.##";X(J,I)
```

```
1570 LPRINT TAB(17);USING"####.##";Y(J,I);
1580 LPRINT TAB(38);USING"####.##";X(J,I)
1590 I=I+1: GOTO 1530
1600 M(J)=I-1
1610 NEXT J
1620 PRINT:PRINT:LPRINT:LPRINT:PRINT TAB(30);"TIME-DISTANCE DIAGRAM"
1630 LPRINT TAB(30);"TIME-DISTANCE DIAGRAM"
1640 FPL$="N"
1650 FOR J=1 TO RX
1660 FOR I=1 TO M(J)
1670 Y(J,I)=Y(J,I)/1000
1680 SY(J,I)=Y(J,I): SX(J,I)=X(J,I)
1690 NEXT I
1700 NEXT J
1710 REM **********************
1720 REM *** COMPUTER PLOT ***
1730 REM **********************
1740 ANA=0
1750 REM
1760 REM *** FIND MAXIMUM X AND Y ***
1770 REM
1780 XMAX=0: YMAX=0
1790 FOR J=1 TO RX
1800 FOR I=1 TO M(J)
1810 IF X(J,I) > XMAX THEN XMAX=X(J,I)
1820 IF Y(J,I) > YMAX THEN YMAX=Y(J,I)
1830 NEXT I
1840 NEXT J
1850 REM
1860 REM *** PLOT X- AND Y-AXIS ***
1870 REM
1880 PRINT CHR$(7): PRINT CHR$(26)
1890 FOR J=1 TO 20
1900 YPOS=J
1910 PRINT CHR$(27)"="CHR$(YPOS+32)CHR$(8+32);"1"
1920 PRINT CHR$(27)"="CHR$(YPOS+32)CHR$(73+32);"1"
1930 NEXT J
1940 FOR K=9 TO 73
1950 YPOS=21: XPOS=K
1960 PRINT CHR$(27)"="CHR$(YPOS+32)CHR$(XPOS+32);"-";
1970 NEXT K
1980 REM
1990 REM *** LABEL AND TIC MARK ***
2000 REM
2010 FOR K=13 TO 73 STEP 5
2020 YPOS=21: XPOS=K
2030 PRINT CHR$(27)"="CHR$(YPOS+32)CHR$(XPOS+32);"+";
2040 NEXT K
2050 I=0
2060 FOR J=1 TO 21 STEP 5
2070 YPOS=J: XPOS=8
2080 YX=YMAX*(1-I/4)
2090 YX=1000*YX
2100 PRINT CHR$(27)"="CHR$(YPOS+32)CHR$(8+32);"+"
2110 PRINT CHR$(27)"="CHR$(YPOS+32)CHR$(73+32);"+"
2120 PRINT CHR$(27)"="CHR$(J+32)CHR$(2+32);USING"###.#";YX
2130 I=I+1
```

```
2140 NEXT J
2150 I=0
2160 FOR K=9 TO 73 STEP 10
2170 XPOS=K-4
2180 XY=XMAX*(2*I/13)
2190 PRINT CHR$(27)"="CHR$(22+32)CHR$(XPOS+32);USING"####.#";XY;
2200 I=I+1
2210 NEXT K
2220 PRINT CHR$(10)
2230 IF RS$="Y" THEN 2240 ELSE 2310
2240 I=0
2250 FOR K=9 TO 73 STEP 10
2260 XPOS=79-K
2270 XY=XMAX*(2*I/13)
2280 PRINT CHR$(27)"="CHR$(22+32)CHR$(XPOS+32);USING"####.#";XY;
2290 I=I+1
2300 NEXT K
2310 REM
2320 REM *** X- AND Y-AXIS NOTES ***
2330 REM
2340 PRINT CHR$(30)
2350 PRINT CHR$(27)"="CHR$(26+32)CHR$(34+32);"DISTANCE (Ft)"
2360 X$(1)="T":X$(2)="I":X$(3)="M":X$(4)="E":X$(5)=" ":X$(6)=","
2370 X$(7)="m":X$(8)="S":X$(9)="e":X$(10)="c"
2380 FOR L=1 TO 10
2390 YPOS=L+5
2400 PRINT CHR$(27)"="CHR$(YPOS+32)CHR$(0+32);X$(L)
2410 NEXT L
2420 REM
2430 REM *** GENERATE GRAPHICAL DISPLAY ***
2440 REM
2450 FOR I=1 TO M(1)
2460 XPOS=8+INT(65*X(1,I)/XMAX)
2470 YPOS=INT(20*(1-Y(1,I)/YMAX))
2480 PRINT CHR$(27)"="CHR$(YPOS+32)CHR$(XPOS+32);"*"
2490 NEXT I
2500 IF RS$="Y" THEN 2510 ELSE 2600
2510 FOR I=1 TO M(2)
2520 XPOS=8+INT(65*(1-X(2,I)/XMAX))
2530 YPOS=INT(20*(1-Y(2,I)/YMAX))
2540 PRINT CHR$(27)"="CHR$(YPOS+32)CHR$(XPOS+32);"o"
2550 NEXT I
2560 REM
2570 REM *** HARDCOPY GRAPHIC DISPLAY ***
2580 REM
2590 LPRINT: LPRINT
2600 FOR I=1 TO RX
2610 NN=M(I)-1
2620 FOR J=1 TO NN
2630 LL1=J: LL2=J+1
2640 FOR I3=LL2 TO M(I)
2650 IF SY(I,LL1) > SY(I,I3) GOTO 2670
2660 LL1=I3
2670 NEXT I3
2680 CHY=SY(I,LL1): CHX=SX(I,LL1)
2690 SY(I,LL1)=SY(I,J): SX(I,LL1)=SX(I,J)
2700 SY(I,J)=CHY: SX(I,J)=CHX
```

```
2710 NEXT J
2720 NEXT I
2730 FOR I=1 TO 21
2740 X1$(I)=" "
2750 NEXT I
2760 FOR J=6 TO 15
2770 X1$(J)=X$(J-5)
2780 NEXT J
2790 CO1=0
2800 FOR CL=1 TO 21
2810 FOR RK=1 TO 66
2820 SYM$(RK)=" "
2830 NEXT RK
2840 FOR I=1 TO M(1)
2850 YP=1+INT(20*(1-SY(1,I)/YMAX))
2860 IF YP=CL THEN XP=1+INT(64*SX(1,I)/XMAX): SYM$(XP)="*"
2870 NEXT I
2880 IF R$$="Y" THEN 2890 ELSE 2930
2890 FOR I=1 TO M(2)
2900 YP=1+INT(20*(1-SY(2,I)/YMAX))
2910 IF YP=CL THEN XP=2+INT(64*(1-SX(2,I)/XMAX)): SYM$(XP)="o"
2920 NEXT I
2930 IF ((CL=1)OR(CL=6)OR(CL=11)OR(CL=16)) THEN 2940 ELSE 3020
2940 SYM$(1)="+": SYM$(66)="+"
2950 YX1=YMAX*(1-CO1/4)*1000
2960 LPRINT TAB(1);X1$(CL);TAB(3);USING"###.#";YX1;
2970 FOR RK=1 TO 66
2980 LPRINT TAB(8+RK);SYM$(RK);
2990 NEXT RK
3000 CO1=CO1+1
3010 GOTO 3220
3020 IF CL=21 GOTO 3090
3030 SYM$(1)="I": SYM$(66)="I"
3040 LPRINT TAB(1);X1$(CL);
3050 FOR RK=1 TO 66
3060 LPRINT TAB(8+RK);SYM$(RK);
3070 NEXT RK
3080 GOTO 3220
3090 FOR RK=1 TO 66
3100 SYM$(RK)="-"
3110 NEXT RK
3120 FOR RK2=0 TO 13
3130 SYM$(5*RK2+1)="+"
3140 IF J=2 THEN PRINT:PRINT "-- REVERSE SHOOTING --":PRINT
3150 IF J=2 THEN LPRINT:LPRINT "-- REVERSEA SHOOTING --":LPRINT
3160 NEXT RK2
3170 YX1=0
3180 LPRINT TAB(1);X1$(CL);TAB(3);USING"###.#";YX1;
3190 FOR RK=1 TO 66
3200 LPRINT TAB(8+RK);SYM$(RK);
3210 NEXT RK
3220 NEXT CL
3230 LPRINT: II=0
3240 FOR RK3=1 TO 13 STEP 2
3250 XY=XMAX*(2*II/13)
3260 LPRINT TAB(6+10*II);USING"####.#";XY;
3270 II=II+1: NEXT RK3
```

```
3280 IF RS$="Y" THEN 3290 ELSE 3340
3290 KK=6: II=0
3300 FOR RK3=1 TO 13 STEP 2
3310 XY=XMAX*(2*KK/13)
3320 LPRINT TAB(11+10*II);USING"####.#";XY;
3330 KK=KK-1: II=II+1: NEXT RK3
3340 LPRINT: LPRINT TAB(34);"DISTANCE   (Ft)"
3350 IF FPL$="Y" THEN 4180
3360 NAN=0
3370 REM ****************************
3380 REM *** REGRESSION ANALYSIS ***
3390 REM ****************************
3400 REM
3410 REM *** SELECT CROSS-OVER DISTANCE ***
3420 REM
3430 ANA=ANA+1
3440 PRINT CHR$(27)"="CHR$(27+32)CHR$(2+32);"  "
3450 PRINT: PRINT: PRINT TAB(10);"REGRESSION ANALYSIS -- TRIAL # ";ANA
3460 LPRINT: LPRINT: LPRINT TAB(10);"REGRESSION ANALYSIS -- TRIAL # ";ANA
3470 PRINT "TYPE-IN 26 TO CLEAR THE SCREEN";: INPUT "  ";W
3480 PRINT CHR$(W)
3490 PRINT "ESTIMATE 1ST, 2ND, ....., 10TH CROSS-OVER DISTANCE"
3500 LPRINT "ESTIMATE 1ST, 2ND, ....., 10TH CROSS-OVER DISTANCE"
3510 PRINT "COMPLETE FORWARD SHOOTING FIRST"
3520 LPRINT "COMPLETE FORWARD SHOOTING FIRST"
3530 PRINT "THEN REVERSE SHOOTING IF AVAILABLE"
3540 LPRINT "THEN REVERSE SHOOTING IF AVAILABLE"
3550 PRINT:PRINT:LPRINT:LPRINT
3560 PRINT "INPUT THE MAXIMUM DISTANCE WHEN FINISH": PRINT
3570 LPRINT "INPUT THE MAXIMUM DISTANCE WHEN FINISH": LPRINT
3580 FOR J=1 TO RX
3590 IF J=1 THEN PRINT "INPUT CROSS-OVER DISTANCE FOR FORWARD SHOOTING"
3600 IF J=1 THEN LPRINT "INPUT CROSS-OVER DISTANCE FOR FORWARD SHOOTING"
3610 IF J=2 THEN PRINT:LPRINT
3620 IF J=2 THEN PRINT "INPUT CROSS-OVER DISTANCE FOR REVERSE SHOOTING"
3630 IF J=2 THEN LPRINT "INPUT CROSS-OVER DISTANCE FOR REVERSE SHOOTING"
3640 PRINT:LPRINT
3650 I=1
3660 PRINT "CROSS-OVER DISTANCE # ";I;: INPUT "  ";XD(J,I)
3670 LPRINT "CROSS-OVER DISTANCE # ";I;"  ";XD(J,I);" (Ft)"
3680 IF XD(J,I) >= XMAX GOTO 3700
3690 I=I+1: GOTO 3660
3700 NEXT J
3710 KC=I
3720 FOR J=1 TO RX
3730 PRINT: LPRINT
3740 IF J=1 THEN PRINT "*** FORWARD SHOOTING ***"
3750 IF J=2 THEN PRINT "*** REVERSE SHOOTING ***"
3760 IF J=1 THEN LPRINT "*** FORWARD SHOOTING ***"
3770 IF J=2 THEN LPRINT "*** REVERSE SHOOTING ***"
3780 I1=1
3790 FOR K4=1 TO KC
3800 PRINT: PRINT
3810 I2=1: K1=I1
3820 FOR K=K1 TO M(J)
3830 IF X(J,K) <= XD(J,K4) THEN 3840 ELSE 3870
3840 TX(I2)=X(J,K): TY(I2)=Y(J,K)
```

```
3850 I1=I1+1: I2=I2+1
3860 NEXT K
3870 I2=I2-1
3880 GOSUB 5210
3890 NEXT K4
3900 NEXT J
3910 KKK=0
3920 FOR J=1 TO RX
3930 IF J=1 THEN PRINT:PRINT "-- FORWARD SHOOTING --":PRINT
3940 IF J=1 THEN LPRINT:LPRINT "-- FORWARD SHOOTING --":LPRINT
3950 FOR K4=1 TO KC-1
3960 IF V(J,K4) > V(J,K4+1) THEN 3970 ELSE 4040
3970 PRINT "LOW VELOCITY ZONE AT ";K4+1;" LAYER --- TRY REGRESSION AGAIN"
3980 PRINT "TREAT LAYERS ";K4;" AND ";K4+1;" AS A SINGLE FORMATION "
3990 PRINT "IF THE VELOCITY DIFFERENCE IS SMALL"
4000 LPRINT "LOW VELOCITY ZONE AT ";K4+1;" LAYER --- TRY REGRESSION AGAIN"
4010 LPRINT "TREAT LAYERS ";K4;" AND ";K4+1;" AS A SINGLE FORMATION "
4020 LPRINT "IF THE VELOCITY DIFFERENCE IS SMALL"
4030 KKK=KKK+1
4040 NEXT K4: NEXT J
4050 IF KKK >= 1 THEN ANA=0: GOTO 1850
4060 PRINT:PRINT "TRY REGRESSION AGAIN (Y/N) ";: INPUT "  ";TR$:PRINT
4070 LPRINT:LPRINT "TRY REGRESSION AGAIN (Y/N)? ";TR$:LPRINT
4080 IF TR$="Y" GOTO 1850
4090 PRINT
4100 PRINT "ELEVATION CORRECTION (Y/N) ";: INPUT "  ";AN$:PRINT
4110 LPRINT "ELEVATION CORRECTION (Y/N)? ";AN$:LPRINT
4120 IF AN$="Y" THEN GOSUB 5640 ELSE 4140
4130 GOTO 1710
4140 PRINT
4150 PRINT "REGRESSION LINE PLOT (Y/N) ";: INPUT "  ";FPL$:PRINT
4160 LPRINT "REGRESSION LINE PLOT (Y/N)? ";FPL$:LPRINT
4170 IF FPL$="Y" GOTO 1710
4180 REM
4190 REM *** CROSS-OVER DISTANCE DETERMINATION ***
4200 REM
4210 FOR J=1 TO RX
4220 FOR I=1 TO KC-1
4230 IF ABS(A(J,I)-A(J,I+1)) <=.0001 THEN 4250 ELSE 4240
4240 XD(J,I)=(B(J,I+1)-B(J,I))/(A(J,I)-A(J,I+1))
4250 NEXT I
4260 NEXT J
4270 IF FPL$="N" GOTO 4450
4280 REM ****************************
4290 REM *** PLOT REGRESSION LINE ***
4300 REM ****************************
4310 FOR J=1 TO RX
4320 I7=1
4330 FOR K3=1 TO KC
4340 IND=XD(J,K3)/XMAX*65
4350 FOR I=I7 TO IND
4360 X2=I/IND*XD(J,K3)
4370 IF J=1 THEN XPOS=I+8 ELSE XPOS=74-I
4380 Y2=X2*A(J,K3)+B(J,K3)
4390 YPOS=1+INT(19*(1-Y2/(YMAX*1000)))
4400 PRINT CHR$(27)"="CHR$(YPOS+32)CHR$(XPOS+32),"-"
4410 NEXT I
```

```
4420 I7=INT(IND)+1
4430 NEXT K3
4440 NEXT J
4450 REM
4460 REM *** PRINT CROSS-OVER DISTANCE ***
4470 REM
4480 PRINT CHR$(27)"="CHR$(25+32)CHR$(2+32)
4490 PRINT: PRINT: LPRINT: LPRINT
4500 PRINT TAB(10);"CROSS-OVER DISTANCE DETERMINATION":PRINT:PRINT
4510 LPRINT TAB(10);"CROSS-OVER DISTANCE DETERMINATION":LPRINT:LPRINT
4520 PRINT "*** FORWARD SHOOTING ***": PRINT
4530 LPRINT "*** FORWARD SHOOTING ***": LPRINT
4540 FOR J=1 TO RX
4550 IF J=2 THEN PRINT "*** REVERSE SHOOTING ***": PRINT
4560 IF J=2 THEN LPRINT "*** REVERSE SHOOTING ***": LPRINT
4570 FOR I=1 TO KC-1
4580 ZTT(J,I)=0: THDX(J,I)=0
4590 IF ABS(A(J,I)-A(J,I+1)) <=.0001 THEN 4660 ELSE 4600
4600 PRINT "NO # ";I;" CROSS-OVER DISTANCE (Ft) = ";XD(J,I): PRINT
4610 LPRINT "NO # ";I;" CROSS-OVER DISTANCE (Ft) = ";XD(J,I): LPRINT
4620 GOTO 4800
4630 REM
4640 REM *** CALCULATION OF UP OR DOWN THROW ***
4650 REM
4660 THDX(J,I)=I
4670 TDIF=B(J,I)-B(J,I+1)
4680 VAD=V(J,I)+V(J,I-1)
4690 VMN=V(J,I)-V(J,I-1)
4700 ZT=TDIF*SQR(VAD/VMN)*V(J,I-1)/1000
4710 ZTT(J,I)=ABS(ZT)
4720 PRINT "POSSIBLE STRUCTURE AROUND ";XD(J,I);" Ft FROM STARTING POINT"
4730 LPRINT "POSSIBLE STRUCTURE AROUND ";XD(J,I);" Ft FROM STARTING POINT"
4740 IF ZT < 0 THEN 4750 ELSE 4780
4750 PRINT "AMOUNT OF DOWN THROW IS ";ABS(ZT);" Ft": PRINT
4760 LPRINT "AMOUNT OF DOWN THROW IS ";ABS(ZT);" Ft": LPRINT
4770 GOTO 4800
4780 PRINT "AMOUNT OF UP THROW IS ";ABS(ZT);" Ft": PRINT
4790 LPRINT "AMOUNT OF UP THROW IS ";ABS(ZT);" Ft": LPRINT
4800 NEXT I
4810 NEXT J
4820 REM ****************************
4830 REM *** THICKNESS ESTIMATION ***
4840 REM ****************************
4850 IF RS$="Y" THEN 5190 ELSE 4860
4860 PRINT: PRINT TAB(10);"*** SUMMARIZED INFORMATION ***"
4870 LPRINT: LPRINT TAB(10);"*** SUMMARIZED INFORMATION ***"
4880 THK(0)=0: SUMD=0
4890 FOR I=1 TO KC-1
4900 SUM=0: L=I
4910 PRINT: PRINT "LAYER # ";I;: PRINT
4920 LPRINT: LPRINT "LAYER # ";I;: LPRINT
4930 IF THDX(1,I)=1 THEN 5120 ELSE 4940
4940 FOR J=1 TO I
4950 SUM1=V(1,I+1)^2-V(1,I-L)^2
4960 SUM1=SQR(SUM1)
4970 IF V(1,I-L)=0 THEN V(1,I-L)=1
4980 CAL=(2*THK(I-L)*SUM1)/(V(1,I+1)*V(1,I-L))
```

```
4990 SUM=SUM+CAL
5000 L=L-1
5010 NEXT J
5020 RT=V(1,I+1)^2-V(1,I)^2
5030 THK(I)=.5*(B(1,I+1)/1000-SUM)*(V(1,I+1)*V(1,I))/SQR(RT)
5040 PRINT "VELOCITY (Ft/Sec) = ";V(1,I)
5050 SUMD=SUMD+THK(I)
5060 SUMD=SUMD+ZTT(1,I)
5070 PRINT "THICKNESS OF BED (Ft) = ";THK(I)
5080 PRINT "DEPTH OF BED (Ft) = ";SUMD
5090 LPRINT "VELOCITY (Ft/Sec) = ";V(1,I)
5100 LPRINT "THICKNESS OF BED (Ft) = ";THK(I)
5110 LPRINT "DEPTH OF BED (Ft) = ";SUMD: GOTO 5140
5120 PRINT "VELOCITY (Ft/Sec) = ";V(1,I): PRINT "THROW (Ft) = ";ZTT(1,I)
5130 LPRINT "VELOCITY (Ft/Sec) = ";V(1,I): LPRINT "THROW (Ft) =";ZTT(1,I)
5140 NEXT I
5150 KKK1=THDX(1,I-1)+1: IF KC=KKK1 THEN 5200 ELSE 5160
5160 LPRINT:LPRINT "LAYER # ";KC:LPRINT "VELOCITY (Ft/Sec) = ";V(1,KC)
5170 PRINT:PRINT "LAYER # ";KC:PRINT "VELOCITY (Ft/Sec) = ";V(1,KC)
5180 GOTO 5200
5190 GOSUB 6090
5200 END
5210 REM ************************************
5220 REM *** LINEAR REGRESSION SUBROUTINE ***
5230 REM ************************************
5240 C1=0: C2=0: D1=0: D2=0: D3=0
5250 S1=S2=S3=0
5260 FOR I=1 TO I2
5270 C1=C1+TX(I): C2=C2+TX(I)^2
5280 D1=D1+TY(I): D2=D2+TX(I)*TY(I): D3=D3+TY(I)^2
5290 NEXT I
5300 REM
5310 REM *** SOLVE FOR UNKNOWN CONSTANTS ***
5320 REM
5330 A(J,K4)=(I2*D2-C1*D1)/(I2*C2-C1^2)
5340 B(J,K4)=(D1-C1*A(J,K4))/I2
5350 A(J,K4)=A(J,K4)*1000: B(J,K4)=B(J,K4)*1000
5360 REM
5370 REM *** PRINT FINAL REGRESSION EQUATION ***
5380 REM
5390 PRINT
5400 LPRINT: LPRINT
5410 LPRINT "REGRESSION EQUATION FOR # ";K4;" LAYER (Y IN mSec & X IN Ft)"
5420 PRINT "REGRESSION EQUATION FOR # ";K4;" LAYER (Y IN mSec & X IN Ft)"
5430 IF B(J,K4) >=0 THEN LPRINT "Y = ";A(J,K4);" * X + ";B(J,K4): GOTO 5440
5440 IF B(J,K4) >=0 THEN PRINT "Y = ";A(J,K4);" * X + ";B(J,K4): GOTO 5480
5450 LPRINT "Y = ";A(J,K4);" * X - ";ABS(B(J,K4))
5460 PRINT "Y = ";A(J,K4);" * X - ";ABS(B(J,K4))
5470 REM
5480 REM *** SOLVE FOR CORRELATION COEFFICIENT ***
5490 REM
5500 S1=I2*C2-C1^2: S2=I2*D3-D1^2: S3=I2*D2-C1*D1
5510 R(J,K4)=S3/SQR(S1*S2)
5520 IF ABS(1-R(J,K4)) <=.0001 THEN R(J,K4)=1
5530 PRINT "CORRELATION COEFFICIENT IS ";R(J,K4)
5540 LPRINT "CORRELATION COEFFICIENT IS ";R(J,K4)
5550 REM
```

```
5560 REM *** ESTIMATE VELOCITY ***
5570 REM
5580 IF ABS(A(J,K4)) <=.0001 THEN PRINT "NO ANSWER FOR VELOCITY": GOTO 5620
5590 V(J,K4)=1000/A(J,K4)
5600 PRINT "VELOCITY (Ft/Sec) = ";V(J,K4)
5610 LPRINT "VELOCITY (Ft/Sec) = ";V(J,K4)
5620 RETURN
5630 REM ****************************************
5640 REM *** ELEVATION CORRECTION SUBROUTINE ***
5650 REM ****************************************
5660 PRINT
5670 PRINT "SELECT DATUM PLANE ELEVATION (Ft): ";: INPUT DAT
5680 LPRINT "SELECT DATUM PLANE ELEVATION (Ft): ";DAT
5690 FOR J=1 TO RX
5700 IF J=1 THEN PRINT:PRINT TAB(10);"FORWARD SHOOTING"
5710 IF J=1 THEN LPRINT:LPRINT TAB(10);"FORWARD SHOOTING"
5720 IF J=2 THEN PRINT:PRINT "REVERSE SHOOTING"
5730 IF J=2 THEN LPRINT:LPRINT "REVERSE SHOOTING"
5740 PRINT: PRINT "ENERGY SOURCE ELEVATION (Ft) ";: INPUT GS
5750 LPRINT: LPRINT "ENERGY SOURCE ELEVATION (Ft) ";GS
5760 PRINT: PRINT "INPUT GEOPHONE ELEVATION (Ft) FOR "
5770 LPRINT: LPRINT "INPUT GEOPHONE ELEVATION (Ft) FOR "
5780 PRINT "TOPOGRAPHIC CORRECTION "
5790 LPRINT "TOPOGRAPHIC CORRECTION "
5800 FOR I=1 TO M(J)
5810 PRINT "GEOPHONE STATION:  ";: INPUT HS(J,I)
5820 LPRINT "GEOPHONE STATION:  ";HS(J,I)
5830  NEXT I
5840 PRINT:PRINT:PRINT:LPRINT:LPRINT:LPRINT
5850 PRINT TAB(3);"TIME-DISTANCE DIAGRAM -- TOPOGRAPHY CORRECTION"
5860 LPRINT TAB(3);"TIME-DISTANCE DIAGRAM -- TOPOGRAPHY CORRECTION"
5870 I1=1
5880 FOR I=1 TO M(J)
5890 IF X(J,I) <=XD(J,1) THEN 5900 ELSE 5930
5900 DIF=GS-HS(J,I): LD=X(J,I)^2-DIF^2: LD=SQR(LD)
5910 Y(J,I)=Y(J,I)*(LD/X(J,I)): I1=I1+1
5920 NEXT I
5930 IF KC =1 THEN 6070
5940 FOR JJ=2 TO KC
5950 I2=I1
5960 FOR I=I1 TO M(J)
5970 IF X(J,I) <= XD(J,JJ) THEN 5980 ELSE 6050
5980 EC1=(GS+HS(J,I)-2*DAT)
5990 EC2=V(J,JJ)^2-V(J,1)^2
6000 EC3=SQR(EC2)/(V(J,JJ)*V(J,1))
6010 EC=EC1*EC3
6020 Y(J,I)=Y(J,I)-EC
6030 I2=I2+1
6040 NEXT I
6050 I1=I2
6060 NEXT JJ
6070 NEXT J
6080 RETURN
6090 REM ************************************
6100 REM *** DIP AND THICKNESS SUBROUTINE ***
6110 REM ************************************
6120 FOR I=0 TO 10
```

```
6130 FOR J=0 TO 10
6140 Z1(I,J)=0: Z2(I,J)=0
6150 NEXT J
6160 NEXT I
6170 VA(1)=.5*(V(1,1)+V(2,1))
6180 TRA1=V(1,2)^2-VA(1)^2
6190 TRA2=V(2,2)^2-VA(1)^2
6200 INC(1)=.5*(ATN(VA(1)/SQR(TRA1))+ATN(VA(1)/SQR(TRA2)))
6210 APH(1,1)=INC(1): BET(1,1)=INC(1)
6220 DIP(1)=.5*(ATN(VA(1)/SQR(TRA2))-ATN(VA(1)/SQR(TRA1)))
6230 VA(2)=VA(1)/SIN(INC(1))
6240 N=KC-1
6250 FOR L=2 TO N
6260 FOR P=2 TO L
6270 IF P=2 THEN 6280 ELSE 6310
6280 APH(L,P-1)=ATN(VA(1)/SQR(V(2,L+1)^2-VA(1)^2))-DIP(1)
6290 BET(L,P-1)=ATN(VA(1)/SQR(V(1,L+1)^2-VA(1)^2))+DIP(1)
6300 GOTO 6330
6310 APH(L,P-1)=GAM(L,P-2)-DIP(P-1)+DIP(P-2)
6320 BET(L,P-1)=DEL(L,P-2)+DIP(P-1)-DIP(P-2)
6330 D=VA(P)/VA(P-1)*SIN(APH(L,P-1))
6340 GAM(L,P-1)=ATN(D/SQR(1-D*D))
6350 E=VA(P)/VA(P-1)*SIN(BET(L,P-1))
6360 DEL(L,P-1)=ATN(E/SQR(1-E*E))
6370 NEXT P
6380 INC(L)=.5*(GAM(L,L-1)+DEL(L,L-1))
6390 APH(L,L)=INC(L): BET(L,L)=INC(L)
6400 DIP(L)=.5*(GAM(L,L-1)-DEL(L,L-1))+DIP(L-1)
6410 VA(L+1)=VA(L)/SIN(INC(L))
6420 NEXT L
6430 N=KC-1
6440 Z1(1,1)=VA(1)*(B(1,2)/1000)/(2*COS(INC(1)))
6450 Z2(1,1)=VA(1)*(B(2,2)/1000)/(2*COS(INC(1)))
6460 FOR J=1 TO N
6470 Z1(J,1)=Z1(1,1): Z2(J,1)=Z2(1,1)
6480 NEXT J
6490 FOR L=2 TO N
6500 IF L=2 GOTO 6690
6510 FOR P=2 TO L-1
6520 SUMP=0: SUMT=0: I=1
6530 IF P=2 GOTO 6630
6540 PR1=1
6550 FOR R1=I TO P-2
6560 PR1=PR1*(COS(DIP(R1+1)-DIP(R1)))
6570 NEXT R1
6580 QX1=Z1(L-1,I)*TAN(APH(L-1,I))-Z1(L,I)*TAN(APH(L,I))
6590 QX3=Z2(L-1,I)*TAN(BET(L-1,I))-Z2(L,I)*TAN(BET(L,I))
6600 SUMP=SUMP+QX1*PR1: SUMT=SUMT+QX3*PR1
6610 I=I+1
6620 IF I <=P-2 THEN 6540
6630 QX2=Z1(L-1,P-1)*TAN(APH(L-1,P-1))-Z1(L,P-1)*TAN(APH(L,P-1))
6640 QX4=Z2(L-1,P-1)*TAN(BET(L-1,P-1))-Z2(L,P-1)*TAN(BET(L,P-1))
6650 SUMP=SUMP+QX2: SUMT=SUMT+QX4
6660 Z1(L,P)=Z1(L-1,P)+SUMP*SIN(DIP(P)-DIP(P-1))
6670 Z2(L,P)=Z2(L-1,P)+SUMT*SIN(DIP(P)-DIP(P-1))
6680 NEXT P
6690 SUM1=0: SUM2=0
```

```
6700 FOR P=1 TO L
6710 QM3=Z2(L,P-1)*(COS(APH(L,P-1)+BET(L,P-1))+1)
6720 QM1=Z1(L,P-1)*(COS(APH(L,P-1)+BET(L,P-1))+1)
6730 IF P=1 THEN 6740 ELSE 6750
6740 QM2=1: QM4=1: GOTO 6770
6750 QM2=VA(P-1)*COS(APH(L,P-1))
6760 QM4=VA(P-1)*COS(BET(L,P-1))
6770 QM=QM1/QM2
6780 YM=QM3/QM4
6790 SUM1=SUM1+QM
6800 SUM2=SUM2+YM
6810 NEXT P
6820 Z1(L,L)=VA(L)*(B(1,L+1)/1000-SUM1)/(2*COS(INC(L)))
6830 Z2(L,L)=VA(L)*(B(2,L+1)/1000-SUM2)/(2*COS(INC(L)))
6840 NEXT L
6850 FOR L=1 TO N
6860 SUM3=0: SUM4=0
6870 FOR P=1 TO L
6880 FM1=Z1(L,P)*COS(APH(L,P)-DIP(L)+DIP(P))/COS(APH(L,P))
6890 FM2=Z2(L,P)*COS(BET(L,P)+DIP(L)-DIP(P))/COS(BET(L,P))
6900 SUM3=SUM3+FM1
6910 SUM4=SUM4+FM2
6920 NEXT P
6930 H1(L)=SUM3/COS(DIP(L))
6940 H2(L)=SUM4/COS(DIP(L))
6950 NEXT L
6960 PRINT: PRINT "*** SUMMARIZED INFORMATION ***"
6970 LPRINT: LPRINT "*** SUMMARIZED INFORMATION ***"
6980 FOR L=1 TO KC-1
6990 PRINT: PRINT "LAYER # ";L;: PRINT
7000 LPRINT: LPRINT "LAYER # ";L;: LPRINT
7010 PRINT "VELOCITY (Ft/Sec) = ";VA(L)
7020 LPRINT "VELOCITY (Ft/Sec) = ";VA(L)
7030 DEG=DIP(L)*360/(2*3.14159)
7040 PRINT "DIP OF NO. ";L;" REFRACTOR (Degree) = ";DEG
7050 LPRINT "DIP OF NO. ";L;" REFRACTOR (Degree) = ";DEG
7060 PRINT "THICKNESS OF BED NEAR STARTING POINT (Ft) = ";Z1(L,L)
7070 LPRINT "THICKNESS OF BED NEAR STARTING POINT (Ft) = ";Z1(L,L)
7080 PRINT "THICKNESS OF BED NEAR ENDING POINT (Ft) =";Z2(L,L)
7090 LPRINT "THICKNESS OF BED NEAR ENDING POINT (Ft) = ";Z2(L,L)
7100 PRINT "DEPTH OF BED AT STARTING POINT (Ft) = ";H1(L)
7110 LPRINT "DEPTH OF BED AT STARTING POINT (Ft) = ";H1(L)
7120 PRINT "DEPTH OF BED AT ENDING POINT (Ft) = ";H2(L)
7130 LPRINT "DEPTH OF BED AT ENDING POINT (Ft) = ";H2(L)
7140 NEXT L
7150 PRINT: PRINT "LAYER # ";KC;: PRINT
7160 LPRINT: LPRINT "LAYER # ";KC;: LPRINT
7170 PRINT "VELOCITY (Ft/Sec) = ";VA(KC)
7180 LPRINT "VELOCITY (Ft/Sec) = ";VA(KC)
7190 RETURN
```

```
**************************
*                        *
*   SEISMIC REFRACTION   *
*                        *
**************************
```

PROBLEM -- EXAMPLE RUN FOR SEISMIC SURVEY

*** FORWARD SHOOTING ***

INPUT -1 FOR TIME AND -1 FOR DISTANCE WHEN COMPLETE

TIME (mSec)	DISTANCE (Ft)
15.00	164.00
20.63	213.30
25.00	264.50
30.50	311.70
35.00	360.90
37.63	410.10
42.50	459.30
46.25	508.50
50.00	557.70
55.00	606.90
57.50	656.10

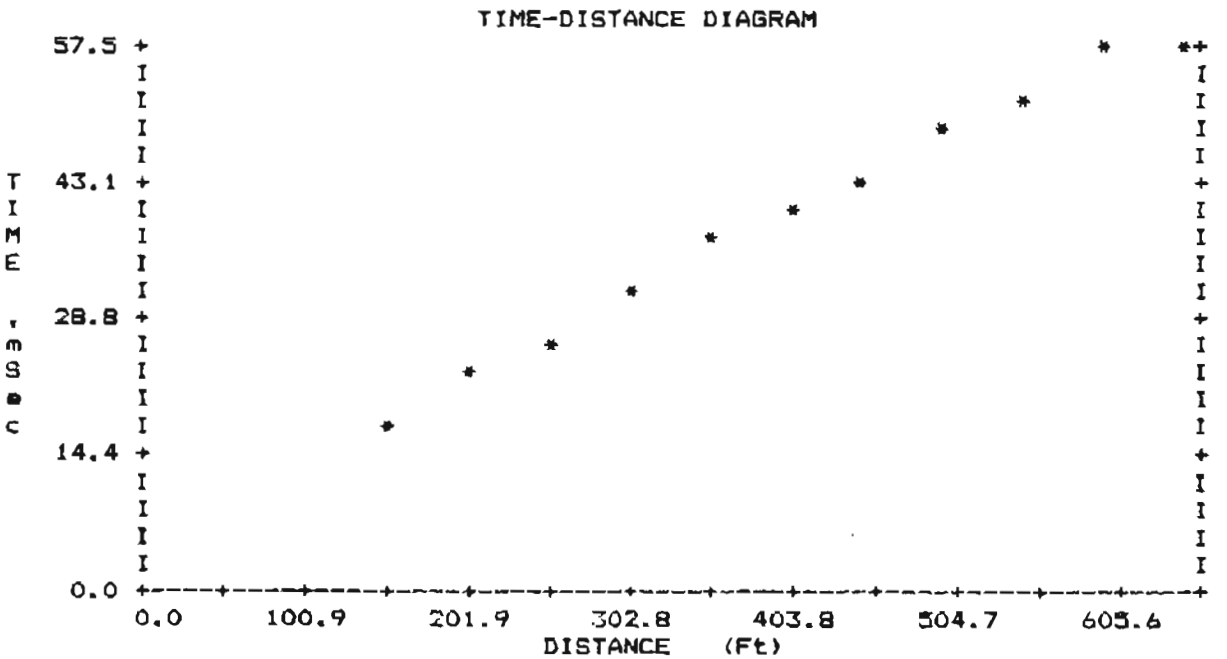

```
        REGRESSION ANALYSIS -- TRIAL #  1
ESTIMATE 1ST, 2ND, ...., 10TH CROSS-OVER DISTANCE
COMPLETE FORWARD SHOOTING FIRST
THEN REVERSE SHOOTING IF AVAILABLE


INPUT THE MAXIMUM DISTANCE WHEN FINISH

INPUT CROSS-OVER DISTANCE FOR FORWARD SHOOTING

CROSS-OVER DISTANCE #  1    370  (Ft)
CROSS-OVER DISTANCE #  2    520  (Ft)
CROSS-OVER DISTANCE #  3    660  (Ft)

*** FORWARD SHOOTING ***


REGRESSION EQUATION FOR #  1  LAYER (Y IN mSec & X IN Ft)
Y =  .101289  * X -  1.40073
CORRELATION COEFFICIENT IS  .998973
VELOCITY (Ft/Sec) =  9872.79


REGRESSION EQUATION FOR #  2  LAYER (Y IN mSec & X IN Ft)
Y =  .0875936  * X +  1.89491
CORRELATION COEFFICIENT IS  .997172
VELOCITY (Ft/Sec) =  11416.4


REGRESSION EQUATION FOR #  3  LAYER (Y IN mSec & X IN Ft)
Y =  .0762209  * X +  7.90819
CORRELATION COEFFICIENT IS  .981948
VELOCITY (Ft/Sec) =  13119.8

-- FORWARD SHOOTING --


TRY REGRESSION AGAIN (Y/N)? N

ELEVATION CORRECTION (Y/N)? Y

SELECT DATUM PLANE ELEVATION (Ft):  1000

        FORWARD SHOOTING

ENERGY SOURCE ELEVATION (Ft)  1001

INPUT GEOPHONE ELEVATION (Ft) FOR
TOPOGRAPHIC CORRECTION
GEOPHONE STATION:   1001
GEOPHONE STATION:   1000
GEOPHONE STATION:   999.5
GEOPHONE STATION:   1000
GEOPHONE STATION:   1000
GEOPHONE STATION:   1001
GEOPHONE STATION:   1001.5
GEOPHONE STATION:   1000
GEOPHONE STATION:   999
GEOPHONE STATION:   999.5
GEOPHONE STATION:   1000
```

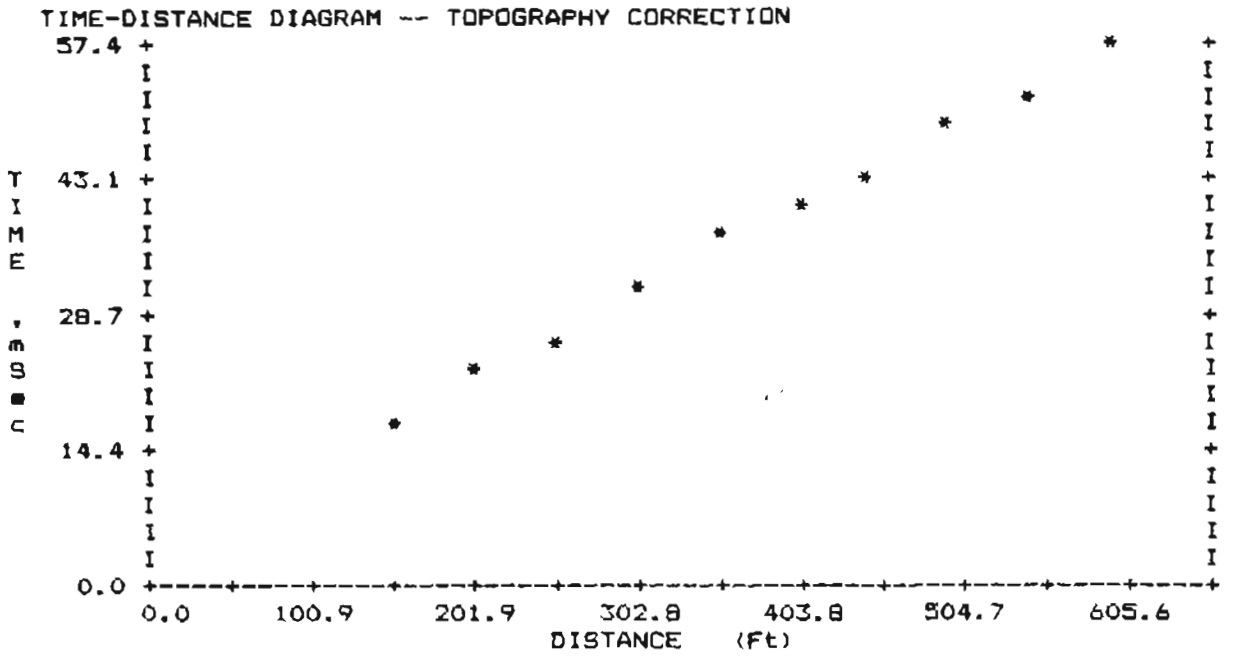


```
        REGRESSION ANALYSIS -- TRIAL #  1
ESTIMATE 1ST, 2ND, ...., 10TH CROSS-OVER DISTANCE
COMPLETE FORWARD SHOOTING FIRST
THEN REVERSE SHOOTING IF AVAILABLE


INPUT THE MAXIMUM DISTANCE WHEN FINISH

INPUT CROSS-OVER DISTANCE FOR FORWARD SHOOTING

CROSS-OVER DISTANCE #  1    380   (Ft)
CROSS-OVER DISTANCE #  2    540   (Ft)
CROSS-OVER DISTANCE #  3    660   (Ft)

*** FORWARD SHOOTING ***


REGRESSION EQUATION FOR #  1  LAYER (Y IN mSec & X IN Ft)
Y =  .101288  * X -  1.40084
CORRELATION COEFFICIENT IS  .998976
VELOCITY (Ft/Sec) =  9872.81


REGRESSION EQUATION FOR #  2  LAYER (Y IN mSec & X IN Ft)
Y =  .0881105  * X +  1.56428
CORRELATION COEFFICIENT IS  .997657
VELOCITY (Ft/Sec) =  11349.4


REGRESSION EQUATION FOR #  3  LAYER (Y IN mSec & X IN Ft)
Y =  .0755422  * X +  8.28674
CORRELATION COEFFICIENT IS  .981661
VELOCITY (Ft/Sec) =  13237.6
```

```
-- FORWARD SHOOTING --

TRY REGRESSION AGAIN (Y/N)? N

ELEVATION CORRECTION (Y/N)? N

REGRESSION LINE PLOT (Y/N)? N


          CROSS-OVER DISTANCE DETERMINATION

*** FORWARD SHOOTING ***

NO #  1  CROSS-OVER DISTANCE (Ft) =  225.009

NO #  2  CROSS-OVER DISTANCE (Ft) =  534.876


          *** SUMMARIZED INFORMATION ***

LAYER #  1
VELOCITY (Ft/Sec) =  9872.81
THICKNESS OF BED (Ft) =  15.6558
DEPTH OF BED (Ft) =  15.6558

LAYER #  2
VELOCITY (Ft/Sec) =  11349.4
THICKNESS OF BED (Ft) =  68.0675
DEPTH OF BED (Ft) =  83.7233

LAYER #  3
VELOCITY (Ft/Sec) =  13237.6
```

APPENDIX B

RESISTIVITY program and the example problem

```
1000 REM ************************************************************
1010 REM ***                                                        ***
1020 REM *** ELECTRIC RESISTIVITY PROGRAM FOR THE SCHLUMBERGER      ***
1030 REM *** SOUNDING SURVEY.  PROGRAMMED BY SCOTT L. HUANG         ***
1040 REM *** 5/20/84.  PORTION OF THE PROGRAM IS MODIFIED FROM      ***
1050 REM *** THE VES PROGRAM.                                      ***
1060 REM ***                                                       ***
1070 REM *** THE RESISTIVITY PROGRAM CALCULATES THE DEPTH AND      ***
1080 REM *** RESISTIVITY OF SUBSURFACE FORMATION BY ASSUMING       ***
1090 REM *** A THEORETICAL CONDITION AND PROGRAM WILL AUTOMA-      ***
1100 REM *** TICALLY ESTIMATE A FIELD APPARENT RESISTIVITY         ***
1110 REM *** CURVE WHICH HAS THE LEAST DEVIATION FROM THE          ***
1120 REM *** ACTURAL FIELD SURVEY CURVE.  TEN ITERATIONS WILL      ***
1130 REM *** BE CONDUCTED FOR EACH COMPUTER RUN.                   ***
1140 REM ***                                                       ***
1150 REM ************************************************************
1160 PRINT TAB(15);"*********************************************"
1170 PRINT TAB(15);"*                                           *"
1180 PRINT TAB(15);"*   RESISTIVITY -- SCHLUMBERGER SOUNDING    *"
1190 PRINT TAB(15);"*                                           *"
1200 PRINT TAB(15);"*********************************************"
1210 LPRINT TAB(15);"*********************************************"
1220 LPRINT TAB(15);"*                                           *"
1230 LPRINT TAB(15);"*   RESISTIVITY -- SCHLUMBERGER SOUNDING    *"
1240 LPRINT TAB(15);"*                                           *"
1250 LPRINT TAB(15);"*********************************************"
1260 PRINT:PRINT:LPRINT:LPRINT
1270 DIM RESIST(50),THICK(50),VV#(50),XAMDA#(50),V(50),VES1#(50),VES2#(50)
1280 DIM DEPTH(50),VES#(50),RADIUS(50),XK#(50),DP(50),RHO(50)
1290 DIM AMDA(50),VV1#(50),VV2#(50),XVES1#(50),XVES2#(50)
1300 DIM SPAC(50),RSQ#(10),DEPTH1(50),RHO1(50),APRH#(50)
1310 PRINT "TITLE FOR THE SURVEY: ";:INPUT TITLE$
1320 LPRINT "TITLE -- ";TITLE$
1330 J=1
1340 PRINT "INPUT APPARENT RESISTIVITY (Ohm-Ft), 1/2 ELECTRODE SPACING (Ft):"
1350 LPRINT "INPUT APPARENT RESISTIVITY (Ohm-Ft), 1/2 ELECTRODE SPACING (Ft):"
1360 PRINT "INPUT -1 FOR RESISTIVITY AND SPACING WHEN COMPLETE"
1370 LPRINT "INPUT -1 FOR RESISTIVITY AND SPACING WHEN COMPLETE"
1380 PRINT:LPRINT
1390 LPRINT TAB(10);"RESISTIVITY";TAB(39);"1/2 SPACING"
1400 PRINT:LPRINT
1410 INPUT APRH#(J),SPAC(J)
1420 IF SPAC(J)=-1 THEN 1450
1430 LPRINT TAB(13);APRH#(J);TAB(43);SPAC(J)
1440 J=J+1: GOTO 1410
1450 NOO=J-1: RADMIN=999999!: RADMAX=0
1460 FOR JJ=1 TO NOO
1470 IF RADMIN >= SPAC(JJ) THEN RADMIN=SPAC(JJ)
1480 IF RADMAX <= SPAC(JJ) THEN RADMAX=SPAC(JJ)
1490 NEXT JJ
1500 PRINT:LPRINT:PRINT:LPRINT
1510 PRINT "ITERATION  (Y/N) ";:INPUT TR$
1520 LPRINT "ITERATION AGAIN (Y/N)? ";TR$
1530 IF TR$="N" THEN 2130
1540 FINAL=0
1550 PRINT "ITERATION UPWARD OR DOWNWARD (UP/DOWN) ";:INPUT ITE$
1560 LPRINT "ITERATION UPWARD OR DOWNWARD (UP/DOWN)? ";ITE$
```

```
1570 IF ITE$="UP" THEN UD=1
1580 IF ITE$="DOWN" THEN UD=-1
1590 PRINT:LPRINT
1600 PRINT "INCREMENTS FOR DEPTH AND RESISTIVITY: ";:INPUT INCD,INCR
1610 LPRINT "INCREMENTS FOR DEPTH AND RESISTIVITY: ";INCD,INCR
1620 LPRINT:PRINT
1630 PRINT "TOTAL NUMBER OF SUBSURFACE LAYERS: ";: INPUT LAYERS
1640 LPRINT "TOTAL NUMBER OF SUBSURFACE LAYERS: ";LAYERS
1650 PRINT "DEPTH (Ft) AND RESISTIVITY (Ohm-Ft): "
1660 LPRINT "DEPTH (Ft) AND RESISTIVITY (Ohm-Ft): "
1670 FOR I=1 TO LAYERS
1680 INPUT DEPTH1(I),RHO1(I)
1690 PRINT TAB(1);DEPTH1(I);TAB(20);RHO1(I)
1700 LPRINT TAB(1);DEPTH1(I);TAB(20);RHO1(I)
1710 NEXT I
1720 FOR LS=1 TO 10
1730 RSQ#(LS)=0
1740 FOR I=1 TO LAYERS
1750 DEPTH(I)=DEPTH1(I)*(1+INCD*(LS-1)*UD)
1760 RHO(I)=RHO1(I)*(1+INCR*(LS-1)*UD)
1770 NEXT I
1780 GOSUB 2140: GOSUB 2460: GOSUB 2730
1790 IF FINAL=0 THEN GOSUB 3480 ELSE 1910
1800 NEXT LS
1810 MIN#=999999!
1820 FOR LS=1 TO 10
1830 IF RSQ#(LS) <= MIN# THEN 1840 ELSE 1850
1840 MIN#=RSQ#(LS): FINAL=LS
1850 NEXT LS
1860 FOR I=1 TO LAYERS
1870 DEPTH(I)=DEPTH1(I)*(1+INCD*(FINAL-1)*UD)
1880 RHO(I)=RHO1(I)*(1+INCR*(FINAL-1)*UD)
1890 NEXT I
1900 GOTO 1780
1910 PRINT:PRINT:PRINT:LPRINT:LPRINT:LPRINT
1920 PRINT TAB(10);"THICKNESS";TAB(26);"DEPTH";TAB(38);"RESISTIVITY"
1930 LPRINT TAB(10);"THICKNESS";TAB(26);"DEPTH";TAB(38);"RESISTIVITY"
1940 PRINT TAB(12);"(Ft)";TAB(27);"(Ft)";TAB(39);"(Ohm-Ft)":PRINT
1950 LPRINT TAB(12);"(Ft)";TAB(27);"(FT)";TAB(39);"(OHM-FT)":LPRINT
1960 FOR I=1 TO LAYERS
1970 PRINT TAB(10);THICK(I);TAB(25);DP(I);TAB(40);RHO(I)
1980 LPRINT TAB(10);THICK(I);TAB(25);DP(I);TAB(40);RHO(I)
1990 NEXT I
2000 PRINT:PRINT:PRINT TAB(10);"1/2 SPACING";TAB(39);"RESISTIVITY"
2010 LPRINT:LPRINT:LPRINT TAB(10);"1/2 SPACING";TAB(39);"RESISTIVITY"
2020 PRINT TAB(13);"(Ft)";TAB(40);"(Ohm-Ft)":PRINT
2030 LPRINT TAB(13);"(Ft)";TAB(40);"(Ohm-Ft)":LPRINT
2040 FOR L=1 TO NRADII
2050 PRINT TAB(11);RADIUS(L);TAB(35);VES#(L)
2060 LPRINT TAB(11);RADIUS(L);TAB(35);VES#(L)
2070 NEXT L
2080 PRINT:PRINT:PRINT "LEAST SQUARE ROOT OF DEVIATION: ";RSQ#(FINAL)
2090 PRINT "AT ";FINAL;" ITERATION"
2100 LPRINT:LPRINT:LPRINT "LEAST SQUARE ROOT OF DEVIATION: ";RSQ#(FINAL)
2110 LPRINT "AT ";FINAL;" ITERATION"
2120 GOTO 1510
2130 END
```

```
2140 REM ***************************
2150 REM *** SPACING SUBROUTINE ***
2160 REM ***************************
2170 THICK(1)=DEPTH(1)
2180 FOR I=2 TO LAYERS
2190 THICK(I)=DEPTH(I)-DEPTH(I-1)
2200 NEXT I
2210 XRATIO#=EXP(LOG(10)/6)
2220 RADIUS(1)=RADMIN
2230 I=2
2240 RADIUS(I)=XRATIO#*RADIUS(I-1)
2250 IF RADIUS(I) >= RADMAX THEN 2280
2260 I=I+1
2270 GOTO 2240
2280 NRADII=I
2290 RADMAX=RADIUS(I)
2300 XMIN=(RADMIN/XRATIO#^10)*1.05
2310 XMAX=(RADMAX*XRATIO#^6)*1.05
2320 XAMDA#(1)=XMIN
2330 I=2
2340 XAMDA#(I)=XRATIO#*XAMDA#(I-1)
2350 IF XMAX-XAMDA#(I) <= 0 THEN 2380 ELSE 2360
2360 I=I+1
2370 GOTO 2340
2380 NRAD=I
2390 NN=LAYERS
2400 SUNN=0
2410 FOR I=1 TO NN
2420 SUNN=SUNN+THICK(I)
2430 DP(I)=SUNN
2440 NEXT I
2450 RETURN
2460 REM ***************************
2470 REM *** KERNEL SUBROUTINE ***
2480 REM ***************************
2490 FOR J=1 TO NRAD
2500 V(J)=1
2510 K=LAYERS-1
2520 KK=LAYERS+1
2530 AMDA(J)=-2/XAMDA#(J)
2540 FOR I=1 TO K
2550 M=KK-I
2560 L=LAYERS-I
2570 P=RHO(M)*V(J)
2580 AK=(RHO(L)-P)/(RHO(L)+P)
2590 PROD=AMDA(J)*THICK(L)
2600 IF PROD < -50 THEN PROD=-50
2610 Q=AK*EXP(PROD)
2620 ABQ=ABS(Q)
2630 IF ABQ <= 0 THEN 2640 ELSE 2660
2640 V(J)=1
2650 GOTO 2670
2660 V(J)=(1-Q)/(1+Q)
2670 NEXT I
2680 NEXT J
2690 FOR J=1 TO NRAD
2700 VV#(J)=V(J)*RHO(1)
```

```
2710 NEXT J
2720 RETURN
2730 REM ************************
2740 REM *** CONVES SUBROUTINE ***
2750 REM ************************
2760 XK#(1)=.0148
2770 XK#(2)=-.0814
2780 XK#(3)=.4018
2790 XK#(4)=-1.5716
2800 XK#(5)=1.972
2810 XK#(6)=.1854
2820 XK#(7)=.1064
2830 XK#(8)=-.0499
2840 XK#(9)=.0225
2850 FOR I=1 TO 50
2860 VV1#(I)=0!
2870 VV2#(I)=0!
2880 NEXT I
2890 NODD=0
2900 NEVEN=0
2910 IF NRAD/2 = INT(NRAD/2) THEN 2950
2920 NODD=NRAD
2930 NN=(NODD+1)/2
2940 GOTO 2980
2950 NEVEN=NRAD
2960 NN=NEVEN/2
2970 GOTO 3060
2980 FOR J=1 TO NN
2990 VV1#(J)=VV#(2*J-1)
3000 NEXT J
3010 MM=NN-1
3020 FOR J=1 TO MM
3030 VV2#(J)=VV#(2*J)
3040 NEXT J
3050 GOTO 3100
3060 FOR J=1 TO NN
3070 VV1#(J)=VV#(2*J-1)
3080 VV2#(J)=VV#(2*J)
3090 NEXT J
3100 REM
3110 M=0
3120 L=1
3130 LL=9
3140 FOR J=L TO LL
3150 REM
3160 XVES1#(J)=VV1#(J)*XK#(J-M)
3170 XVES2#(J)=VV2#(J)*XK#(J-M)
3180 NEXT J
3190 REM
3200 SMVES1#=0
3210 SMVES2#=0
3220 FOR J=L TO LL
3230 SMVES1#=XVES1#(J)+SMVES1#
3240 SMVES2#=XVES2#(J)+SMVES2#
3250 NEXT J
3260 VES1#(L)=SMVES1#
3270 VES2#(L)=SMVES2#
```

```
3280 L=L+1
3290 LL=LL+1
3300 M=M+1
3310 IF LL > NRAD THEN 3330
3320 GOTO 3140
3330 IF NRAD=NODD THEN 3350
3340 GOTO 3420
3350 FOR J=1 TO NN
3360 VES#(2*J-1)=VES1#(J)
3370 NEXT J
3380 FOR J=1 TO MM
3390 VES#(2*J)=VES2#(J)
3400 NEXT J
3410 GOTO 3460
3420 FOR J=1 TO NN
3430 VES#(2*J-1)=VES1#(J)
3440 VES#(2*J)=VES2#(J)
3450 NEXT J
3460 REM
3470 RETURN
3480 REM ***
3490 REM *** LEAST SQUARE SUBROUTINE ***
3500 REM ***
3510 K=0
3520 FOR J=1 TO NOO
3530 FOR I=1 TO NRADII
3540 IF (SPAC(J)>=RADIUS(I))AND(SPAC(J)<=RADIUS(I+1)) THEN 3550 ELSE 3600
3550 XX#=VES#(I+1)-VES#(I)
3560 INTR#=VES#(I)+(SPAC(J)-RADIUS(I))/(RADIUS(I+1)-RADIUS(I))*XX#
3570 RSQ#(LS)=RSQ#(LS)+(INTR#-APRH#(J))^2
3580 K=K+1
3590 GOTO 3610
3600 NEXT I
3610 NEXT J
3620 RSQ#(LS)=RSQ#(LS)/K
3630 RSQ#(LS)=SQR(RSQ#(LS))
3640 RETURN
```

```
**********************************************
*                                            *
*   RESISTIVITY -- SCHLUMBERGER SOUNDING     *
*                                            *
**********************************************

TITLE -- EXAMPLE RUN FOR RESISTIVITY SURVEY
INPUT APPARENT RESISTIVITY (Ohm-Ft), 1/2 ELECTRODE SPACING (Ft):
INPUT -1 FOR RESISTIVITY AND SPACING WHEN COMPLETE

          RESISTIVITY                    1/2 SPACING

              37000                          15.5
              70000                          31
              90000                          46
              74000                          61.5
              64000                          76
              40000                          92
              26000                          107
              18000                          122
              11000                          137
               8800                          152
               6500                          167
               5000                          182
               3800                          197
               2950                          212
               2150                          227
               1980                          242
               1700                          257
               1680                          272
               1700                          287
               1600                          302


ITERATION AGAIN (Y/N)? Y
ITERATION UPWARD OR DOWNWARD (UP/DOWN)? UP

INCREMENTS FOR DEPTH AND RESISTIVITY:  .05              .05

TOTAL NUMBER OF SUBSURFACE LAYERS:  3
DEPTH (Ft) AND RESISTIVITY (Ohm-Ft):
 5.4                22655
 21.6               226550
 999999             566
```

THICKNESS (Ft)	DEPTH (FT)	RESISTIVITY (OHM-FT)
5.4	5.4	22655
16.2	21.6	226550
999977	999999	566

1/2 SPACING (Ft)	RESISTIVITY (Ohm-Ft)
15.5	50069.57058097547
22.7509	63226.80447371651
33.3937	73630.83485384769
49.0153	74566.4596171476
71.9446	60397.39750241566
105.6	35396.52507961623
155	13308.43469762605
227.509	2744.071480481635
333.937	583.577126809063

LEAST SQUARE ROOT OF DEVIATION: 6791.7900390625
AT 1 ITERATION
ITERATION AGAIN (Y/N)? N